63-2-4

RADIO CORPORATION OF AMERICA
RCA LABORATORIES

UNCLASSIFIED

RESEARCH IN ELECTRON EMISSION FROM SEMICONDUCTORS

REPORT NO. 16 CONTRACT DA36-039-SC-87388 FINAL REPORT
PROJECT NO. 3A99-13-001-01
(CONTINUATION OF CONTRACT DA36-039-SC-78155)

1 OCTOBER 1960 TO 30 SEPTEMBER 1962

PLACED BY:
U. S. ARMY ELECTRONICS RESEARCH AND DEVELOPMENT LABORATORY
FORT MONMOUTH, N. J.

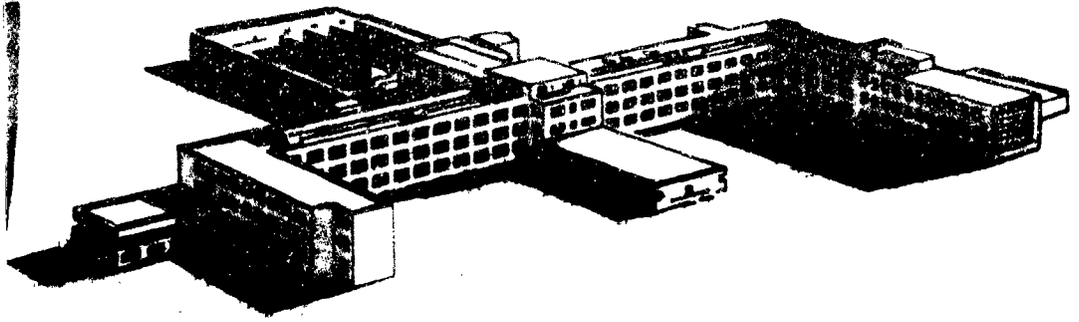

DAVID SARNOFF RESEARCH CENTER
PRINCETON, NEW JERSEY

UNCLASSIFIED

RESEARCH IN ELECTRON EMISSION FROM SEMICONDUCTORS

Report No. 16 Contract DA36-039-SC-87388 Final Report
(Continuation of Contract DA36-039-SC-78155)

Technical Requirements: SCL-5587B, 27 June 1960

Department of the Army Project No.: 3A99-13-001-01

Period Covered: 1 October 1960 to 30 September 1962

Objective: Research leading to a better theoretical understanding of thermionic and hot electron emission and to new materials with useful electron emission characteristics.

Report prepared by:

R. E. Simon
Project Engineer

E. K. Gatchell

W. H. McCarroll

C. R. Fuselier

Report Approved by:

G. A. Morton, Director
Conversion Devices Laboratory

Work on Contract done by: R. E. Simon, Project Engineer
G. O. Fowler
C. R. Fuselier
E. K. Gatchell
W. H. McCarroll
J. J. Quinn
W. E. Spicer

CONVERSION DEVICES LABORATORY
Electron Tube Division
RCA Laboratories
Princeton, N. J.

TABLE OF CONTENTS

	page
PURPOSE	1
ABSTRACT	1
CONFERENCES	2
FACTUAL DATA	3
I. Introduction	3
II. Literature Survey	5
III. The Range of Excited Electrons in Semiconductors and Metals	9
IV. P-N Junction Emitter	12
A. Description of Requirements	12
B. Diffusion and Fabrication	16
C. Characteristics of the Emitter without Injecting Contact	20
1. Thickness Measurement of the Thin Junction	20
2. i-v Characteristics	22
D. Voltage Profiles over Front Surface	26
E. Emission Measurements	29
F. Hot Electron Emitter with Injecting Contact	32
G. Metal Semiconductor Contact	36
V. Surface Treatment	37
A. Heat Treatment	37
B. Argon Bombardment	39
VI. Cesium on Silicon	44
A. Development of Method of Deposition	44
B. Condensation of Cesium on Silicon	45
C. Effect of Cesium on Silicon	47
D. Band Structure of Silicon from Photoemission Measurements	50
CONCLUSIONS AND RECOMMENDATIONS	52

FIGURE CAPTIONS

1. Electron temperature as a function of applied field for germanium as derived by several investigators.
2. Energy loss per unit path length by electron-electron interaction for a 2 ev electron in germanium as a function of electron concentration in the semiconductor conduction band.
3. One half the transition rate, $-E_I/E_o$, in units of the Fermi energy E_o, as a function of momentum p/p_o, in units of the Fermi momentum p_o for a hot electron in a metal.
4. The mean free path of an electron in aluminum as a function of its initial energy above the Fermi energy.
5. Energy band diagram of hot electron emitter.
6. Energy band diagram of hot electron emitter with injecting contact.
7. Surface concentration, C_o, of phosphorus in Si vs temperature.
8. Diffusion constant of phosphorus in Si vs 1/T.
9. Silicon wafer showing geometry of hot electron emitter and of surface conductance unit.
10. Hot electron emitter with rear contacts for imaging.
11. Diagram for definition of sheet conductance.
12. Sheet conductance vs number of boiling water-HF treatments.
13. N_D vs distance for thin junction.
14. Possible current transport mechanisms through junctions.
15. i-v characteristics of thick junction only and thick plus thin junction.
16. i-v curves for different current transport mechanisms through junction.
17. Diagram showing lateral current flow in thin junction.
18. Front surface potential vs radius for high σ_s.
19. $\frac{\Delta V(\text{Predicted})}{\Delta V(\text{Measured})}$ as a function of R_s.
20. $\frac{\Delta V(\text{Predicted})}{\Delta V(\text{Measured})}$ as a function of bias.
21. Pictures of luminescence of sample S-30.
22. Tube for testing hot electron emitter.

23. Emission current as a function of voltage across p-n junction.

24. i-v curves of hot electron emitter junction during the processing of the tube.

25. Tube for imaging the hot electron emitter surface.

26. Pictures showing light emitting and electron emitting regions, the latter being imaged on phosphor screen.

27. Geometry of first type of hot electron emitter with injecting contact.

28. Geometry of second type of hot electron emitter with injecting contact.

29. i-v curves of hot electron emitter with injecting contact.

30. Photographs of luminescence of hot electron emitter with injecting contact.

31. Experimental tube used to investigate the cesium-silicon metal semiconductor contact.

32. i-v characteristics as a function of heat treatment and cesium treatment of an etched crystal.

33. Experimental tube used for argon ion-bombardment of silicon crystals.

34. i-v characteristics of a crystal containing shallow and deep diffused regions before and after argon bombardment with 1000 ev ions.

35. Second design of argon ion bombardment tube.

36. Tube for deposition of cesium on silicon and on tungsten by molecular beam technique.

37. Tube used for measurement of the mean condensation time of cesium on tungsten. For measurements on silicon, W_1 was replaced by a silicon crystal.

38. Ion current as a function of time (or cesium deposition) in experiments on mean condensation time of cesium on silicon.

39. $1-I/I_\infty$ plotted as a function of time where I is the cesium ion current from surface ionization detector and I_∞ is the limiting value of this current. The slope of the line is equal to the mean time of adsorption of a cesium atom on tungsten.

40. $1-I/I_\infty$ as a function of time for cesium on silicon.

41. White light photoemission from a freshly cleaved silicon crystal as a function of time in a cesium atmosphere.

42. White light photoemission from an etched crystal of silicon and a tungsten filament as a function of the number of cesium atoms incident on the surfaces.

43. Experimental tube for the study of the effect of cesium on resistance and photoemission from heat treated silicon.

44. Effect of cesium on the resistance and white light photoemission from silicon cleaned by high temperature heat treatment.

PURPOSE

Hot electron emission is to be studied with the following aspects in mind:

(1) Basic investigation of hot electron emission with voltage applied across a semiconductor p-n junction varying over a wide range.

(2) Production of low electron affinity surfaces by suitable activation processes with alkali metals.

(3) Attempts to produce p-n junctions parallel to the vacuum interface to obtain electron emission from larger areas.

ABSTRACT

The work performed under this contract directed toward the study of hot electron emission from semiconductors is reviewed and summarized in this report. These studies include a review of the literature on hot electron effects in semiconductors and the theoretical study of electron-electron interactions in semiconductors and metals. The requirements for a p-n junction hot electron emitter are discussed, and a method of preparation of these emitters of silicon and studies of their properties are described. An emitter with an injecting contact is described but emission measurements on this device have not yet been made. Attempts to clean silicon in vacuum by low temperature heating and by argon bombardment without annealing are discussed. Measurements on the interaction of cesium with silicon are reported. While it has not yet been possible to produce an emitter with optimum properties, the groundwork for such an emitter has been laid.

CONFERENCES

During the final months of this contract, the following conferences took place for the purpose of discussing work in progress under the contract:

Place: Fort Monmouth, N. J.

Date: July 9, 1962

Attendance: Signal Corps- Messrs. Hieslmair and Kaplan
RCA - Messrs. Simon and Gatchell

Place: RCA Laboratories, Princeton, N. J.

Date: August 9, 1962

Attendance: Signal Corps- Mr. Hieslmair
RCA - Messrs. Simon, Gatchell,and Fuselier

Place: RCA Laboratories, Princeton, N. J.

Date: October 5, 1962

Attendance: Signal Corps - Mr. Hieslmair
RCA - Messrs. Simon, Gatchell, and Fuselier

FACTUAL DATA

I. Introduction

When a large electric field is applied across a semiconductor, conduction band electrons are accelerated to energies greater than their normal energies in the solid. If the kinetic energy associated with their motion in a direction perpendicular to the surface is made larger than the surface barrier, these electrons may be emitted into vacuum. If the number of electrons with energy great enough to escape from the solid can be made appreciable, this effect may be used to produce a cold cathode, hot electron emitter.

The object of this contract has been to study the possibility of producing a useful hot electron emitter. The program of research has included a survey of the literature on high field effects in bulk semiconductors and in reverse biased p-n junctions. During these studies questions arose about the effect of electron-electron interactions in semiconductors on the mean free path of hot electrons. A theoretical program to study this effect was instituted. This was subsequently extended to include the study of the mean free path of energetic electrons in metals.

It was concluded that a p-n junction provided a convenient method of producing a high field region near the surface of a crystal and the development of technqiues for preparing and measuring the properties of thin diffused junctions in silicon was undertaken. Silicon was chosen as the material with which to work because of the advanced nature of the technology of this material. This program has included the preparation of an n-p-n structure in which a forward biased p-n junction could be used to inject carriers which upon drifting to the thin junction would gain enough energy to be emitted.

In order to get appreciable electron emission, it is necessary to reduce the normally high electron affinity of the silicon. This can be done by treating the silicon surface with cesium. It has been shown that the minimum electron affinity can be achieved only if the cesium is applied to a clean or almost clean silicon surface. Part of our effort has been directed toward producing clean silicon surfaces in vacuum by heat treatment and by argon bombardment. Unfortunately, our results on electron emission have been limited by this aspect of our program.

A method of deposition of cesium on silicon by molecular beam techniques has been developed. The interaction of cesium on silicon has been studied as part of our program.

The culminating results of our studies would be the measurement of hot electron emission from thin diffused p-n junctions which have been cleaned in vacuum and then treated with cesium to minimize the electron affinity. Because of difficulties associated with producing a clean surface in vacuum it has not been possible to measure hot electron emission under ideal conditions. However, measurements of emission have been made during the course of our work as part of the evaluation of our junctions and will be included below.

An electric field can be applied across a semiconductor to obtain electron emission by means other than by use of a p-n junction. Part of our program has been to study the contact between cesium and p-type silicon to see if an inversion layer is formed across which a field could be applied.

Although the goals of our program have not been fully achieved, it is felt that sufficient progress has been made to indicate that further investment in this program to solve the remaining problems would yield significant information. This would be useful in determining the practicality of hot electron emitters.

II. Literature Survey

Following is a brief summary of the literature survey. No references are given. For a more complete description and references see the First and Second Quarterly Reports on this contract.

Hot electron effects were first observed in measurements on uniformly doped crystals containing no p-n junctions. Much of the experimental and theoretical work described in the literature has been performed on this type of sample simply because this type of geometry is amenable to theoretical treatment.

The basic experiments performed were measurements of the field dependence of mobility in germanium and silicon. These experiments showed that the mobility of semiconductors is non-ohmic in the high field region. The measurements have been made over frequencies ranging from dc to microwave frequencies.

A simple qualitative explanation of the high field effect on mobility can be given: When an electric field is applied across a semiconductor, kinetic energy is given to the relatively free electrons in the conduction band (and holes in the valence band). In equilibrium, this energy must be transmitted to the lattice through electron collisions with lattice vibrations. With high fields applied across the crystal, the electrons in thermal equilibrium with the lattice cannot give up energy to the lattice as fast as they receive energy from the field. Therefore, the electron temperature becomes higher and the electrons interact more strongly with the lattice. Electrons, because of their higher average velocity, collide more frequently with the lattice and the mobility decreases as the field increases.

A more rigorous theory of the high field mobility depends upon a solution of the Boltzmann transport equation taking into account the following electron interactions: (1) electron-acoustical phonon scattering, (2) electron-optical phonon scattering, (3) electron-electron scattering, (4) electron-impurity scattering, and (5) intervalley scattering. A rigorous theory would also take into account the complex band structure of the semiconductor in the energy region of interest.

While the formulation of the problem appears to be straightforward, the solution is complex and approximations have been made in the solutions. These include assumption of simple band structure and neglect of some of the interactions. Of particular interest has been the neglect (usually) of the pair production interaction, which occurs with high probability when an electron has energy greater than the threshold for pair production. This implies that even though the electron temperature is consistent with the mobility which depends on the behavior of the average electrons in the distribution, it may not predict the electron emission which depends upon the behavior of the electrons in the high energy tail of the distribution.

The electron temperatures as a function of field derived from theory for germanium are summarized in Fig. 1. Despite the different approximations made, they are in order of magnitude agreement. Also shown on this curve is the electron temperature as derived from measurements of the thermal noise temperature of the electron distribution under high fields. This experiment, suggested independently in our survey, has been performed by Erlback and Gunn.[1]

As a result of the literature survey, it was suggested that hot electron effects might be possible in materials which do not have strong optical phonon

---

1. E. Erlback and J. B. Gunn, Phys. Rev. Lett. 8, 280(1962).

interactions. These may include the useful electroluminescent materials.

The use of reverse biased p-n junctions makes possible the attainment of very high fields at low voltage. In addition, the non-destructive nature of the breakdown has made p-n junctions the natural configuration for the study of very high field effects in semiconductors.

Historically, the mechanism of breakdown was at first believed to be the result of tunneling of carriers across the band gap. It was subsequently shown that the breakdown was more usually the result of a multiplication-avalanche process. Breakdown occurs by tunneling when junctions with widths less than ~500 Å are used. Multiplication occurs when an electron gains sufficient energy to excite a valence band electron into the conduction band. The threshold for this effect was measured and a theory of the breakdown was developed in analogy with Townsend breakdown in a gas discharge. The theory was expressed in terms of $\alpha_i(E)$, the number of pairs produced by an electron or hole per unit path length. Measurement of α_i has subsequently been the objective of several experiments. The mean free path for a hot electron in a solid has been measured to be ~140 Å for optical scattering.

It has been shown that the breakdown in silicon usually occurs over small localized regions called microplasmas. These are evident in the light emission which was found to be localized and in the current through the junction which was found to consist of pulses. It has been shown that microplasmas are correlated with dislocations and, in a junction with no dislocations, uniform light emission can be obtaired indicating that dislocations play a role in microplasma formation. Uniform light emission has also been obtained using an injecting contact and operating the reverse biased junction below the breakdown voltage. A theory of microplasma breakdown has been suggested indicating that the ionization region is 500 Å wide, is 500-600 Å in diameter, and has

a space charge density of 10^{18} charges/cm^3.

The effect of the surface on the breakdown characteristics has been established experimentally and theoretically. It was shown that adsorbed atoms on the surface of a crystal can decrease the width of the depletion layer thereby decreasing the breakdown voltage.

The treatment of a p-n reverse biased junction in the high field region is exceedingly complex because not only must all the interaction discussed above be taken into account but the spatial dependence of the field and the crystal impurity density must be considered. Only qualitative agreement with experimental data has been obtained from the few attempts to derive a theory of a p-n junction under high field.

The literature survey has served to increase our knowledge of the phenomena associated with hot electron emission. It has shown us which mechanisms may play a role in limiting emission. It has provided a basis for the design of an emitter. The survey has also shown that not enough is now known about hot electron emitters to predict their performance. On the basis of this conclusion, our experimental program designed to produce an emitter was undertaken.

III. The Range of Excited Electrons in Semiconductors and Metals

In metals, with their high electron concentrations and in semiconductors with heavy doping, electron-electron interactions may be a source of energy loss for hot electrons. With the impurity concentration required for the p-n junctions, the possibility of electron-electron interactions was present so a calculation of energy loss by this mechanism was made. A similar calculation of the energy loss of energetic electrons in metals was made because of the interest in emitters based on metal-semiconductor contacts and because of the interest in metal-oxide-metal tunnel emitters which depend upon the transfer of hot electrons through metal films.

The calculations of the energy loss of excited electrons both in metals and in semiconductors due to electron-electron interaction are based upon the self energy approach to interactions in an electron gas. In the case of a metal the electron gas is assumed to be degenerate while in the semiconductor the electrons are assumed to obey classical statistics.

Very roughly, the calculation is based on the following reasoning. An excited electron polarizes the electron gas as it moves through it. The polarization cloud which it induces around itself acts back on the original electron giving rise to a self energy. The self energy has a real and imaginary part. The imaginary part can be interpreted in terms of a transition rate for real scattering events as follows. If ψ is the wave function of the excited state then

$$|\psi|^2 \propto e^{-2|E_{I(p)}|t}$$

where $E_{I(p)}$ is the imaginary part of the self energy and the state ψ damps out in time. Thus, the factor $2|E_{I(p)}|$ can be interpreted as the total transition rate for real scattering processes and its inverse can be thought of as the

lifetime of the state. By weighing each scattering event contributing to the total scattering rate by the amount of energy lost by the excited electron in the scattering event, one can obtain a rate of energy loss. Dividing the rate of energy loss by velocity of the electron gives $\frac{dE}{dX}$ the loss of energy per unit length along the path of the electron.

The imaginary part of the self energy of an electron can be expressed in terms of the dielectric constant of the electron gas. For the Boltzmann gas of the semiconductor, the dielectric constant was derived. For the degenerate gas, the dielectric constant derived by Lindhard[2] was used.

There are contributions to the energy loss from two distinct sources. In one contribution the energy lost by the excited particle goes into the creation of collective oscillations (plasmons) of the electron gas. The second contribution corresponds to excitation of individual particle states in the electron gas by the incident electron.

For the case of the non-degenerate electron gas in a semiconductor the energy loss per unit path length of a 2 ev electron in germanium is given in Fig. 2. Assuming a mean free path for optical phonon scattering of about 100 to 200 A, and an energy loss in a collision with an optical phonon of .04ev, the rate of energy loss in optical phonon collisions is $\frac{dE}{dX} \geq 2\times10^{-4}$ ev/Å. The greatest rate of energy loss via conduction electron scattering (at $n=10^{18}$) is 3.7×10^{-5} ev/Å. Thus, it is concluded that for $n \leq 10^{18}$ optical phonon scattering is more important than electron scattering.

For the case of an energetic electron in a metal, $-E_I$, which is one half the transition rate, is plotted in Fig. 3 in units of E_o, the Fermi energy, as a function of momentum p in units of p_o, the Fermi momentum.

---

2. J. Lindhard, Kgl. Dans. Videnskab, Selskab, Mat. - fys. Medd, 28, No. 8(1954).

The mean free path of an electron in a metal is given by

$$L(\mathcal{E}_i, \mathcal{E}_f) \approx \frac{\left(\frac{24\alpha r_s}{\pi}\right)^{1/2} \left[E_o^2 \left(\frac{1}{\mathcal{E}_f^2} - \frac{1}{\mathcal{E}_i^2}\right) + 2E_o \left(\frac{1}{\mathcal{E}_f} - \frac{1}{\mathcal{E}_i}\right) a_o\right]}{\left[\tan^{-1}(\pi/\alpha r_s)^{1/2} + \frac{(\alpha r_s/\pi)^{1/2}}{(1+\alpha r_s/\pi)}\right]}$$

where $\alpha = (4/9\pi)^{1/3}$, r_s is the radius of a sphere equal in volume to the volume per electron in units of the Bohr radius a_o, and $\mathcal{E}_f$ and $\mathcal{E}_i$ are the initial and final excitation energies, respectively. Fig. 4 shows the mean free path of an electron in aluminum ($r_s \approx 2$, $E_o \approx 12$) as a function of the initial excitation energy. It is seen that long mean free paths are possible for lower energy electrons. It should be noted that phonon interactions have not been considered. For a more detailed account of this theory, see reference 3.

---

3. J. J. Quinn, Phys. Rev. 126, 1453(1962).

IV. P-N Junction Emitter

A. Description of Requirements

Drawing upon the results of the literature survey on energy loss mechanisms, described in Section II, an analysis of the requirements for a hot electron emitter was carried out. A high electric field is required to raise the kinetic energy of the electrons, so that an appreciable number may be emitted. The electric field must be above $\sim 10^4$ volts/cm for significant emission. The most convenient method to achieve such an electric field is to use a p-n junction. Any practical emitter will have a reasonably large emitting area and, for almost any application, the electrons must leave the emitter with approximately the same potential at all parts of the emitting surface. These two considerations dictate the choice of a p-n junction whose plane is parallel to the emitting surface as shown in Fig. 5.

The aim of the study conducted under this contract was to specify, insofar as possible, the geometry of the emitter and the conductivity of the semiconductor regions comprising the emitter. The shape of the junction field, the width of the depletion layer, the operating voltage, and method of carrier injection are all important considerations in determining the design of the emitter. The literature survey on energy loss mechanisms suggested several large band gap materials with very interesting possibilities as hot electron emitters. Among intermediate band gap materials, silicon looked like the most promising. Silicon was also chosen for reasons previously indicated.

The current through the emitter p-n junction shown in Fig. 5 consists of i_e, the current emitted, and i_c, the current that is not emitted. i_c flowing laterally along the surface produces an unwanted IR potential drop along the surface. Since this potential drop reduces the total useful emitting area of the emitter and produces a velocity spread in the emitted beam, it is imperative

to make the thin n-region highly conductive to reduce the lateral potential drop. The hot electrons passing through the junction to the surface must pass through the n-region, and in so doing, lose energy. If the energy loss is such that the electron cannot surmount the potential barrier, it will not be emitted. Therefore, as thin an n-region as is consistent with the conductivity requirement is desired. It is possible that the requirement of high surface conductance can be met by depositing a monatomic layer of cesium on the silicon surface.

The chemisorbed cesium atom can donate its electron to the conduction band of the semiconductor, reducing the electron affinity of the surface and raising the conductance of the n-layer at the same time. This point will be more fully discussed in Section VI.

A high conductance n-layer is also required for the optimum field distribution within the depletion layer of the p-n junction. If the p-region is of lower resistivity than the n-region, then the maximum electric field will be concentrated very close to the n-region and consequently to the emitting surface. This is the optimum field distribution for hot electron emission.

The doping of the p-region is dictated by the requirements on the mechanism for current transport through the p-n junction. An electron in the p-region, within a diffusion length of the junction, will diffuse to the high field region of the junction depletion layer, will gain kinetic energy from the field, and, if the losses are not too great, can be emitted. An alternative transport process which becomes important when the electric field reaches 10^6 volts/cm is quantum mechanical tunnelling of carriers through the forbidden gap. In this process, an electron in the valence band on the p-side makes a transition to the conduction band on the n-side. Because this process can occur for electrons in very deep states in the valence band as well as those near the top, many electrons will arrive in the conduction band of the n-material with

little excess kinetic energy and thus cannot be emitted. The tunnelling process depends on the width of the depletion layer and this, in turn, will be determined principally by the doping in the more lightly doped p-region. To avoid tunnelling, an upper limit of $N_A = 10^{17}$ acceptors/cm^3 was chosen. With the requirement $N_D \gg N_A$, the junction parameters are specified.

If the voltage across such a junction is raised in order to give the electrons more kinetic energy, then at about 10-15 volts, the current through the junction will increase rapidly due to the phenomenon of pair production and the resulting current multiplication. Pair production presents a very serious limitation in raising the kinetic energy of the electrons. Once the threshold for the process is attained (about 3/2 the band gap), the process occurs with a very short mean free path ~ 25 Å. This means that energetic electrons are rapidly degraded in energy and will have little chance of reaching the surface with enough energy to be emitted. The excess carriers produced by the avalanche breakdown will dissipate energy thereby reducing the efficiency of the emitter. Since they must pass through the thin n-region on their way to the contact, these carriers will also contribute to the lateral potential drop along the surface of the emitter. From these two standpoints, multiplication is undesirable. However, the requirement of a high electric field is paramount. The emission current depends very strongly on electric field and it is likely that some multiplication will accompany meaningful emission. The voltage across the junction which will optimize the emission efficiency cannot be predicted and will have to be determined empirically.

An injecting contact can be used to augment the number of electrons reaching the high field region in the depletion layer. Because the emission current depends on the number of electrons accelerated as well as their probability of escape, injecting extra carriers provides a simple means of

increasing the emitted current. Furthermore, an injecting contact would make possible certain experiments that would clarify the behavior of the device. In particular, up to the present all experimental data on hot electrons show a very sharp dependence of emission current on the applied voltage. Since some multiplication is probably occurring in practically all the experiments reported to date, it is very difficult to separate the dependence of hot electron emission on electric field from the dependence of hot electron emission on multiplication. A source of additional electrons, which can be controlled by varying the injecting junction potential at a fixed value of field strength in the accelerating region, provides a powerful tool for this study. It is for this reason, as well as to increase emission current, that emphasis has been placed on fabricating an emitter with an injecting contact.

In summary, the emitter envisioned in the study consisted of three regions as shown in Fig. 6: an injection n-region $N_{Dinj} \gg N_A$, a p-region (with $5x10^{16} > N_A > 10^{17}$) less than one diffusion length wide, and a thin n-region less than 1000 Å thick on the surface. The surface layer must be treated to lower the electron affinity to as low a value as possible. The possibility of replacing the thin n injecting region by a metal was also considered and some experiments to see if this is practical were envisioned. In view of the state of the art, diffusion seemed the most practical way of fabricating the junctions.

Other aspects of the problem which have an important bearing on the operation of the emitter will be discussed in describing the behavior of the junctions fabricated and studied under this contract. These include microplasmas, the i-v characteristics, and surface treatment. In view of the importance of the surface problem, a summary of the work on the devices is first presented in Sections B through G, largely ignoring the surface problem,

followed by a detailed description of the surface studies in Sections V and VI.

B. Diffusion and Fabrication

In order to produce a junction less than 1000 Å thick by diffusion, it is necessary to know the parameters involved in the diffusion. The first point to recognize is that the diffusion equation may not be accurate for such thin diffusions.[4] The solution to the diffusion equation, appropriate to the plane geometry shown in Fig. 5, is given below:

$$N_D(x) = C_o \operatorname{erfc} \frac{x}{2\sqrt{Dt}}$$

where

N_D = Number of donor atoms/cm^3
C_o = Density of donor atoms at the surface
D = Diffusion constant
x = Distance in from the surface
erfc = Error function complement

This solution depends on the assumption that the source for the diffusant is infinite and that the diffusant impurity concentration, C_o, is a constant during the diffusion. The junction plane occurs at x_j where

$$N_A = C_o \operatorname{erfc} \frac{x_j}{2\sqrt{Dt}}$$

where

N_A = Number of acceptor atoms/cm^3 of the bulk p-type semiconductor

While shallow diffusions do not follow this equation well, it was nevertheless felt that a knowledge of D and C_o as a function of temperature was important as a rough indication of the depths of the diffusions. Therefore, a series of measurements of these quantities was undertaken.

The diffusion constant for phosphorus in silicon was determined over the temperature range from 822° to 1200°C for times of from 1 to 22 hours. The

4. E. Tannenbaum, Solid State Electronics 2, 123(1961).

"box" method was used and the 5% phosphorus source was employed in all runs. The "box" method will be described below when the device fabrication is discussed.

Sheet resistivities of the diffused layers were measured by the four point probe method.[5] The diffused layer was lapped at a small angle and stained with a standard $HF:HNO_3$ solution[6] to delineate the junction. The depth of the junction was determined from measurements of the angle and width of the exposed region using a metallurgical microscope having stage and depth micrometers. The above data were used to determine the surface concentration using the curves of Backenstoss[7] as corrected by Irvin.[8] An error function complement (erfc) distribution was assumed. A plot of surface concentration vs temperature (Fig. 7) shows that it is constant with temperature from 1200°C to about 950°C after which it falls off rapidly to where it is approximately $10^{20}/cm^3$ at 850°C.

The junction depths and surface concentrations were then used to calculate the diffusion constants for a graphical solution of the error function complement. The data obtained are plotted as a function of temperature as shown in Fig. 8.

These diffusion constant data were used to calculate the conditions for the shallow diffusion step. The junction depth based on an erfc distribution of phosphorus for 15-minute diffusions at 900° and 850°C are 1820 Å and 980 Å, respectively. These figures probably represent minimum junction depths since it appears from the work of Tannenbaum that initially there is a positive deviation from the erfc distribution. On the basis of these measurements and calculations, a 15-minute diffusion at 850°C was decided upon as a starting point for shallow diffusion studies.

---

5. F. M. Smits, Bell System Tech. J. 37, 711(1958).
6. F. J. Biondi, Transistor Technology, Vol. III, Van Nostrand Co., Princeton, N. J., p. 85, 1958.
7. G. Backenstoss, Bell System Tech. J. 37, 711(1958).
8. J. Irvin, Bell System Tech. J. 41, 387(1962).

The contact to the thin silicon n-layer which is less than 1000 Å in thickness requires special consideration. The standard method of alloying an ohmic contact is clearly unsuitable since it would penetrate the layers and short out the junction. It was felt that contact by means of an adjacent thick diffused layer, continuous with the thin layer, would be the surest and easiest method to use. The deep diffused junction, about 5 microns deep, presents no special problem.

Because the fabrication of an emitter with an injecting contact is difficult, it was felt that work on an emitter without the injecting contact should be initiated first. The circular geometry adopted is shown in Fig. 9. The thick outer ring provides the contact to the thin region in such a manner that the plane of the thin junction never intersects the surface. If the junction plane intersects the surface, hot electrons can be emitted without passing through the thin n-layer. Since this edge emission is not useful and obscures the emission through the thin n-region, we were anxious to avoid it. The deep diffused region has a higher breakdown than the thin region so that emission should occur from the thin region before it comes from the thick n-p junction at the surface.

A rectangular unit which is pictured in Fig. 9 was fabricated simultaneously with the circular one on the same wafer. This rectangular geometry was chosen to measure the surface conductance. After the processing of the wafer, it could be cut in half. One could etch through the thin n-region completely, if desired, and still mount the circular unit in a tube for emission measurement.

The following procedure was followed in constructing the wafer. Silicon wafers with resistivity 0.5 $\pm$0.1 ohm cm were lapped and optically polished to a thickness of about 0.010". The wafer was then etched in CP-4*

*The composition of CP-4 is HNO_3:HF:CH_3COOH in the ratio 5:3:3. If ten drops of the acid mixture is added, the reaction starts rapidly.

for about one minute to remove surface damage caused by the polishing. The patterns shown in Fig. 9 are formed by means of the photoresist[9] technique.

In the photoresist technique, the oxidized silicon wafer is coated with a material that can be rendered insoluble to HF by light. After the wafer has been coated, it is exposed to light through a stencil. The wafer, covered with photoresist, is then put in a solution. The solution dissolves the photoresist that has been exposed to light and leaves the unexposed region protected. HF can then be used to dissolve that part of the SiO_2 that is unprotected and cannot attack the SiO_2 that is protected. The resulting SiO_2 pattern on the surface of the crystal serves as a mask against diffusion.

The diffusion of phosphorus is carried out in a closed box from a source consisting of a mixture of SiO_2 and P_2O_5. A 5% concentration of P_2O_5 is used.[10] The diffusion takes place at 1200°C for one hour in an ambient of dry nitrogen. The resulting diffusion produces a thick n-region about 5 microns deep.

The last step in the construction is the diffusion of the thin n-region. This process requires an oxide mask which can be much thinner than the one for the previous thick diffusion. The oxide growth conditions are the same as before except that the time is one hour. The thin diffusion proceeds with the same diffusant source employed in the diffusion of the thick contact. This time, however, the length of the diffusion time is reduced to 15 to 30 minutes at a temperature of 845°-865°C.

Certain samples were prepared to be placed in an image tube. For this purpose, it is undesirable to make probe contact to the thick region with tungsten probes on the same side of the crystal on which the thin diffusion exists. This requires folding over the thick diffused region as shown in Fig. 10. Masking

---

9. F. J. Biondi, Transistor Technology, Vol. III, Van Nostrand Co., Princeton, N. J., 1958.

10. D'Asaro, Solid State Electronics 1, 3(1960).

techniques, identical to those described above, were employed to construct wafers with this slightly different geometry.

C. Characteristics of the Emitter without Injecting Contact

1. Thickness Measurement of the Thin Junction

Since the depth of the thin junction is a crucial parameter in determining the behavior of the hot electron emitter, a measurement of it which is independent of the diffusion equation is highly desirable. One method that was readily available was the boiling water technique devised by Moll and his coworkers.[11] This is a method for removing a known amount of silicon in small steps and measuring the sheet conductance after each step. The silicon surface is stripped by first oxidizing the surface (by means of one minute immersion in boiling water) followed by an HF etch. The HF etch removes only the SiO_2, formed during the boiling water immersion, and does not attack Si. Moll and his colleagues calibrated this technique by very careful weighing and arrived at a value of 33 Å/step. Subsequently, this measurement was checked by an independent interferometry measurement which yielded a value of 23 Å/step.[12] One sample, prepared for interferometric measurement, was then also checked by the weighing technique and the two techniques gave the same value of 23 Å/step. The surface preparation used in the initial measurement by the weight technique was different from that used in the interferometric technique. They attributed the difference in the two measurements to unrelieved strain which was present in the optically polished samples, but not present in the samples prepared for weight measurement. Inasmuch as the surface preparation of our emitters closely resembled the surface preparation Moll et al used when they calibrated the boiling water technique by weighing, we accepted the 33 Å/step value as applying to our emitter surfaces. Since they had performed a careful measurement and cross-checked it, we did

11. J. L. Moll, N. I. Meyer, and D. J. Bartelink, Phys. Rev. Letters 7, 87(1961).
12. J. W. Beck, J.A.P. 33, 2391(1962).

not feel that an independent measurement was warranted or necessary.

The boiling water technique in conjunction with surface conductivity measurement can be used to determine the donor concentration profile and the depth of the end of the depletion region beneath the emitter surface. σ_s, the surface conductivity, is defined by the measurement of the conductance of a square sheet shown in Fig. 11(a). σ_s is meaningful only if the thickness, t, is small compared to the other dimensions. σ_s is independent of d and is readily derived from a conductance measurement on a sample which is not square (see Fig. 11(b)). If G is the conductance measured on the rectangular sample shown in Fig. 11(b), then

$$\sigma_s = G \frac{b}{a}$$

The surface conductance of the thin n-layer is given by

$$\sigma_s = \int_o^D Ne\mu d\chi$$

$$\frac{d\sigma_s}{d\chi} = Ne\mu$$

$$N = \frac{d\sigma_s / d\chi}{e\mu}$$

where

N = density of electrically active donor impurities
D = depth of depletion layer edge beneath the surface
μ = mobility
e = electron charge
χ = distance in from the surface of the emitter

Fig. 12 shows a plot of σ_s versus the number of boiling water steps performed on one of the rectangular units. Fig. 13 shows a plot of N derived from the above equation and the curve of Fig. 12. The mobility data of Backenstoss were used in the calculation. Since mobility is a function of doping, a self-consistent approximation was used to arrive at N. If the thickness of the thin layer becomes comparable to or smaller than the mean free path

for scattering, a correction may be important. However, no such correction was applied to the data plotted in Fig. 12.

2. i-v Characteristics

The i-v characteristics of the emitter may have an important effect on the characteristics of a hot electron emitter. Once the surface problem is solved and significant emission is obtained, the question of efficiency becomes important. For high efficiency, it is necessary that the electron transport mechanism through the junction be such that the maximum number of electrons passing through the junction be excited to as high a kinetic energy as possible.

Fig. 14 shows two types of transport that can limit the efficiency. The first (Fig. 14(a)), tunnel emission, has already been discussed. The carriers, shown in the diagram, tunnelling through the depletion layer cannot surmount the surface barrier and contribute to emission. As was pointed out in Section IV(A), we chose the doping of the p-region so that tunnelling would not occur.

A second mechanism is indicated in Fig. 14(b). There are no free carriers in the depletion layer. However, electrons from the valence band may make transitions into the conduction band assisted by means of generation-recombination centers. The square boxes in the diagram represent generation-recombination centers[13] in the forbidden energy gap.

Only a fraction of the electrons arriving in the conduction band by this mechanism can be emitted. These emitted electrons will have been generated in that part of the depletion layer that is shown shaded in Fig. 14(b). Therefore, the efficiency of the emitter may be determined by the distribution of impurity centers in the depletion region. In all semiconductors except Ge, the bulk of the current passing through the junction is carried by this generation-recombination mechanism.

---

13. A. K. Jonscher, Principals of Semiconductor Devices, J. Wiley, New York, p. 36, 1960.

A third mechanism for current transport across the junction is surface leakage. An inversion layer may cover either the n- or the p-region and thus present a parallel path for current flow, bypassing the p-n junction. We have strong indirect evidence that this is not a significant source of current transport in our devices. Fig. 15 shows two sets of i-v curves taken on a typical circular unit before and after the thin diffusion. The significant feature to note is that the i-v characteristic of the device with both the thick and thin diffusions is much "leakier" or "softer" than the i-v characteristic of the device with the thin junction alone. After the thick diffusion is made, there appears to be very little leakage as is shown in Fig. 15(a). In Fig. 15(b), an effect that resembles surface leakage has been introduced solely by performing the thin diffusion. The boundary of the thin diffusion, indicated by the dotted line in Fig. 9, lies entirely within the thick region. It is difficult to imagine any mechanism being introduced by the thin diffusion process which can produce surface leakage not already present after the thick diffusion. The thin diffusion is carried out in the same box, using the same diffusant source, in the same oven, ambient gas flow and quartz tubing as the thick diffusion. It is interesting to note that the same "leakage" is observed in thin Ge diffused junctions, only the effect is much more severe in the case of Ge.[14] The fact that the thick diffusion and the thin diffusion i-v curves behave in this manner is important in evaluating the behavior of the devices. As long as the voltage is kept below the breakdown voltage of the thick junction, one can be sure that any hot electron emission is coming from the thin junction which is the principal area of interest. Thus, the thick region not only provides us with a region for contact but also serves as a guard ring.

Finally, consider the possibility that the excess current due to the thin diffusion is simply the result of multiplication. The thin diffusion

---

14. Quarterly Report No. 3, "Research Study for Increasing the Sensitivity of Photoemitters," ERDL Contract DA44-009-ENG-4913, 1 July 1962 - 30 September 1962.

would be expected to produce breakdown at a lower voltage, and the effect of multiplication is seen at lower voltages than the breakdown voltage. The current enhancement due to multiplication begins to appear at voltages lower than breakdown and might therefore account for the excess current introduced by the thin diffusion.

To test this hypothesis, an attempt was made to calculate the i-v curve using the multiplication data of Batdorf, Chynoweth, Dacey, and Foy.[15] Their junctions were quite similar to ours: phosphorus was diffused into 0.2 to 0.3 ohm cm p-type silicon to a depth of 2000 Å, and their light emission showed only a few microplasmas. Their data shows that when $V/V_B = 1/4$ (where V_B = breakdown voltage), then M = 1. If we take V_B = 28 volts for our experimental i-v curve shown in Fig. 16, then at $V/V_B = 1/4$ (meaning V, in our case, = 7 volts), i should contain no component due to multiplication. The dashed curve of Fig. 16 is based on their multiplication data normalized at 7 volts for our junction. The dashed curve thus represents what our i-v curve should look like if the increase in current is due solely to multiplication. It is at once obvious that our experimental curve is more rounded or "leaky" than the curve predicted by the multiplication data.

It should be emphasized that the experimental curve presented in Fig. 16 is typical of our results. It is, of course, the actual experimental curve, but numerous other i-v curves on other samples have all yielded the same general behavior. It is of interest in this connection to note that the experimental i-v curves of Batdorf, et al are more rounded than predicted by their multiplication data.

---

15. Batdorf, Chynoweth, Dacey, and Foy, J.A.P. 31, 1154(1960).

Fig. 16 also illustrates i-v curves arbitrarily normalized for the other current transport mechanisms discussed: leakage by an inversion layer and generation-recombination. There are two curves for "leakage," one representing a weak inversion layer and the other a strong inversion layer yielding somewhat different voltage dependences.[16] The generation-recombination mechanism can also give two different voltage dependences as illustrated in Fig. 16. The two extremes are the limiting forms for voltage dependence of a diffused junction. Lawrence and Warner[17] have carried out an explicit calculation for the width of the depletion layer of a diffused junction and show a $V^{1/2}$ and $V^{1/3}$ behavior as asymptotes. If one makes the assumption that generation-recombination centers are distributed uniformly throughout the depletion layer, then the current due to this mechanism should be proportional to depletion layer width and therefore should have some voltage dependence intermediate between $V^{1/2}$ and $V^{1/3}$.

It is easy to dismiss the current transport mechanism envisioned in the original Shockley[18] model of a p-n junction. The Shockley model predicts a current of 10^{-12} amps independent of voltage for 1 volt $< V < V_{Breakdown}$. It is worth noting that at room temperature, the only semiconductor for which the simple p-n Shockley model obtains is Ge.

It is apparent from a cursory inspection of Fig. 16 that our i-v experimental curve fits none of the theoretical curves. It is difficult to imagine any change in normalization procedure that would produce a fit. Furthermore, a linear combination of any of the theoretical curves cannot reproduce the experimental i-v curves. The work Goetzberger and Stephens[19] suggests

16. W. Erikson, H. Statz, and G. A. Demars, J.A.P. 28, 133(1957).
17. Lawrence and Warner, B.S.T.J. 39, 389(1960).
18. W. Shockley, Electrons and Holes in Semiconductors, D. Van Nostrand, New York, p. 309, 1950.
19. A. Goetzberger and C. Stephens, J.A.P. 32, 2640(1961).

a possible explanation. Their junctions were formed in p-type, 0.4 ohm cm silicon with phosphorus diffusion. The depth of their junctions was somewhat greater than ours since the diffusion was carried out at 900°C for 1.5 hours (our conditions were 850°C for 0.5 hour). They found that there are two distinct groups of microplasmas. If one associates the onset of a microplasma with a localized breakdown in the region at which the breakdown is taking place, then their data show not one single breakdown voltage but a spread of breakdown voltages. The spread of a larger group of microplasmas is 5 volts wide centered at 27.3 volts, while the spread of the smaller group is 1 volt wide centered at 23.8 volts. They attribute the two groups as being due to 2 separate types of imperfections. The spread in breakdown voltage that they report is too narrow to account for our measured i-v characteristic. It should be noted, however, that Batdorf, et al,[15] succeeded in making one perfect junction which showed uniform emission with no microplasmas.

In conclusion, we can say that no known mechanism adequately explains our i-v data. It is recommended that future work in the area of hot electron emission include a more detailed experimental study of the i-v characteristics in view of their importance in determining the usefulness of hot electron emission.

D. Voltage Profiles over Front Surface

As has been pointed out in the introduction (Section IV-A), one of the requirements that is placed on a broad area hot electron emitter is that the potential distribution across the front surface be small. Measurements of the potential drop across a typical sample, S-30, were made with a tungsten probe delicately touching the silicon surface by use of a high impedance electrometer DC amplifier in order to eliminate the effect of the tungsten-Si contact.

If one assumes a uniform current density J_o(amps/cm^2) through the thin junction of our device (see Fig. 17), then

$$dV(r)\text{(voltage change between r and r+dr)} = \frac{J_o \pi r^2}{2\pi r \sigma_s} dr$$

where

V(r) = the voltage on the surface at r

J_o = the current/cm^2 through the junction

σ_s = the surface conductance in mhos per square

$$V(r) - V(o) = \int_o^r dV = \frac{J_o r^2}{4\sigma_s}$$

and $$\Delta V = V(r_o) - V(o) \frac{J_o r_o^2}{4\sigma_s} = \frac{i}{4\sigma_s}$$

where

i = the total current through the thin junction.

V(o) - V(r) is plotted in Fig. 18 for sample S-30. The experimental points follow the predicted parabolic behavior (solid line) quite well. This measurement was done before any of the thin surface was etched off with σ_s = 0.0018 mhos/sq. (A companion rectangular unit was put through the same boiling water and HF treatments as S-30 so that the surface resistance could be measured.)

As the thickness of the thin region was reduced, V vs r curves were periodically taken. In Fig. 19, the ratio of $\frac{\Delta V(\text{predicted})}{\Delta V(\text{measured})}$ is plotted as a function of R_s ($R_s \equiv 1/\sigma_s$) for two different values of bias and in Fig. 20, we plot $\frac{\Delta V(\text{predicted})}{\Delta V(\text{measured})}$ as a function of voltage applied across the junction, V_{pn}, for the highest value of σ_s, 0.00012 mhos/sq. The following facts are observed:

(1) At values of $\sigma_s > 0.001$ mhos/sq, the predicted voltage drop is in reasonable agreement with the measured value even for bias values close to breakdown.

(2) The predicted ΔV behavior is followed to somewhat higher values of σ_s as the bias voltage is increased. At half the breakdown voltage

the predicted value is reasonably well followed to $\sigma_s < 0.00044$ mhos/sq.

(3) At the highest value of $\sigma_s \sim 10^{-4}$ mhos/sq (corresponding to a thin n-region of the order of 200 Å), the predicted ΔV is 5 times the measured ΔV. This deviation from the predicted ΔV is followed all the way down to 0.4 volt bias across the junction.

The departure from the predicted value of ΔV implies that the current through the thin junction area is not uniform. An examination of the luminescence supports this picture. Luminescence from sample S-30 is shown in Fig. 21. The various photographs were taken for successively longer exposure times. The brightest spots occur at the intersection of the thick and thin regions and there are at least two other groups of microplasmas of more or less equal light intensity. The breakdown between the outer edge of the thick diffusion and the p-region can be seen. It is evident that the bulk of the light emission and hence breakdown current is occurring inside the diameter of the thin region and that the contribution from the edge of the thick n- to p-region is small.

The microplasmas with different breakdown voltages explain the non-uniform current in the breakdown region and therefore non-uniform J_o and the departure from the predicted voltage profile distribution. In fact, to explain the obeyed behavior at high voltages in the microplasma region is something of a puzzle. One has to assume a uniform density of microplasmas which is not very reasonable from the appearance of the pictures. These pictures are representative of those taken on other samples. None of the pictures taken on emitters without the injecting contact showed uniform light emission.

While the voltage profile measurements were made on a sample without Cs coverage, they may be made on a cesium covered surface if and when the need arises. Furthermore, the techniques developed can be applied to such samples in the vacuum if the need arises.

E. Emission Measurements

The measurement of hot electron emission current made during the contract period falls into three classes. The first is a DC measurement for which the circuit is shown in Fig. 22. The second is a pulse measurement wherein a pulse generator replaces the variable reverse bias DC supply. The results of both DC and pulsed measurements for a rectangular unit are shown in Fig. 23. The third type of observation of emission was carried out by means of a phosphor screen onto which the source of the emitted electrons was imaged.

The following procedure was used to prepare the wafers for emission studies: The wafers were subjected to a series of boiling water treatments to reduce the thickness of the thin layer. In general, about 900 Å were removed. The wafer was then mounted in a tube with two tungsten probes on the p-region and two on the n-region to allow i-v measurements after sealing. The tubes were then sealed onto a glass system and baked at a temperature of 200°C to 450°C for times ranging between 2 hours and 6 hours. The i-v characteristics frequently changed as a result of the baking. This was attributed to changes in the inversion layer, formed on the surface, which can be responsible for part of the leakage current. The optimum baking conditions to keep the i-v curves as "hard" as possible was 200°C and 6 hours. The vacuum after the bake was usually around 5×10^{-8} torr.

Cesium was subsequently introduced into the tube. This was accomplished first by heating a mixture of Si and Cs_2CrO_4 to the reaction temperature which liberates Cs vapor in an auxiliary side tube. The whole system was then baked which serves to drive the Cs from the side tube onto the crystal surface. The process was monitored by measuring the white light photoemission from the n-layer. An empirical value of white light photoemission was used to determine

when the optimum Cs coverage was reached. The tube was then ready for emission measurements.

While this method of treating the Si surface with Cs is not quantitative, the procedure has yielded useful results. The more sophisticated method described in Section VI is definitive. However, it is somewhat more cumbersome and, since our silicon surfaces were not well controlled in these experiments, we felt its use was not warranted at this time. Once the silicon surfaces are better defined, the refined method of depositing cesium will, of course, be used.

The cesium treatment often produced drastic changes in the i-v curves. Fig. 24 shows the i-v curves as a function of the treatments described above. The effect of Cs on the junction characteristics is the most striking feature of these data. It is most graphically seen in comparing the i-v curve on the 3.2 ma/Div scale before and after the Cs deposition. With this type of Cs treatment, the cesium is not confined to the thin n-region and the cesium layer can produce a conducting path that shorts out the junction. This merely highlights the need for controlled cesium deposition.

The emitted electrons were imaged onto a phosphor screen. The wafers fabricated for imaging are pictured in Fig. 10 and were mounted in a tube shown in Fig. 25. The processing was identical to that described above. Once hot electron emission was observed, the phosphor screen could be moved in front of the crystal and, by using a collecting voltage of 2000 volts, the pattern of the emitted electrons could be seen on the phosphor screen. By moving the screen out of the way, one could observe microplasma luminescence from the crystal and thus a comparison between emission and microplasma light emission could be obtained.

Fig. 26 shows photographs of microplasma luminescence and photographs of the hot electrons being imaged onto the phosphor screen and the

conditions under which the photographs were taken are listed below each photograph. The photographs were taken on the same sample. The spacing between the crystal and the phosphor screen was 1/4" which is too large to expect good imaging definition. Furthermore, it was difficult to hold the phosphor screen exactly parallel to the crystal surface during the glass sealing operation. Any non-parallelism will produce some distortion of the image of the source of electrons.

While it is difficult to identify the identical pattern of microplasmas in the light emission photographs with the pattern of emitted electrons in the photographs of the phosphor screen, the qualitative similarity is striking. Electrons from the outer ring, delineating the boundary between the thick n-region and the p-region, are visible in one photograph of the phosphor screen while none of the photographs of the microplasma light emission showed light emission from this ring. The difference is probably due to the much greater sensitivity of the phosphor photographic film combination compared to the photographic film alone.

The photographs presented in Fig. 26 are much more convincing than those appearing in a recent paper on hot electron emission.[20] While Hodgkinson's photographs suggest that both the microplasma luminescence and the hot electrons emanate from discrete spots on the crystal surface, his photographs show very little correlation between the two effects. We believe that our pictures, taken before his publication, provide much stronger evidence than his data does for his conclusion that light emission and hot electron emission originate from the same spots.

---

20. Hodgkinson, Solid State Electronics 5, 269(1962).

F. Hot Electron Emitter with Injecting Contact

The importance of, and reasons for, a hot electron emitter with an injecting contact have already been discussed in Section A above. In order to fabricate a useful hot electron emitter with an injecting contact, there are two principal requirements which must be satisfied.

(a) The injection efficiency, γ, should be high, preferably ≈ 1. γ is defined as $\equiv i_e + i_e' / i_T$ where the current symbols are defined below. The total current through the junction contact, i_T, is made up of three components as shown in Fig. 6. i_e represents the injected electron current that crosses the base and is captured by the high field region of the back biased thin junction. i_h is the hole current through the injecting junction and is not useful for emission.

(b) i_e'/i_e should be as small as possible. i_e' represents the injected electron current that recombines in the p-type or base region and cannot therefore contribute to electron emission.

Since the first approach toward fabricating a hot electron emitter was not successful, it will be only briefly described. The geometry of the unit is shown in Fig. 27. The shaded region was a standard circular thick-thin diffusion of the same dimensions as that shown on Fig. 9. The injecting contact is shown as the crosshatched region in Fig. 27. The facilities of the development group at the RCA Somerville plant were used to fulfill the rather stringent fabrication requirements of this device. The diffusion in which the thick injecting contact was made had to be sufficiently deep so that the p-type base layer left was thin (comparable to the electron diffusion length). The top and bottom of the crystal wafer had to be kept parallel, and the diffusion had to be well controlled. Units that satisfied these criteria were successfully constructed

but showed no electron transport across the p-region. A calculation based on simple junction theory[21] and utilizing the diffusion parameters predicted $\gamma = .75$. The thick injecting n-region was formed by a long high-temperature diffusion of phosphorus (1275°C for 120 hours). We believe that this high temperature for such a long period degraded the minority carrier lifetime to such an extent that electron transport across the p-region was negligible.

The second approach, which was more successful, is described with reference to Fig. 28. A 0.5 ohm cm p-type silicon wafer that had been polished and etched was placed in a jig for electro etching. The electro etching was done in an electrolyte of ethanol with 10% HF and at a current density of 0.5 amps/cm^2. The hole was cut to a depth varying between 75 μ and 100 μ. This process, which was used by A. Goetzberger,[22] was followed by a 2-μ thick diffusion (15 minutes at 1200°C) over the entire wafer. The thick diffused regions in the bottom and sides of the hole were removed selectively by chemical etching. The final step was a thin diffusion using the box technique for 15 minutes at 845°C to 865°C producing the standard thin diffused junction 1500 Å below the surface.

Goetzberger[22] has described the operation of the device shown in Fig. 5 which he calls a three-layer diode and we call a hot electron emitter with injecting contact. If the device is biased as shown in Fig. 6 with the lead to the p section removed

$$\text{Then} \qquad \alpha = \frac{i_e}{i_T}$$

where the symbols are those shown in Fig. 6.

Let M = multiplication in the back biased junction

---

21. A Tanenbaum and O. Thomas, B.S.T.J. 37, 699(1958).
22. A. Goetzberger, J.A.P. 31, 2260(1960).

(In this treatment, α is to be regarded as the α that obtains when multiplication does not occur. See, for example, Jonscher.[23])

Current conservation requires $M\alpha = 1$

M depends very strongly on the electric field and hence the voltage across the junction. Therefore, as the voltage is increased and current multiplication begins, there is a limiting voltage set by the equation for current conservation. A negative resistance occurs as this condition is reached. Fig. 29 shows the i-v characteristic obtained on one of our hot electron emitters with injecting contact. The oscillations are attributed to the negative resistance region and the frequency and range over which the oscillation occurs are set by the external circuit parameters of the equipment used to display i-v curves on the oscilloscope. For comparison, an i-v curve of the thick-thin junction is shown when the emitter is left floating. These pictures are thus confirmation of transistor operation of the hot electron emitter with injecting contact.

A very interesting feature of a hot electron emitter with injecting contact is the light emission pattern observed. When operated with the base p-region floating, the condition $M\alpha = 1$ forces the current to be uniform over the thin junction area. Microplasmas are not observed. Fig. 30 shows photographs of the light emission of one of our units operated with base region floating and with emitter region floating. The difference in the pictures is evident. One microplasma only shows up in the photograph taken with the base floating. This is due to an edge effect.

There is some shading across the face of the thin junction due to the fact that the thin region was not exactly parallel to the flat side of the crystal wafer. This was caused by a relatively crude jigging technique employed in the electro etching. The brightest section of the light emission pattern corresponded to the deepest part of the electro etched hole.

---

23. A. K. Jonscher, Principles of Semiconductor Device Operation, ch. 5, J. Wiley, New York, 1960.

As a final confirmation of transistor action, the α of the transistor was measured and from α a value of L_e, the diffusion length for electrons in the p-material, was derived. The measurement was carried out at low DC bias to eliminate multiplication effects. α was measured with the help of the following equation:

$$i_c = i_{co} + \alpha(i_e + i_e')$$

where $i_T = i_e + i_e'$ ($i_e + i_e'$ shown in Fig. 6 and in our case $i_h \approx 0$)

i_{co} = collector current when $i_e + i_e' = 0$

α was measured to be 0.25. (The calculation involved a correction factor for the fact that the emitting area was five times the area of the collecting area.) The calculated value of the injection efficiency, γ, was ≈ 1.0. γ was calculated using the known diffusion parameters.

$$\alpha = \gamma\beta = 0.25$$

where β = the transport factor; taking $\gamma = 1$, $\beta = 0.25$

Transport theory[24] gives:

$$\beta = \left(1 - \frac{1}{2}\ \frac{W^2}{D_e \tau}\right)$$

where W = width of base region

τ = minority carrier lifetime

D_e = diffusion constant for electrons

Using the relation $L_e = \sqrt{D\tau}$, we obtained a reasonable value of 37 μ for L_e.* The principal error in L_e comes from the fact that W is not uniform.

Unfortunately, the sample on which these measurements were made cracked during the operation of mounting in a tube so that hot electron emission measurements on the unit could not be made. We feel that the utility of the injecting contact for hot electron emission has not yet been explored and that its possibilities should be vigorously pursued.

---

24. W. Shockley, M. Sparks and G. K. Teal., Phys. Rev. 83, 151(1951).

*A value of 20 μ was obtained in similar Si junctions by A. Goetzberger, Air Force Cambridge Research Laboratories Report 62-286, July 15, 1962.

G. Metal Semiconductor Contact

An alternate way of producing a high field region near the surface of a crystal is by means of an inversion layer at a metal semiconductor contact. This system has the advantage of bringing the high field region close to the surface and utilizing the high conductivity of the metal to pass off those electrons which get through the inversion layer but are not emitted. The calculation of the mean free path of electrons in metals suggests that not many electrons will be lost in passing through a thin metal film.

In view of these possibilities, experiments were performed to see if a metal-semiconductor contact between cesium and silicon would be useful. According to the simple theory of contacts, it was expected that the contact of cesium to p-type silicon would be rectifying. Indeed, experiments on the velocity distribution of photoelectrons from cesium treated silicon indicate that an inversion layer is produced.

In our experiments, the i-v characteristic between bulk cesium and p-type silicon was investigated. The tube used for this experiment is shown in Fig. 31. A silicon crystal which was heavily oxidized was inserted in a closely fitting glass sleeve. After evacuating the tube, cesium was liberated. The crystal was then cleaved, exposing a fresh surface. Cesium was distilled to the crystal, the cesium collecting in a pool on the crystal. Contacts were made to the cesium pool and to the crystal.

In no case were rectifying contacts observed. It is possible that cesium reacted with silicon so that a good metal-semiconductor contact was not made. These results, however, are not considered conclusive and it is felt that metal-semiconductor contacts are potentially promising enough to be worth considerably more effort.

V. Surface Treatment

A. Heat Treatment

In order to get appreciable electron emission, it is necessary to reduce the normally high electron affinity of silicon. It has been shown, as will be discussed in the next section, that the deposition of cesium on clean silicon reduces the electron affinity from about 4.1 ev to 1.5 ev. This is the minimum value obtained with cesium on silicon and thus it appears that it is desirable to deposit cesium on a clean surface. In addition, it seems desirable to eliminate any oxide on the surface since this is simply another impediment to hot carriers on their way to the surface.

It is known that a clean surface on silicon can be obtained by heat treatment at 1600°K for one hour.[25] The result of such a treatment is to produce a clean surface. However, if this treatment is carried out in a conventional borosilicate vacuum system, boron from the glass which deposits on the crystal during sealing of the tube will diffuse into the crystal resulting in a surface with a p-type skin with a surface concentration of approximately 10^{19} boron atoms per cm^3.[26]

It is not possible to utilize this heat treatment on our thin diffused crystals. First, the high temperature heat treatment is carried out at a temperature much higher than the diffusing temperature and would result in the smearing out of our impurity profile resulting in a degraded junction. Second, the effect of the boron diffusion into the crystal would be to compensate for the phosphorus again ruining the junction. The high temperature treatment has been useful, however, to prepare surfaces for the study of cesium on clean silicon surfaces.

---

25. F. G. Allen, J. Eisinger, H. D. Hagstrum, J. T. Law, J. Appl. Phys. 30 1563(1959)

26. F. G. Allen, T. M. Buck, and J. T. Law, J. Appl. Phys. 31, 979(1960).

Attempts have been made to produce a clean or nearly clean surface by moderate heat treatment after careful etching and mounting in a tube. It should be noted that whenever a crystal is sealed into a tube, it is exposed to water vapor. This may result in additional oxide growth on the surface. During the previous contract, a silicon crystal was given the following treatment. First, it was etched with $HF\text{-}HNO_3$ followed by a rinse in HNO_3 then H_2O. This should have resulted in a film of 15-25 Å on the surface.[27] The crystal was then sealed into a tube and heat treated at 400-450°C for several hours. As a result, an n-type layer was produced on the crystal surface. It was shown, however, that upon deposition of cesium on this surface, a photothreshold of 2.2 ev was obtained compared to 1.5 ev on a clean surface. It was concluded that this treatment was not promising.

During this contract, an attempt was made to prepare a clean surface by a different etching treatment followed by moderate heat treatment. A silicon crystal containing a p-n junction perpendicular to the surface was etched with $HF\text{-}HNO_3$ followed by an etch in HF. This results in a crystal with an oxide layer on the surface which is initially 12 Å and grows as thick as 30 Å in 5×10^5 seconds.[28] The crystal after being sealed in a tube was heated at temperatures ranging from 250°C for 15 hours to 10 minutes at 895°C. The current-voltage characteristics of the junction as a function of heat treatment are shown in Fig. 32. It can be seen that the junction characteristics were degraded by heat treatment at temperatures as low as 250°C. The effect was especially drastic after heat treatment at 740°C. Measurements of photoconductivity as a function of the distance of a point light from the junction indicate that no appreciable change in the surface conductivity type occurred until the heat treatment at 895°C was carried out. After this treatment,

---

27. R. J. Archer, J. Phys. Chem. Solids 14, 104(1960).
28. R. J. Archer, J. Electrochem. Soc. 104, 619(1957).

the surface became p-type, apparently due to diffusion of boron from the surface into the crystal. It seems likely that the effect on the i-v characteristic at 740°C and above was the result of this diffusion into the crystal. In addition to this experiment, a thin diffused junction was heated to 775°C for 15 minutes. This resulted in degradation of the i-v characteristics and, after cesiation, these crystals showed small electron emission. The crystal must be heated at temperatures considerably below 740°C if a detrimental effect is not to occur where a junction intersects the surface. Since heating at 450°C and subsequent cesium deposition in the experiment described previously did not result in a low electron affinity surface, it was concluded that moderate heat treatment was not likely to result in a good surface for electron emission.

B. Argon Bombardment

An alternate method which has been used to prepare a clean surface in vacuum is by bombardment of the surface with argon ions.[29] The action of the ions is to sputter oxide atoms and ultimately silicon atoms off the surface. This technique appeared to have promise for reducing the thickness of the n-type layer as well as producing a clean surface. It was recognized that the bombardment produces damage in the crystal which must be annealed out when energetic ions are used. It was felt, however, that by using ions with energy near the threshold for sputtering, this damage would be limited to a thin layer near the surface and be inconsequential.

In the first experiment, a silicon crystal, which had been heat treated at 1600°K to introduce a known impurity concentration, was bombarded with 1000 ev argon ions. It was established by means of measurements of conductivity as a function of cumulative incident current that silicon could be removed

29. J. A. Dillon, and H. E. Farnsworth, J. Appl. Phys. 29, 1195(1958).

at a controlled rate. That a clean surface resulted was shown by comparing the behavior of the argon bombarded surface with that of a crystal cleaned by heating as a function of cesium coverage. The experimental tube used is shown in Fig. 33.

An attempt was made to clean a crystal containing the thin n-type diffused layer with thick diffused n-regions for contacts with 1000 ev ions. It was found that the conductance between the thick n-regions decreased from 3×10^{-3} mhos to 1.5×10^{-5} mhos as a result of bombardment which could only have removed 30 Å of material. In addition, the i-v characteristic reverted to what it was before the thin n-region was diffused as shown in Fig. 34. It was concluded that the damage in the crystal as a result of 1000 ev bombardment penetrated at least 1500 Å into the crystal.

Consequently, it was decided to attempt to clean a silicon crystal by bombardment with low energy ions in the range of energy of 50 ev. With ions of this energy, the sputtering yield can be no bigger than 0.1 atom per incident ion.[30] The surface conductivity as a function of incident number of ions appeared to be similar to the measured values of conductivity as a function of number of boiling water treatments. It appeared, however, that the junction was reached after bombardment with fewer atoms (by at least a factor of 10) than should be necessary to sputter the n-layer from the crystal. It is concluded then that even with 50 ev ions considerable damage has occurred.

As a result of this ion bombardment with 50 ev ions, hot electron emission currents of 4×10^{-6} amps/cm^2 were observed from the crystal. This was observed after bombardment with 1.46×10^{17} ions/cm^2. Further bombardment reduced the emission. The hot electron emission was increased by a factor of $\sim$40 by depositing cesium on the crystal surface. The peak emission, however, occurred

---

30. R. V. Stuart, and G. K. Wehner, J. Appl. Phys. 33, 2345(1962).

with only about 10^{14} cesium atoms/cm^2 on the surface.

These results have been repeated (without cesium) on two other crystals with similar results. These experiments have been performed with a tube of different geometry shown in Fig. 35. No improvement over the first results, however, were obtained.

There were several interesting aspects to these experiments which required further clarification. First, it appeared that 50 ev ions could produce damage deep in the crystal. Second, the observation that the peak in the emission as a function of cesium coverage occurred with only 10^{14} cesium atoms/cm^2 while the peak in photoemission usually occurred with 4 or $5x10^{14}$ cesium atoms on the surface was surprising.

During the last quarter, an experiment was performed which bears upon these two questions. The tube shown in Fig. 35 was used to perform another argon bombardment experiment. This tube included a phosphor screen which could be moved in front of the crystal so that the source of emission current could be imaged. The screen could be moved away for bombardment and for viewing the crystal. The crystal contained a circular diffused emitter, consisting of a ring of thick diffused n-type silicon with a thin n-layer diffused in the center of the ring. Light emission from one spot in the thin junction could be seen.

Initially, the discharge was excited in the tube with the crystal biased positive at a potential of 67 volts. Under these conditions, the crystal should not be bombarded and, in fact, an 8 ma electron current flowed to the crystal. However, as a result of this treatment, hot electron emission current of $6x10^{-9}$ amps was seen. No emission had been seen before the bombardment. Imaging the emission showed that it came from one discrete spot. Little

or no change was seen in the i-v characteristic nor in the light emission pattern as a result of this or any subsequent treatment with the discharge with the crystal biased positively. Further research showed that the emission was highest after a treatment of three minutes; a longer or shorter treatment resulted in less emission. The emission could always be restored by treating the crystal for three minutes. An attempt was made to observe photoemission from the sample with white light, but no emission was seen.

The crystal bias was reversed so that the crystal was bombarded with 67 ev ions. After a 1 minute bombardment with .05 ma, the emission decreased to 7×10^{-10} amp and the light emission was barely visible. After one more minute of bombardment, the emission was immeasurably low and no light emission could be seen. Further bombardment yielded no change in these results. After the first two minutes of bombardment, the i-v characteristic between the n- and p-regions became sharper.

As a result of this experiment and the preceding ones, several tentative conclusions can be drawn. (1) The electron emission seen as a result of exposing the crystal to a discharge appears to be a result not of bombardment but of the exposure of the crystal to a discharge. (2) Bombardment of the crystal with 67 ev ions appears to introduce damage into the crystal to depths of 1500 Å.

The most likely explanation for the effect of exposure to the discharge on emission is that a low work function material is liberated in the tube as the result of bombardment of the glass walls by ions and deposited on the surface. This hypothesis is consistent with the observation that a full cesium treatment is not required to produce peak emission. This possibility was first suggested to us by L. Holland. Subsequently, we have found several references which support this assumption. Bills and Evett[31] have reported the presence of sodium

31. D. G. Bills and A. A. Evett, J. Appl. Phys. 30, 567(1959).

and potassium ions in a vacuum tube when the glass walls were exposed to oxygen and nitrogen ions. They suggest, however, that this may not be the case when argon ions are used. Ruedl and Bradley[32] have observed sodium and potassium in their system as a result of bombardment of copper by inert gas ions. While they do not say where the ions come from, it seems reasonable that they are the result of ions striking the glass walls.

The extent of damage produced by the low energy bombardment is surprising. An estimate of the depth of penetration of a 1000 ev argon ion is $\sim$100 Å.[33] The damage may however, extend considerably further. Little work has been done on the depth of damage caused by ion bombardment. It was estimated that 30 Kev ions produced a damaged layer about 1 micron deep.[34] Measurements of electron diffraction of silver crystals bombarded with argon ions with energy as low as 12 ev produced disoriented crystallites on the surface.[35] The crystallites were estimated to be 100 Å deep. The mechanism by which the crystallites were formed was believed to be production of point defects at the surface followed by their diffusion into the crystal. Dislocations can also be formed as a result of bombardment. In these measurements, crystallites were observed. It is possible, however, that lesser damage penetrated considerably deeper.

The results of argon bombardment, if confirmed, indicate that it will not be possible to clean diffused hot electron emitters in vacuum by argon bombardment without annealing. Since annealing requires temperatures of 800°C or higher, it will not be possible to make use of this treatment.

---

32. E. Ruedl and R. C. Bradley, J. Phys. Chem. Solids 23, 885(1962).
33. J. Lindhard and M. Scharff, Phys. Rev. 124, 128(1961).
34. V. F. Gianola, J. Appl. Phys. 28, 868(1957).
35. G. J. Ogilvie, J. Phys. Chem. Solids 10,222(1959).

VI. Cesium on Silicon

A. Development of Method of Deposition

In order to obtain an optimum surface for electron emission, it seemed desirable to develop a method of depositing cesium on silicon in a controlled fashion. This method should also have the characteristic that cesium could be deposited on certain regions of a crystal without contaminating regions where p-n junctions intersect the surface since the junctions might be shorted out by the metal layer.

A method which satisfies these requirements is the molecular beam method. Cesium metal is distilled into a chamber containing a small hole. The cesium chamber temperature, T, is carefully controlled in order to maintain the cesium vapor pressure, p, at a constant value. By using the kinetic gas equations, the number of cesium atoms which pass through the small hole per second can be calculated. A molecular beam is formed by using cooled defining apertures. It can be shown that the number of molecules which strike a unit area parallel to the oven aperture plane at a distance r from the small hole is

$$N = \frac{5.83\times10^{-2} L\, ap}{\pi r^2 (MT)^{1/2}} \quad \text{molecules/cm}^2\text{/sec} \tag{1}$$

where a is the area of the oven opening, M is the molecular weight of the effusing molecules and L is Avagadro's number.[36] A tube with a typical cesium beam forming chamber is shown in Fig. 36.

While it is possible to calculate the rate of deposition from this formula, it was deemed desirable to check the calibration by other methods. Two methods were used. (1) The ion current from a hot tungsten filament was measured with a beam of cesium atoms incident. Since each atom incident on a hot filament evaporates as an ion, the current from the filament measures the beam flux.[2] The

---

36. I. Estermann, Rev. Mod. Phys. 18, 300(1946).

other method is to measure the photoemission as a function of cesium coverage on a tungsten filament. The photoemission goes through a maximum when approximately one monolayer covers the filament. The apparatus was considered reliable when the cesium atom flux measured by each method, and calculated from equation 1 agreed within 15 percent. Subsequently, it was assumed that the beam flux was given by equation 1.

B. Condensation of Cesium on Silicon

The rate of condensation of cesium on silicon depends not only on the incident rate of atoms but on the condensation coefficient and the rate of desorption from the surface. An experiment was performed to investigate these effects on silicon at room temperature.

The experimental tube is shown schematically in Fig. 37. A beam of cesium atoms was directed toward the surface of a crystal. A constant fraction of those atoms which were reflected or desorbed was detected by a hot tungsten filament ionization detector. In a preliminary experiment, a tungsten filament (W_1 in Fig. 37) was the target. Subsequently, this was replaced by an unoriented silicon crystal.

The measured current from the filament is shown in Fig. 38 for two experiments on a silicon crystal cleaned by high temperature heat treatment before each experiment. It is seen that, initially, few or no cesium atoms were reflected or desorbed from the surface. After about 6×10^{14} atoms/cm^2 were adsorbed on the surface, cesium atoms were desorbed or reflected from the surface. The number reflected or desorbed increased and gradually became constant with time. In our second experiment, after saturation was reached, the incident beam was suddenly cut off. Curve 3 of Fig. 38 shows that the desorption or reflection current decreased gradually. This shows that the cesium incident on the silicon

was all adsorbed not reflected, since a discontinuous drop would be expected if cesium in the incident beam was being reflected. The observation that the desorption current reached a limiting value is believed to have occurred when the rate of desorption was equal to the rate of adsorption. An alternate explanation, that the rate of desorption became independent of the coverage, has been discarded because of the low coverages possible with the cesium flux used.

A more quantitative description of the processes involved in this experiment can be derived in terms of τ, the mean adsorption time for an adsorbed atom on the surface. It is assumed that τ_1 is the mean sticking time for surface concentrations n given by $o < n < n_1$, τ_2 for $n_1 < n < n_2$, τ_3 for $n_2 < n < n_3$, and so on. It is also assumed that desorption can occur from each of these groups with their mean desorption time, but the lower groups are immediately filled from the higher groups. It will be seen that $n_1, n_2 \ldots$ may correspond to distinct monolayers.

Using this model, it can be shown that the ion current from the surface ionization detector is given by

$$I = I_\infty (1-e^{-t/\tau_1}) \qquad t < t_1$$

$$I = I_\infty \left[1 - \left(1 - \frac{n_1}{N\tau_1}\right) e^{-t_1 - t/\tau_2}\right] \qquad t_1 < t < t_2$$

$$I = I_\infty \left[1 - \left(1 + \frac{n_1}{N\tau_2} - \frac{n_1}{N\tau_1} - \frac{n_2}{N\tau_2}\right) e^{-t_2 - t/\tau_3}\right] \qquad t_2 < t < t_3$$

and so on

where I_∞, the limiting value of I, is given by eAN

where N is the incident flux on the silicon surface

e is the electronic charge

A is a geometric factor

This theory indicates that a plot of $\log(1-I/I_\infty)$ against time should

consist of a series of straight lines with slope τ_1, τ_2.... intersecting at t_1, t_2.... The data for cesium on tungsten and silicon are shown in Figs. 39 and 40. From the slopes, values of τ_i and n_i can be obtained, and are shown in Table I. Note that n_1 and n_2 correspond approximately to complete monolayers of cesium on silicon. It is interesting to observe that the second group of atoms on tungsten are less tightly bound than the third group.

Table I

	Cs-W		Cs-Si	
i	$\tau_{i(sec)}$	n_i(atoms/cm^2)	τ_i(sec)	n_i(atoms/cm^2)
1	$>10^5$	5.15×10^{14}	$>10^5$	6×10^{14}
2	43.3	5.6×10^{14}	5684	1.25×10^{15}
3	143	5.8×10^{14}	279	1.5×10^{15}*

*n_3 represents the limiting coverage rather than a completed third group.

These results show that all incident atoms up to coverages of one monolayer are tightly bound. At coverages below n_i, the number of adsorbed atoms is equal to the number of incident atoms. Since for peak electron emission, coverages of one monolayer are required, these results indicate that cesium on clean silicon at room temperature will be a stable system.

C. Effect of Cesium on Silicon

The effects of cesium on silicon which are of greatest interest with respect to hot electron emission are those on electron affinity and surface conductance. To study the effect on the electron affinity it has been found useful to measure photoemission, as a function of cesium coverage and the spectral response of photoemission.

An experiment was performed in which cesium was deposited on a clean silicon surface produced by cleavage in vacuum. The experimental tube was saturated with cesium vapor, then the crystal was cleaved in vacuum and the white light photoemission as a function of time was measured. Fig. 41 shows that the emission went through a maximum, then decreased. A spectral response curve showed that a photothreshold of 1.5 ev resulted.

When cesium was deposited on silicon with no cleaning, using the molecular beam technique, the photoemission did not go through a peak but rose to a maximum value and remained constant as the surface concentration was increased. These results are shown in Fig. 42. The i-v characteristic of this crystal which contained a p-n junction perpendicular to the surface, showed a drastic change at a coverage of 1×10^{14} atoms/cm^2 becoming more conductive, but showed no further change with subsequent deposition. In a second experiment on an uncleaned surface the cesium behaved similarly with respect to photoemission but showed no effect on the i-v characteristic. Previous measurements have shown that cesium does not produce a low electron affinity surface on unclean silicon.

An experiment was performed in which cesium was deposited on the surface of a heat treated crystal and both photoemission and electrical conductivity were measured as a function of deposition time. The experimental tube used for this experiment is shown in Fig. 43. Contacts were made to the crystal as shown in the inset in Fig. 43. Current contacts were clamped to the crystals. The voltage probes were movable and could be placed in contact with the crystal by tilting the tube. A tungsten probe was in contact with the back surface of the crystal. In order to make a good contact with the voltage probes heavy deposits

of cesium were placed on the crystal on the area to be contacted by the voltage probes prior to deposition of cesium between the probes. The crystal used in this experiment was heat treated at 1600°K to clean it before the deposition of cesium.

The measurements of photoemission and conductivity vs cesium deposited across the crystal are shown in Fig. 44. The photoemission went through a peak as a function of cesium coverages as had been previously observed for a clean surface. The resistance which was measured periodically as a function of deposition decreased rapidly initially and then changed slope and subsequently changed only slightly. The peak in the photoemission and change in the slope of the resistance occurred at the same coverage.

These results are consistent with the idea that at the coverage at which the peak occurred in photoemission a transition occurred in the type of adsorption from chemisorption to physical adsorption. The decrease in resistance occurs because electrons are donated to the silicon, which compensate the 10^{19} holes/cm^3 and then go into the conduction band reducing the crystal resistance. This is possible since the inversion layer formed by the cesium is expected to be $\sim$100Å thick. If then 5×10^{14} electrons are contributed to the silicon, the inversion layer contains a density of 5×10^{20} electrons/cm^3. If this model is correct, it was expected that the resistance of the crystal should initially increase due to the compensation of some of the holes by electrons. Attempts to observe this were not successful because of experimental difficulties.

These experiments show that the electron affinity and electrical resistance of silicon can be reduced by addition of cesium to clean silicon. These effects are expected to be useful in producing a hot electron emitter.

D. Band Structure of Silicon from Photoemission Measurements

Analysis of our measurement of spectral response of photoemission and velocity distribution of emitted electrons from cesium treated silicon showed that these measurements would yield considerable information about the band structure of silicon.[37] The velocity distribution measurements were undertaken to attempt to gain information on the energy loss mechanisms of hot electrons in solids. These measurements, initially made under this contract have been refined and extended under a contract (ERDL Contract No. DA44-009-ENG-4913) more specifically related to photoemission. Since these results are about to be published, they will not be described here. The value of the measurements and the methods of analysis will be indicated below.

The value of photoemission studies are due to two of the characteristics of photoemission. First, only those electrons excited into states which lie above the vacuum level can escape from the semiconductor. As a result, in the spectral distribution of the photoemission quantum yield, only those absorption peaks associated with transitions to conduction band states which lie above the vacuum level will produce peaks in the spectral distribution data. Transitions in which the final state lies below the vacuum level may produce minima in the photoemission yield curves corresponding to maxima in the absorption curves.

The second useful characteristic of photoemission for investigating band structure lies in the possibility of measuring the energy distribution of the emitted electrons. Quantitative information about the shape of the energy band may be obtained from the structure in the energy distribution of the emitted photoelectrons.

The principal transitions in the absorption spectra of silicon as determined from reflectivity measurements have been identified by Ehrenreich, Philipp and Phillips.[38] The principal transitions in the absorption spectra are shown

37. W. E. Spicer, R. E. Simon, J. Phys. Chem. Solids (in press).
38. H. Ehrenreich, H. R. Philipp, J. C. Phillips, Phys. Rev. Let. 8, 59(1962).

in Table II. The L_3' to L_1 transition is not seen in reflectivity of silicon but has been predicted by Tauc and Abraham from their studies of germanium silicon alloys. From Table II, it is expected that the $\Gamma_{25'}$ to Γ_{15} and L_3' to L_3 transitions would give maxima in the photoemission response at 3.5 ev and 5.3 ev but the X_4 to X_1 and perhaps the L_3' to L_1 transitions would give minima since in these transitions, the final state of the electron is lower in energy than the vacuum level. In the velocity distribution it is expected that peaks in energy would be seen at 0.9 ev and 1.5 ev.

Table II

Optical Transition	Photon Energy at Absorption Peak	Energy of final state with respect to lowest conduction band minimum	Predicted energy of emitted electrons (electron affinity =1.5 ev)
$\Gamma_{25'}$ to Γ_{15}	3.5 ev	2.4 ev	0.9 ev
L_3' to L_1	3.7 ev	1.2 ev	------
X_4 to X_1	4.5 ev	0.2 ev	------
L_3' to L_3	5.3 ev	3.00 ev	1.5 ev

The predicted behavior has been seen verifying the band structure of silicon. In addition, with refined measurements, the L_3' to L_1 has been observed* and the energies of the final states of the transitions have been determined. This could not be done with absorption data which yields information only on the energy difference between states.

---

* There is some question as to the assignment of this transition-- see ref. 3.

CONCLUSIONS AND RECOMMENDATIONS

The preparation of a p-n junction hot electron emitter with optimum emission properties requires the solution of many diverse problems. Our approach has been to attack these problems simultaneously with the aim of bringing the results together to form emitters with optimum properties, these emitters to be the subject of intensive studies. While almost all the problems associated with the preparation of these emitters have been solved, it has not been possible to bring together these solutions in a single emitter. The outstanding problem remaining to be solved is the preparation of a clean or nearly clean surface prior to cesium treatment on a crystal containing a thin diffused junction.

The problems which have been attacked have been presented above. The results of these studies are outlined below:

1. A survey of the literature has shown that the mechanisms involved in hot electron processes in semiconductors are complex and no adequate treatment from which the properties of a hot electron emitter can be predicted is now available.
2. Based upon the present knowledge of p-n junctions in semiconductors, the requirements for a hot electron emitter have been specified.
3. Theoretical examination of the electron-electron interaction in semiconductors and metals shows that the energy loss by this mechanism is smaller than by interaction with optical phonons for concentrations of less than 10^{18} electrons/cm^3. In metals, an expression for the mean free path of hot electrons has been derived.
4. The closed box method has been applied to the diffusion of phosphorus in thin regions in silicon.
5. The diffusion constant for diffusion of phosphorus in silicon at relatively low temperatures, 828°C to 1200°C, has been measured.

6. A method of making contact to thin n-layers by means of deep diffused layers has been developed.
7. Measurements of the thickness of the thin diffused layers have been made by stripping off thin sections by the boiling water-HF technique.
8. Possible mechanisms responsible for the shape of the i-v characteristic of the thin junctions have been considered but no explanation for their softness has been found.
9. Measurements of the voltage profile across the surface of the thin n-layer with the junction reverse biased indicate that the bulk of the current is flowing uniformly through the junction.
10. Emission measurements have been made on crystals with a surface treatment such that the electron affinity was 2.5 ev. Under these conditions, appreciable emission cannot be expected.
11. A correlation between light emission and electron emission from microplasmas has been noted.
12. Crystals containing a n-p-n configuration have been constructed. Uniform light emission through the thin diffused region has been observed, but these have not yet been tested for electron emission.
13. Measurements on crystals etched and subjected to low temperature ($< 800^{\circ}C$) heat treatment indicate that a low electron affinity surface cannot be obtained by this treatment followed by cesium deposition.
14. Heat treatment above $740^{\circ}C$ detrimentally affects the junction characteristics.
15. Argon bombardment appears to produce a clean surface.

16. When used without annealing, argon bombardment appears to result in damage comparable in depth to the thin junction depth even when 50 ev ions are used.
17. Exposure of a crystal to a glow discharge appears to result in the deposition of a low work function material on the surface.
18. A molecular beam method has been developed for accurately depositing cesium on emitter junctions.
19. Deposition of cesium on clean silicon produces a surface with an electron affinity of 1.5 ev.
20. The mean time for adsorption of cesium on silicon at room temperature has been found to be $> 10^5$ sec for the first monolayer. Times for the second and third layer as well as for cesium on tungsten have been obtained.
21. Resistance and photoemission measurements on silicon as a function of cesium coverage indicate that approximately one monolayer of cesium is chemically adsorbed on silicon.
22. Information on the band structure of silicon has been obtained from measurements of the spectral response of photoemission and velocity distribution of photoemitted electrons.
23. Attempts to produce a rectifying cesium, clean silicon metal-semiconductor contact have not been successful.

It is recommended that this work be continued with major emphasis on developing a method of producing a clean surface on thin diffused emitters. This will allow a device with optimum properties to be constructed and tested. In addition, it is felt that further work should be directed toward improving the characteristics of the p-n junction and the injecting contact. In addition,

it is felt that the metal-semiconductor contact has sufficient potential so that further work should be done on it.

It is believed that progress has been made on the basic steps which must be taken to properly evaluate the possibilities of hot electron emission. Further effort should yield proportionately greater results since the remaining problems have been well defined by the work performed under this contract.

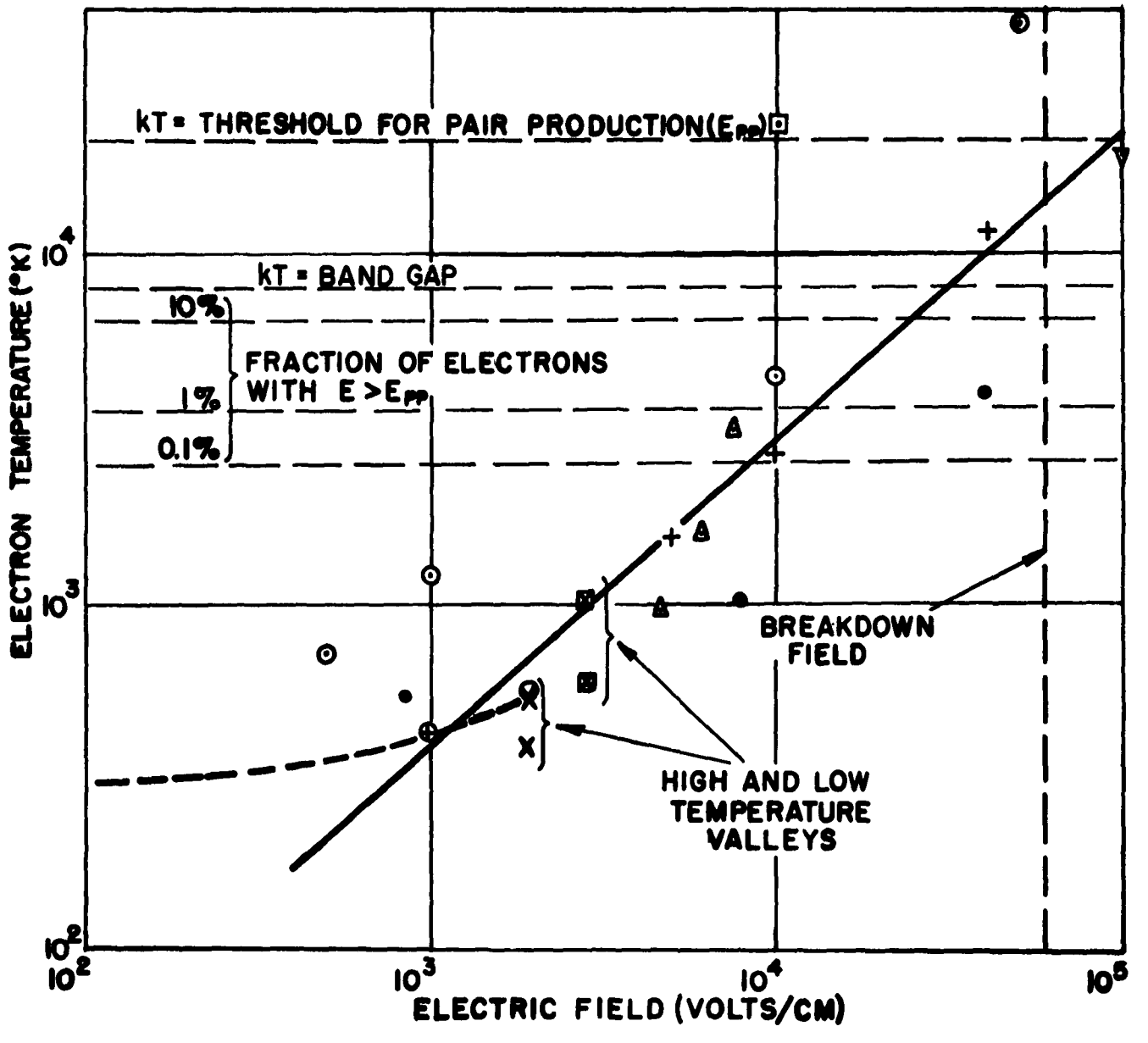
kT = THRESHOLD FOR PAIR PRODUCTION(E_{pp})
kT = BAND GAP
10%
1%
0.1%
FRACTION OF ELECTRONS WITH E > E_{pp}
BREAKDOWN FIELD
HIGH AND LOW TEMPERATURE VALLEYS
ELECTRON TEMPERATURE (°K)
10^4
10^3
10^2
10^2
10^3
10^4
10^5
ELECTRIC FIELD (VOLTS/CM)
o SHOCKLEY
⊡ YAMASHITA
⊙ ADAWI
▲ YAMASHITA & INOUE
--ERLBACH AND GUNN
▽ CHUENKOV
X PAIGE
+ STRATTON
■ SHIBUYA & SASAKI

FIG. 1

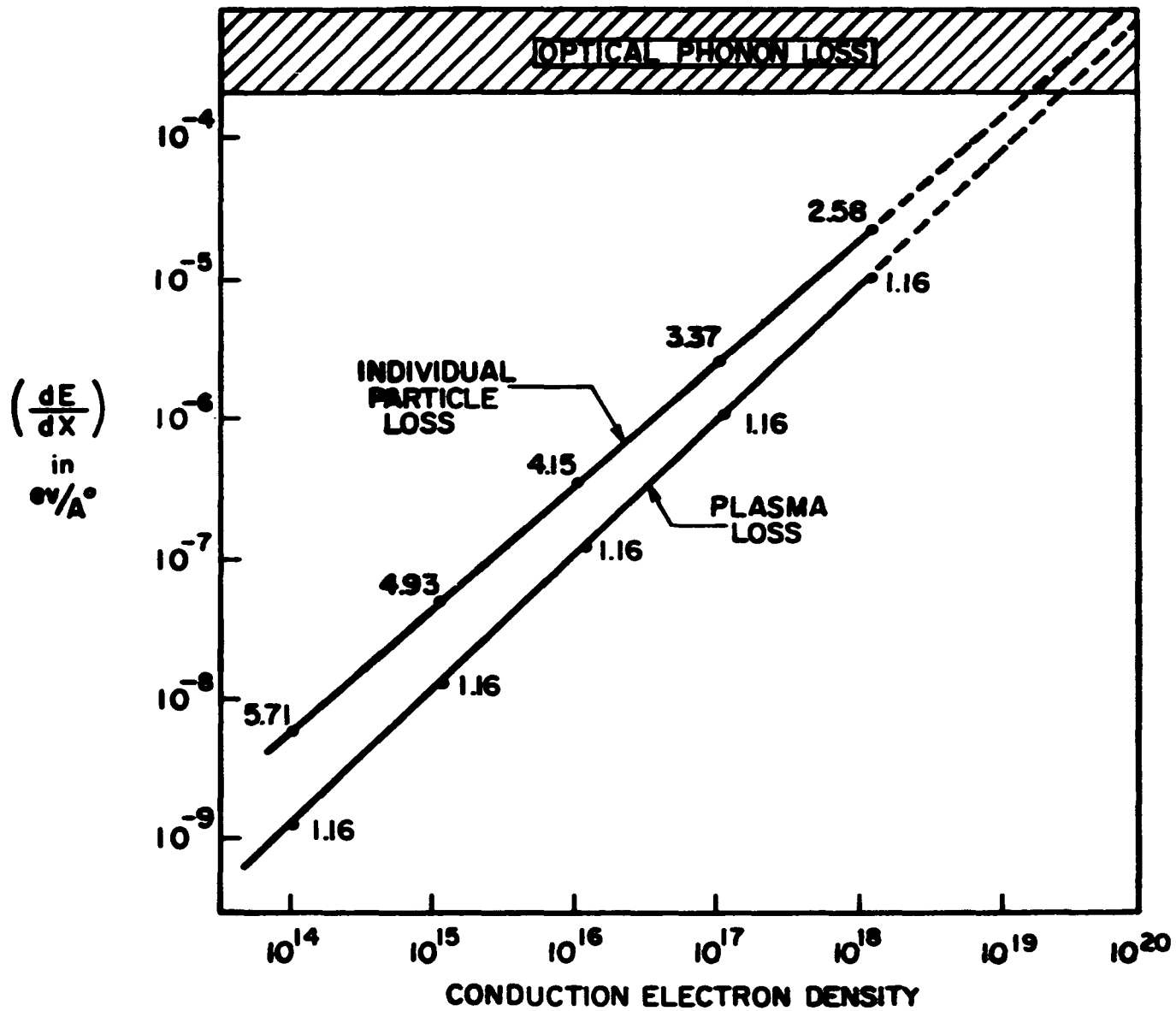
[OPTICAL PHONON LOSS]
10^{-4}
10^{-5}
10^{-6}
10^{-7}
10^{-8}
10^{-9}
$\left(\frac{dE}{dX}\right)$ in ev/A°
2.58
1.16
3.37
INDIVIDUAL PARTICLE LOSS
1.16
4.15
PLASMA LOSS
1.16
4.93
1.16
5.71
1.16
10^{14}
10^{15}
10^{16}
10^{17}
10^{18}
10^{19}
10^{20}
CONDUCTION ELECTRON DENSITY

FIG. 2

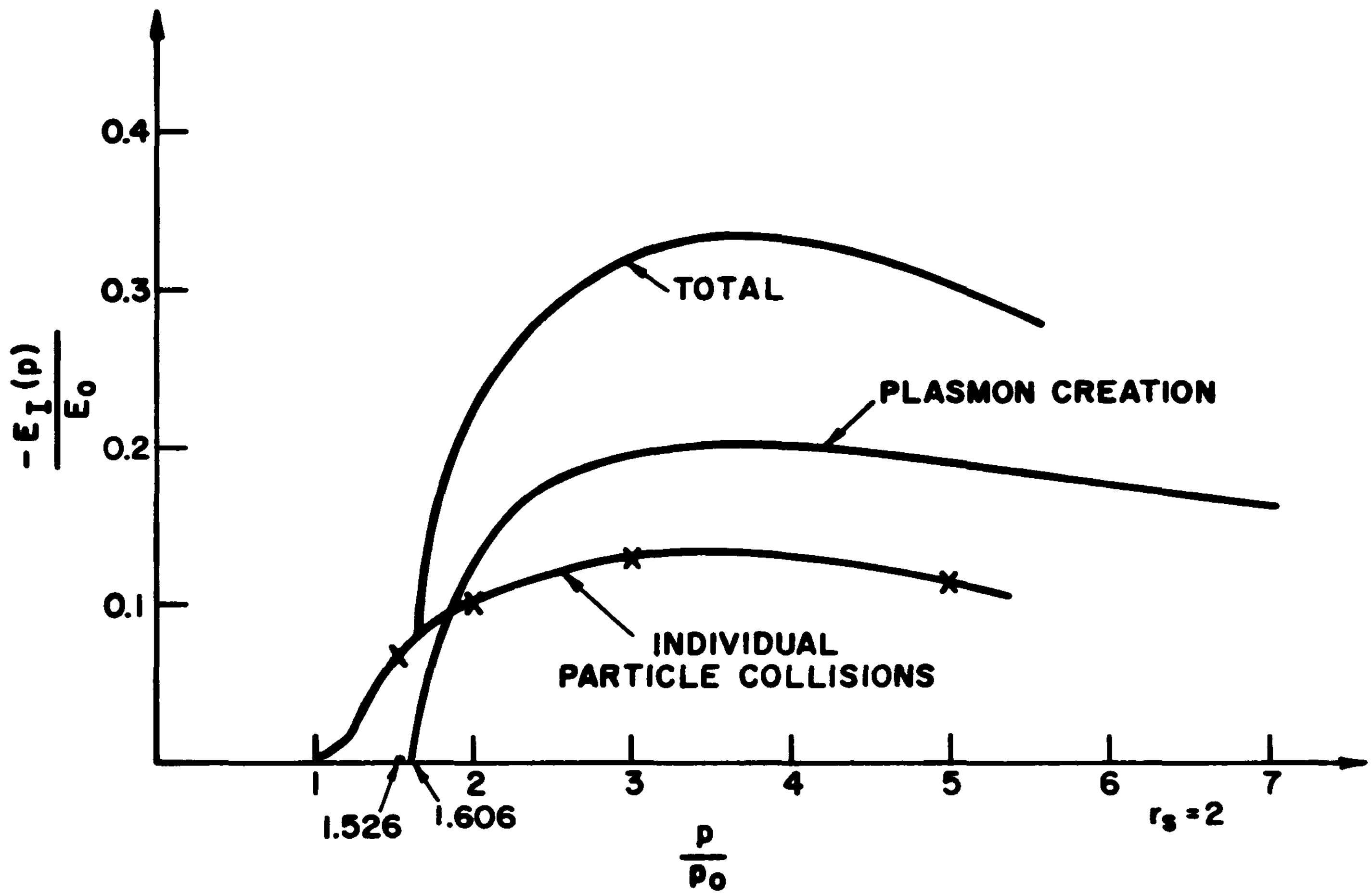

TOTAL
PLASMON CREATION
INDIVIDUAL
PARTICLE COLLISIONS
$-\frac{E_I(p)}{E_0}$
0.1
0.2
0.3
0.4
1
2
3
4
5
6
7
1.526
1.606
$r_s = 2$
$\frac{p}{p_0}$

FIG. 3

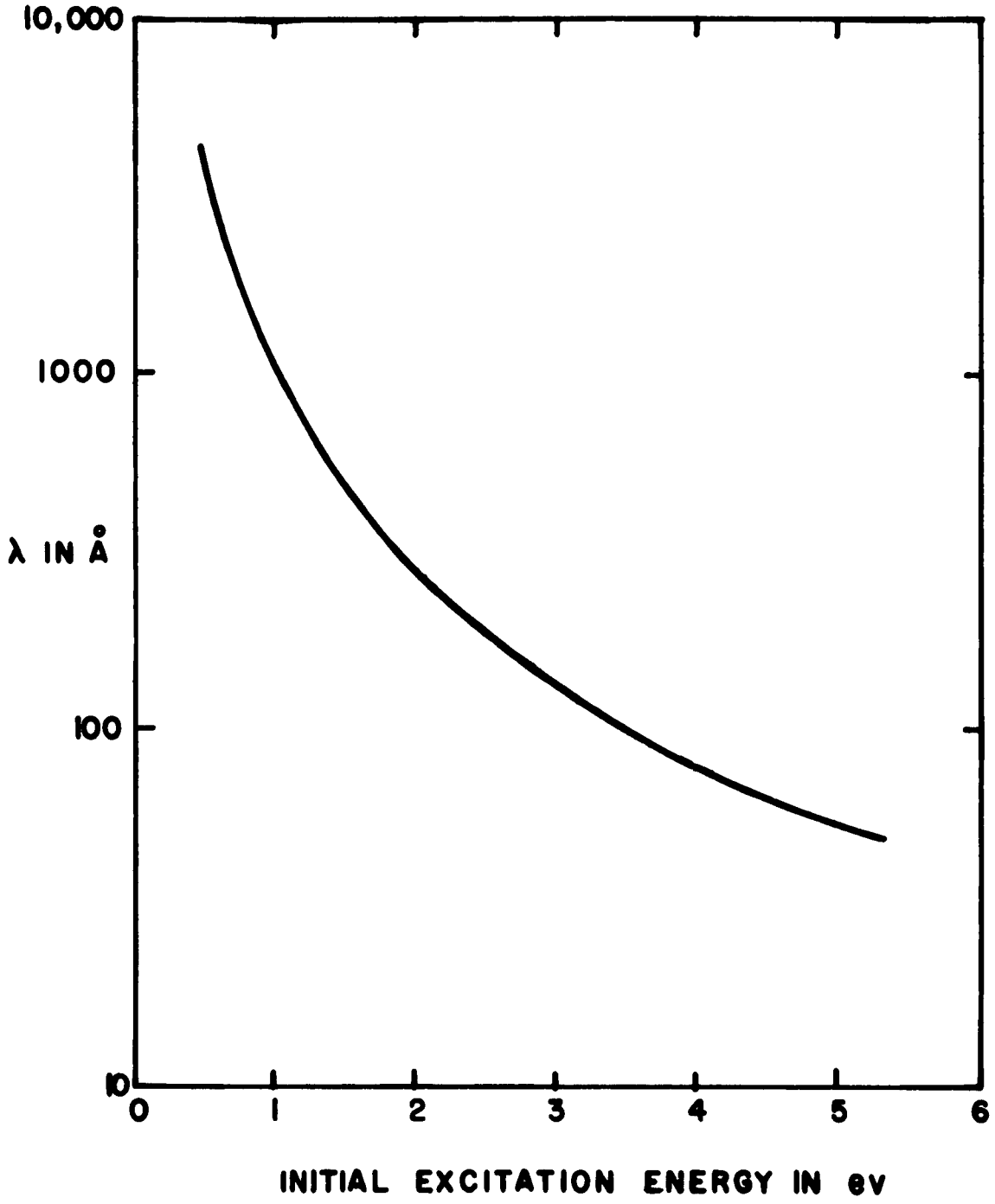
10,000
1000
100
10
λ IN Å
0
1
2
3
4
5
6
INITIAL EXCITATION ENERGY IN eV

FIG. 4

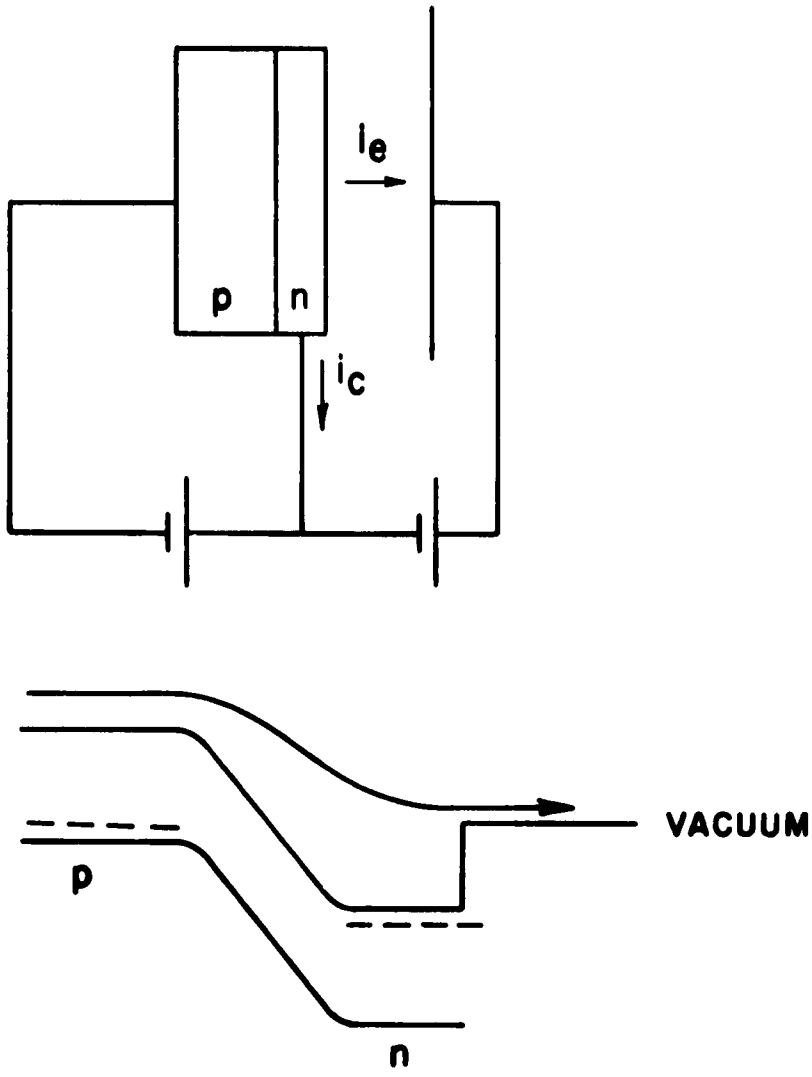

FIG. 5

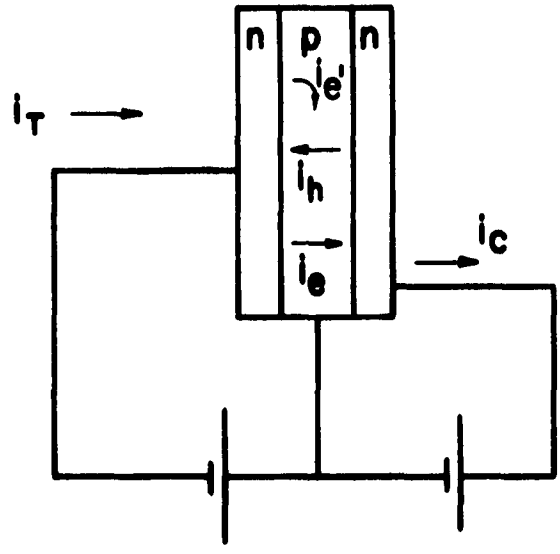
n
p
n
i_T
$i_{e'}$
i_h
i_e
i_C

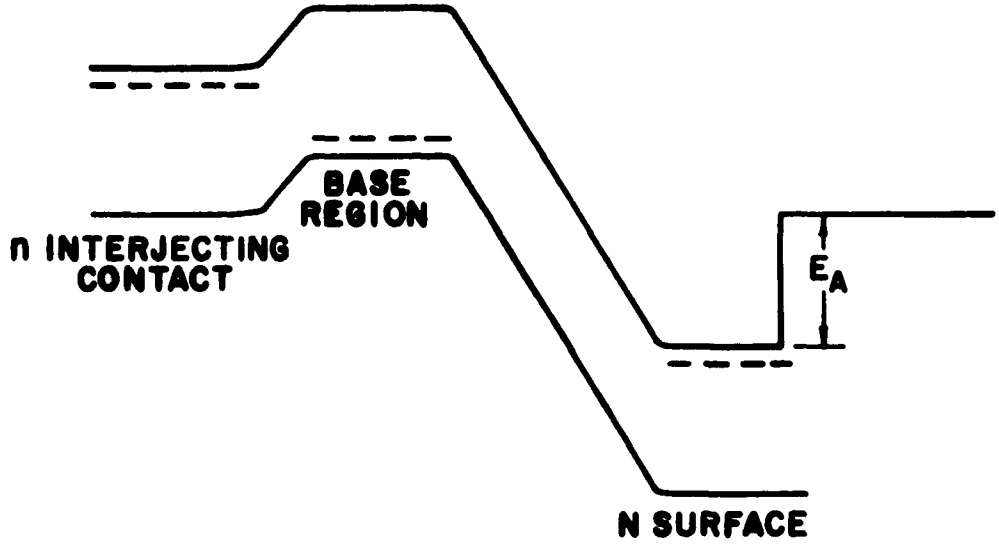
BASE
REGION
n INTERJECTING
CONTACT
E_A
N SURFACE

FIG. 6

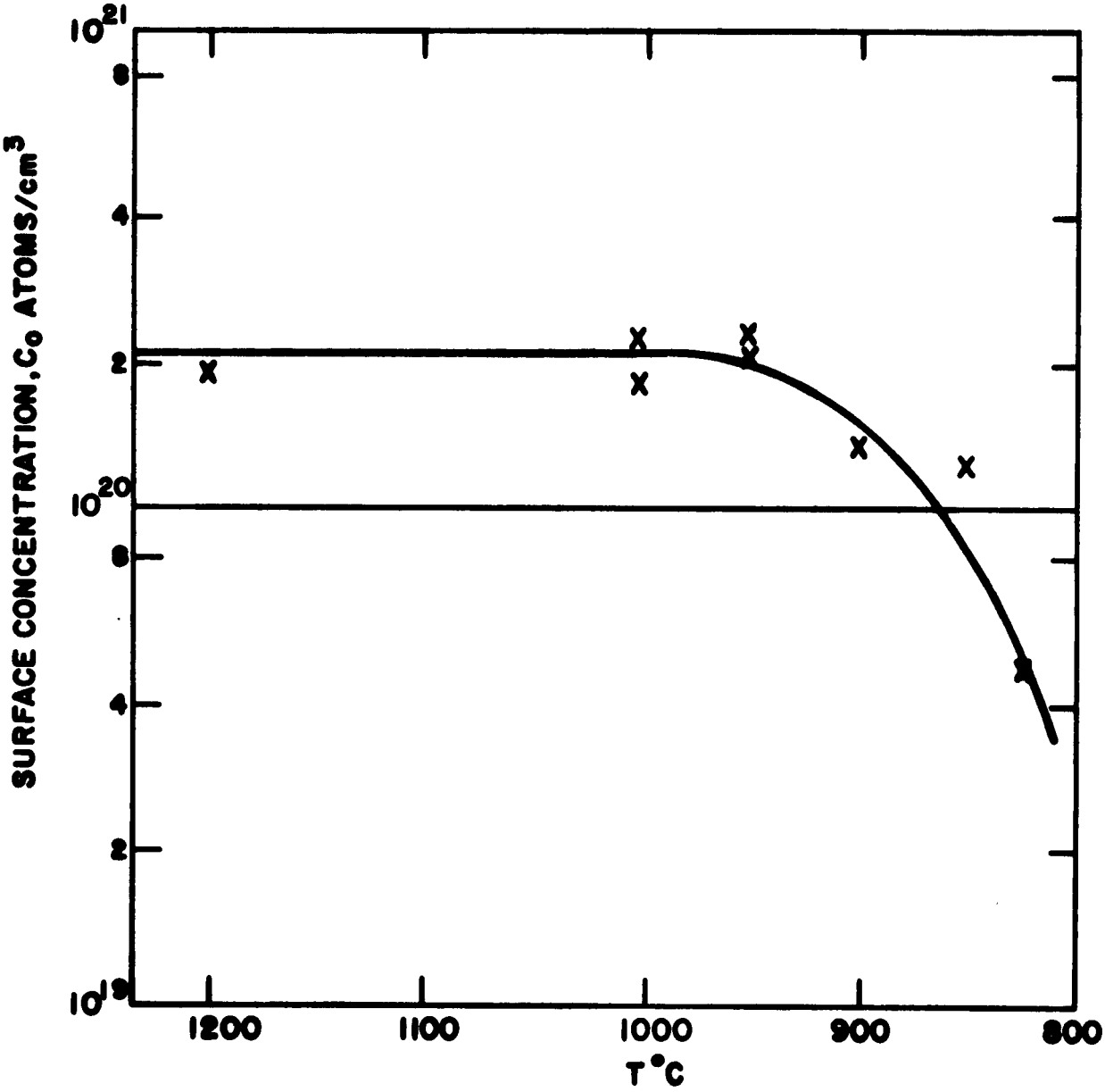
SURFACE CONCENTRATION, C_o ATOMS/cm^3
10^{21}
8
4
2
10^{20}
8
4
2
10^{19}
1200
1100
1000
900
800
T°C

FIG. 7

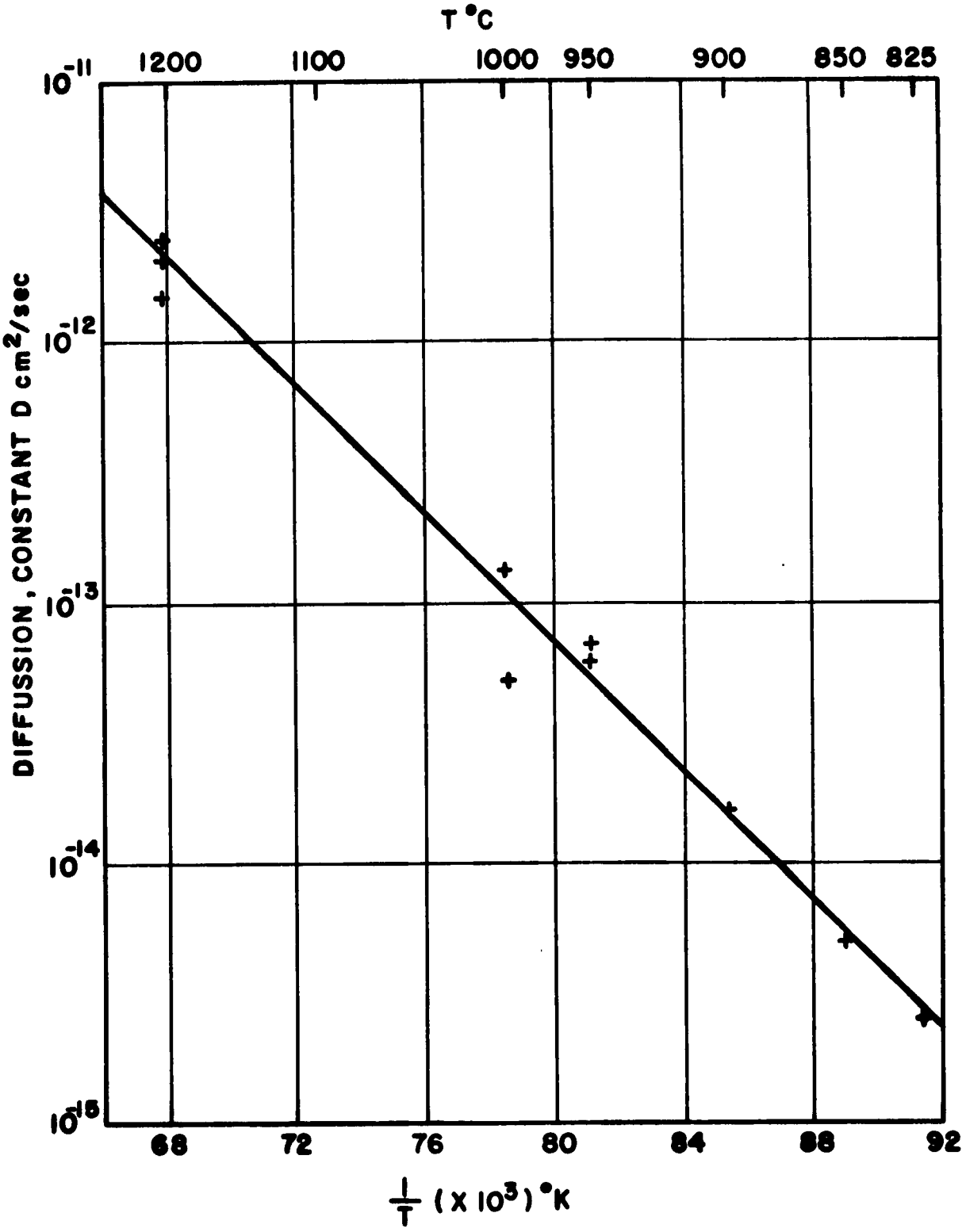
T °C
1200
1100
1000
950
900
850
825
10^{-11}
10^{-12}
10^{-13}
10^{-14}
10^{-15}
DIFFUSSION, CONSTANT D cm²/sec
68
72
76
80
84
88
92
$\frac{1}{T}$ (X 10^3) °K

FIG. 8

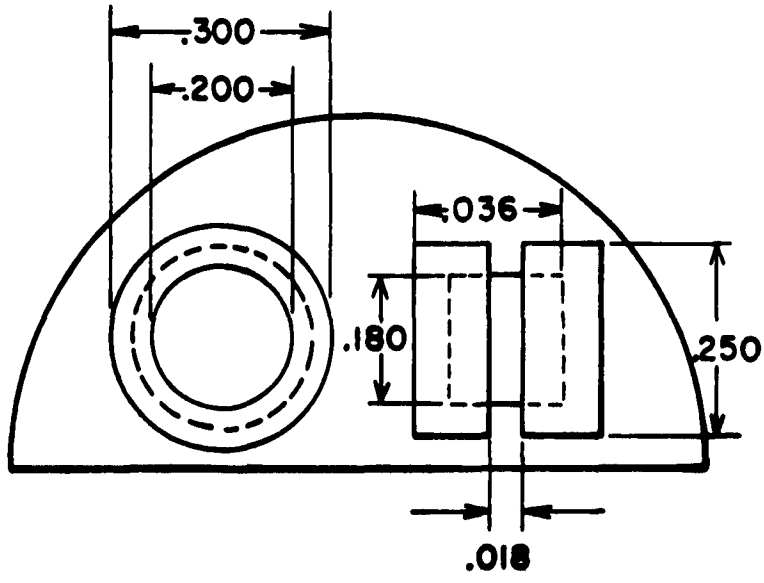

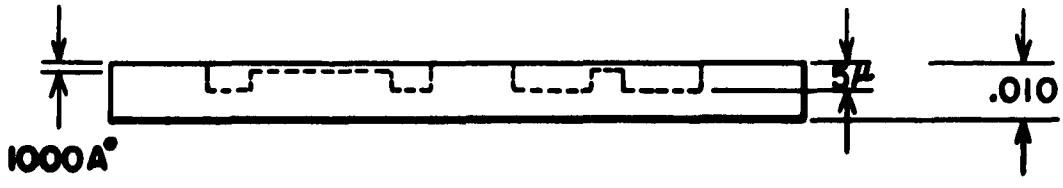

FIG. 9

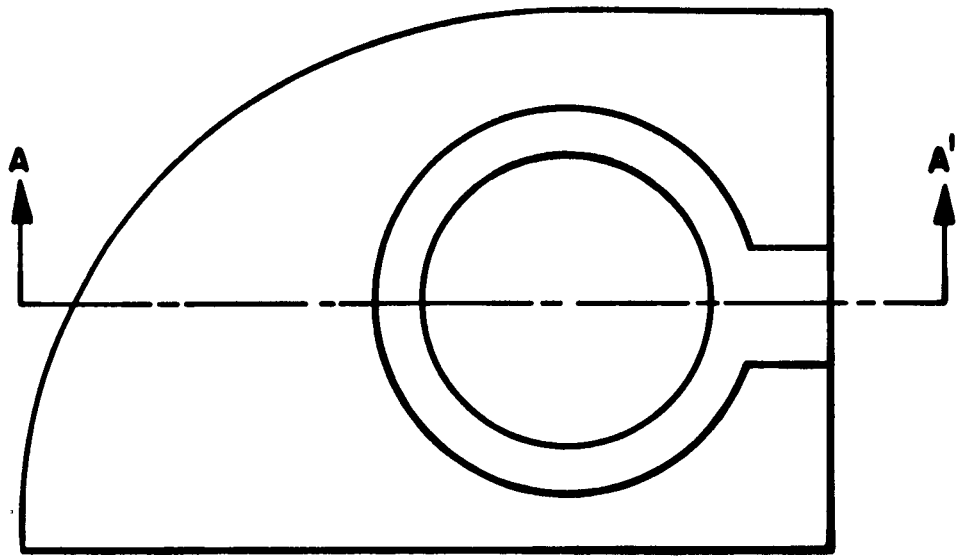

N TYPE SILICAN

P TYPE SILICAN

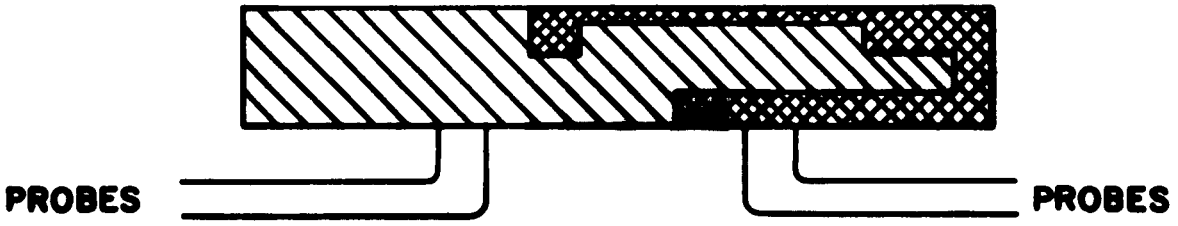

SECTION AA'

FIG. 10

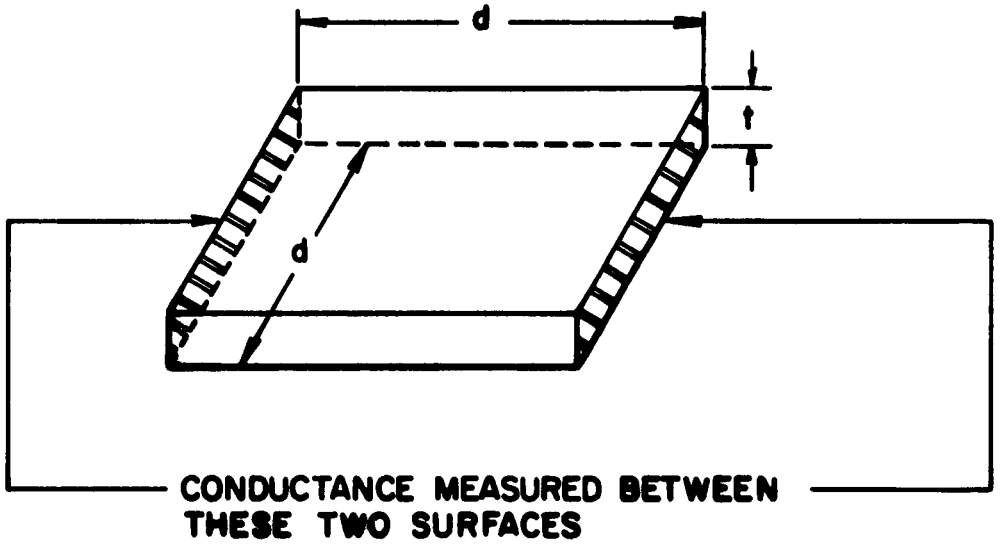

FIG. II (a)

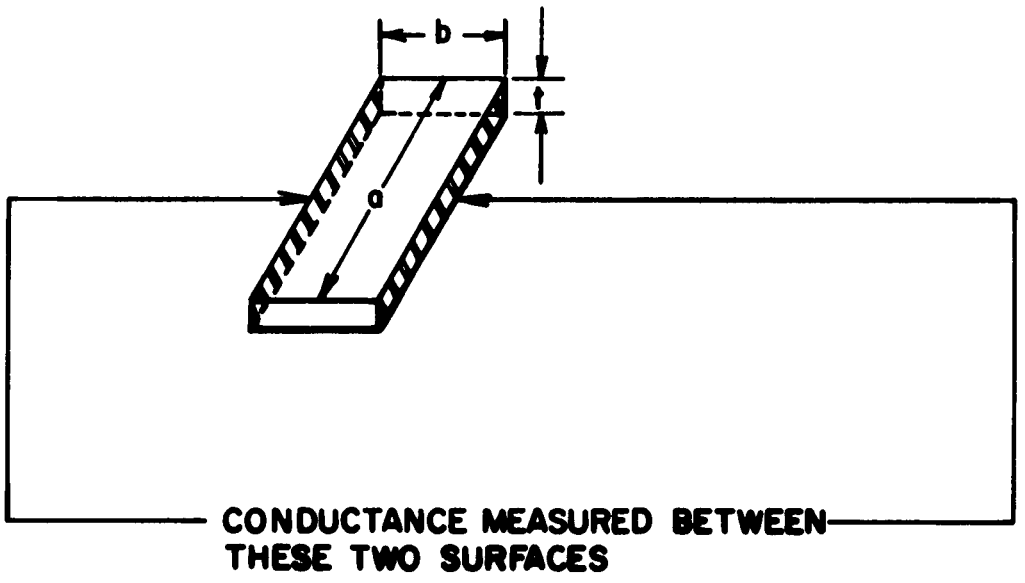

FIG. II (b)

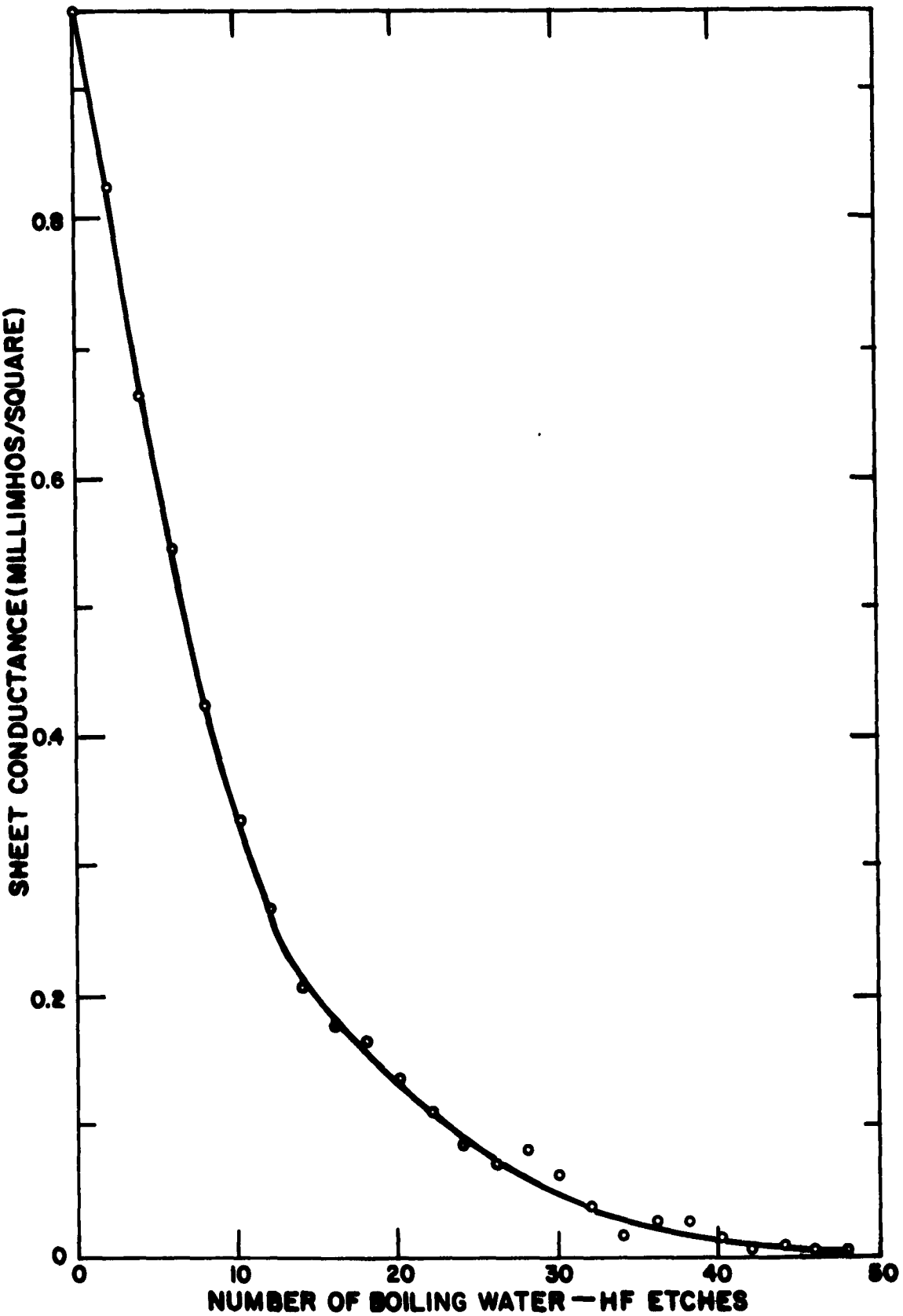
SHEET CONDUCTANCE (MILLIMHOS/SQUARE)
0.8
0.6
0.4
0.2
0
0
10
20
30
40
50
NUMBER OF BOILING WATER—HF ETCHES

FIG. 12

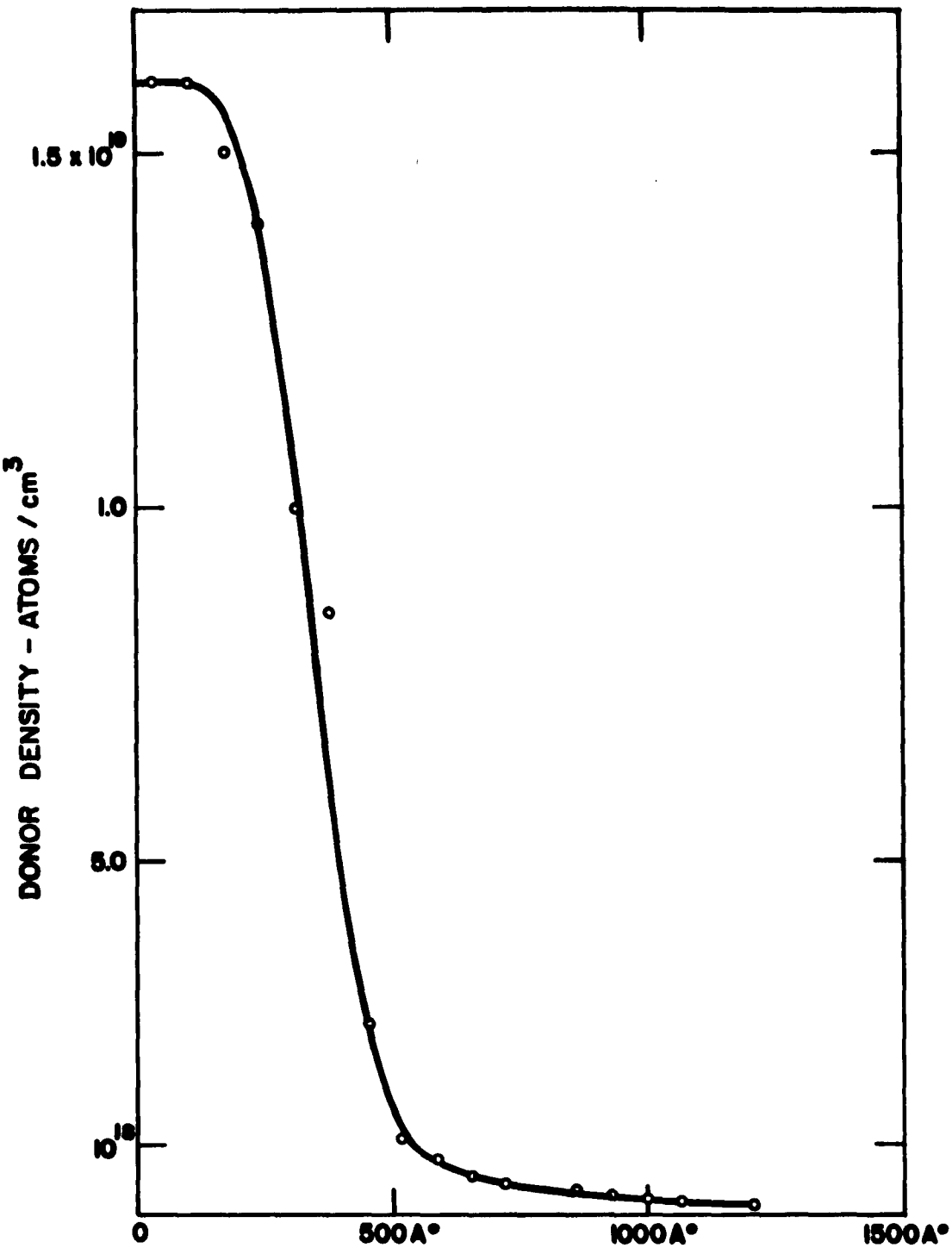
DONOR DENSITY - ATOMS / cm3
1.5 x 10^18
1.0
5.0
10^18
0
500A°
1000A°
1500A°

FIG. 13

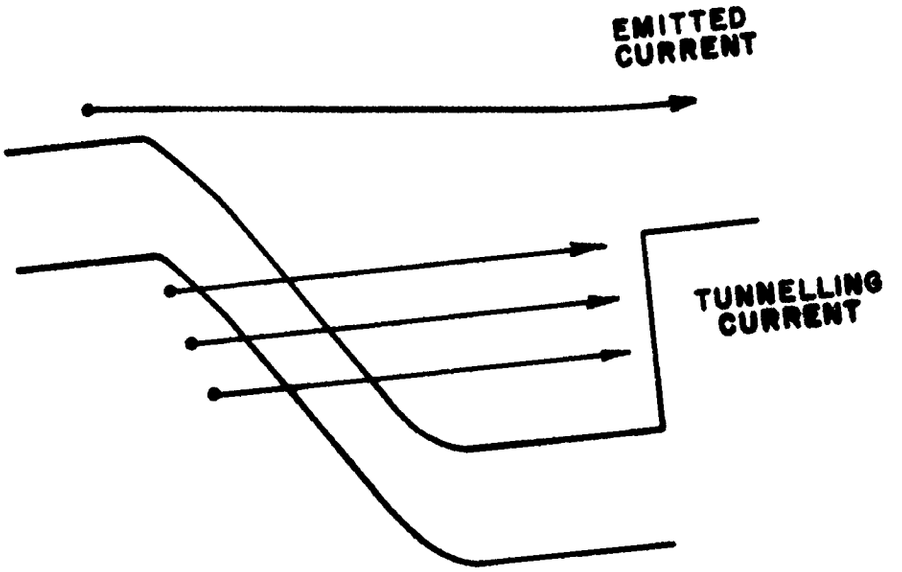

FIG. 14 (a)

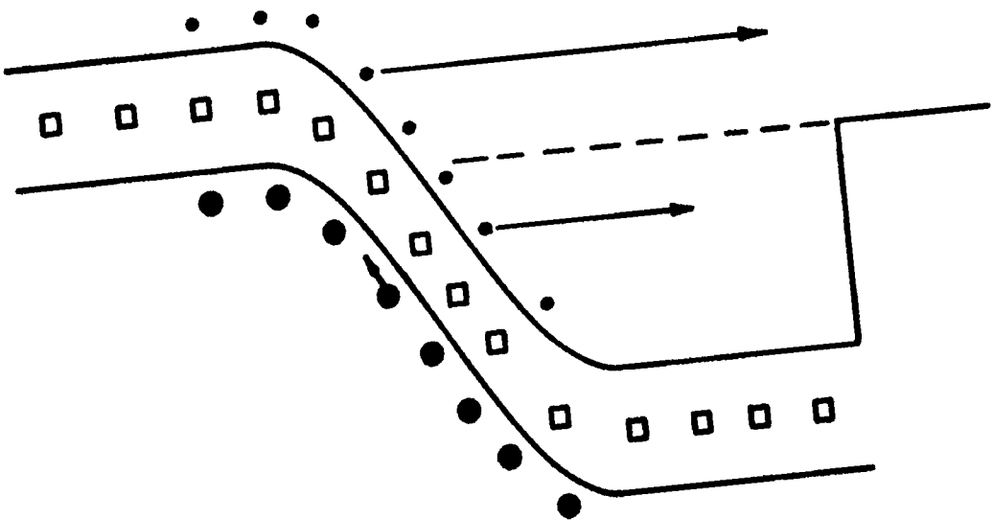

FIG. 14 (b)

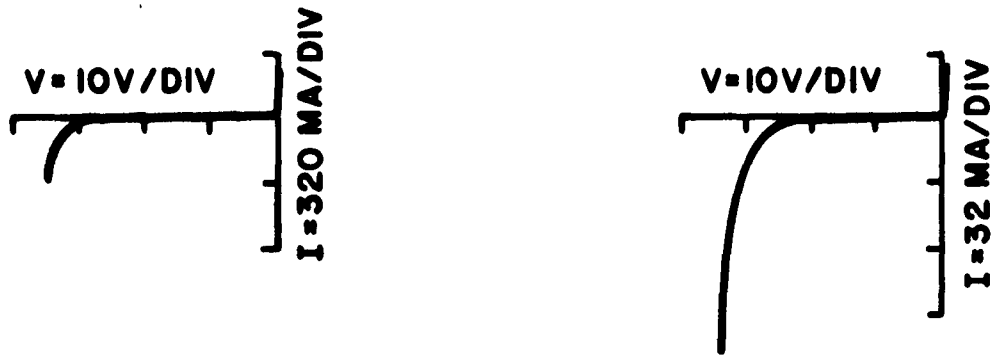

THICK JUNCTION ONLY

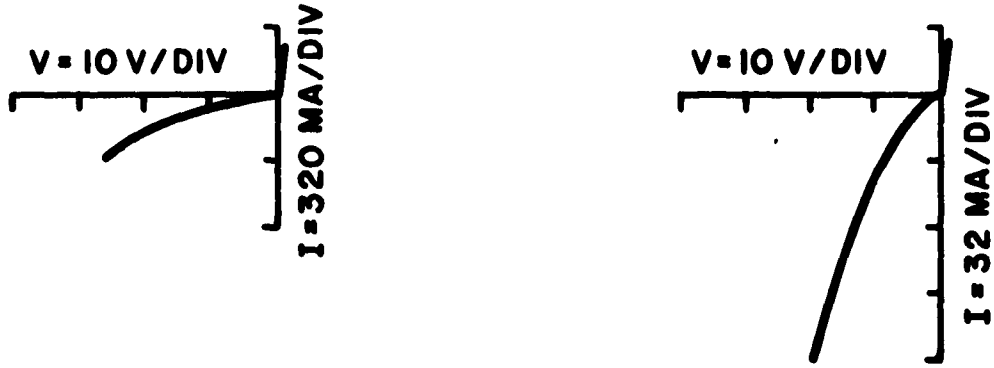

THICK AND THIN JUNCTION

FIG. 15

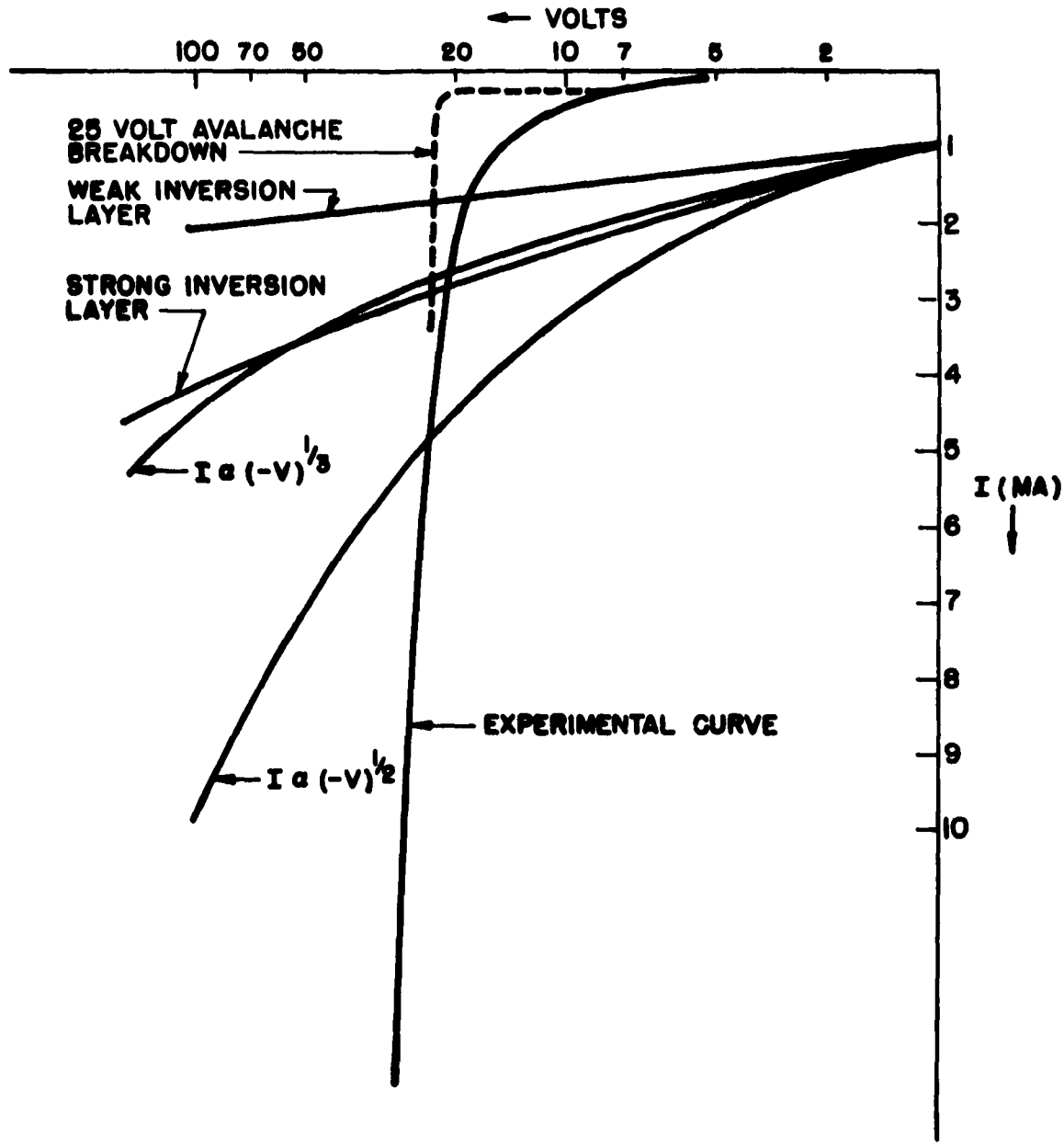
VOLTS
100 70 50 20 10 7 5 2
25 VOLT AVALANCHE BREAKDOWN
WEAK INVERSION LAYER
STRONG INVERSION LAYER
I α (-V)^1/3
I α (-V)^1/2
EXPERIMENTAL CURVE
I (MA)
1 2 3 4 5 6 7 8 9 10

FIG. 16

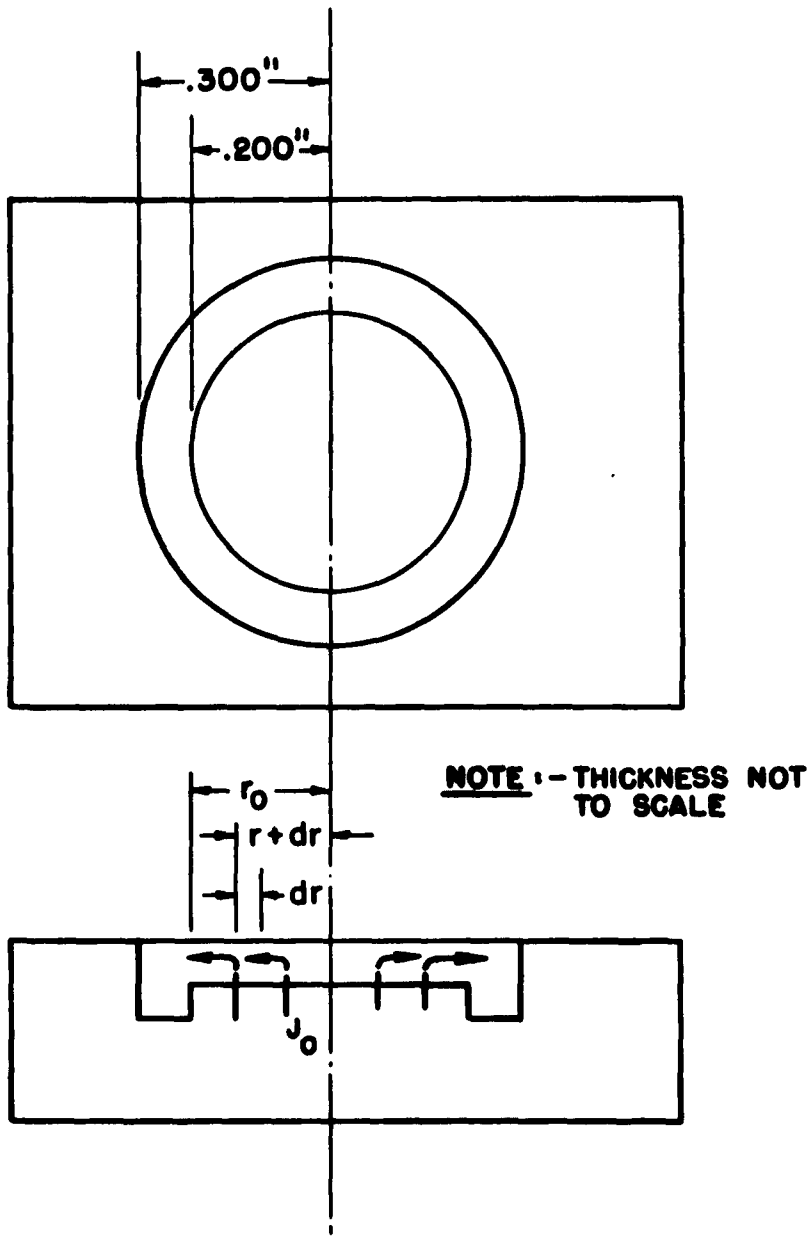

FIG. 17

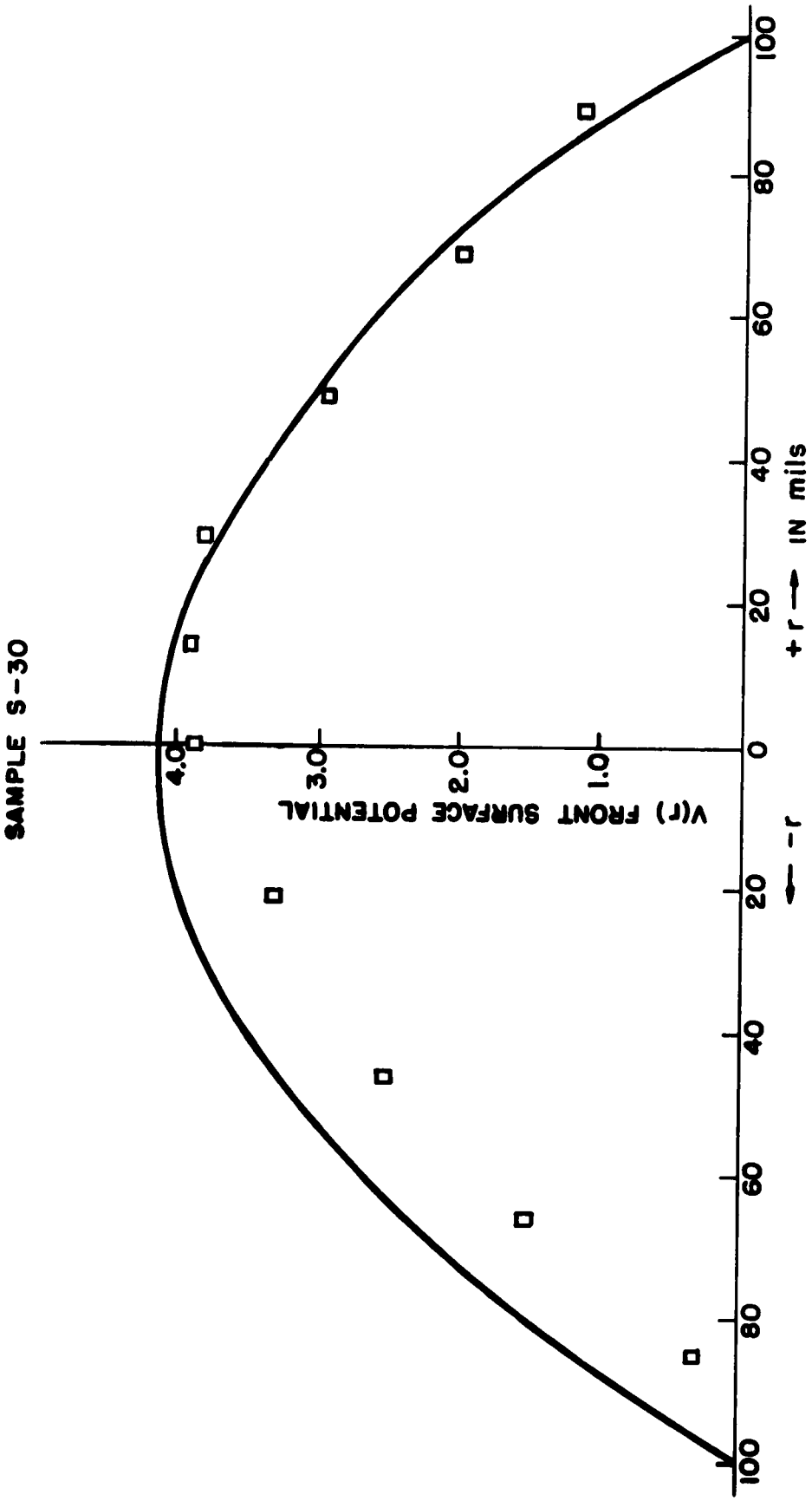
SAMPLE S-30
V(r) FRONT SURFACE POTENTIAL
4.0
3.0
2.0
1.0
0
20
40
60
80
100
+r IN mils
-r

FIG. 18

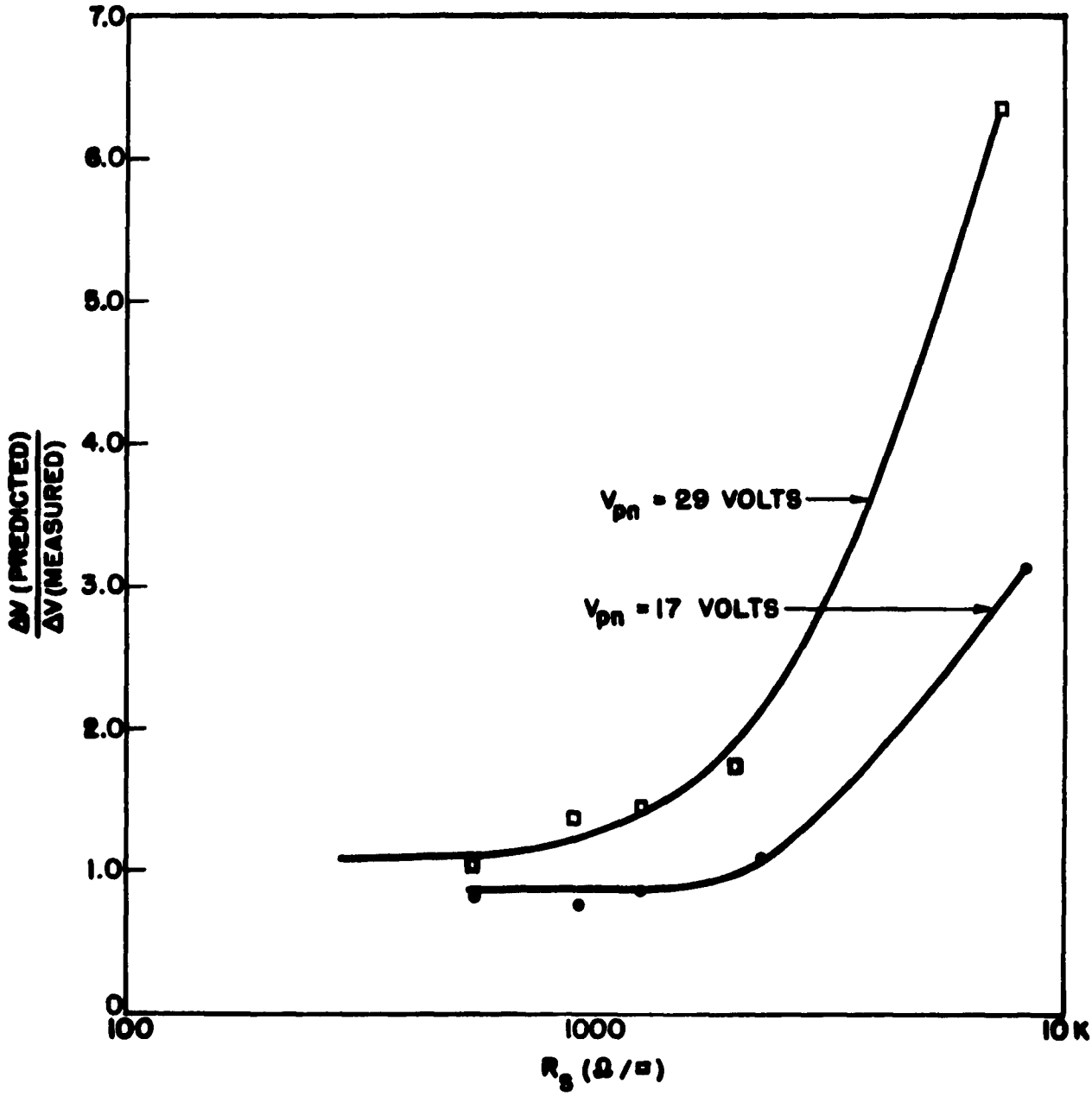
7.0
6.0
5.0
4.0
3.0
2.0
1.0
0
100
1000
10K
$\frac{\Delta V\ (PREDICTED)}{\Delta V(MEASURED)}$
$R_S\ (\Omega/\square)$
V_{pn} = 29 VOLTS
V_{pn} = 17 VOLTS

FIG. 19

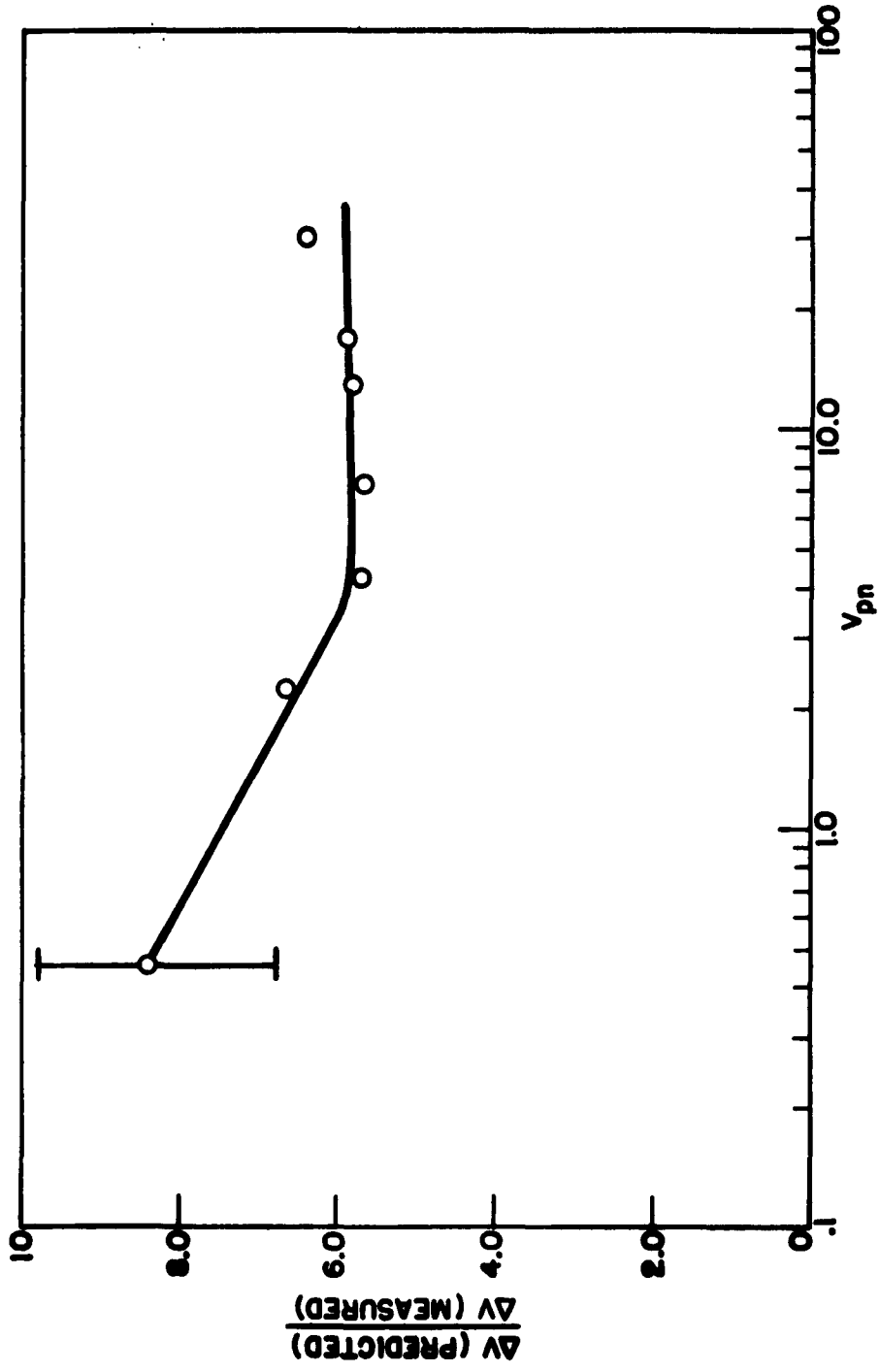

FIG. 20

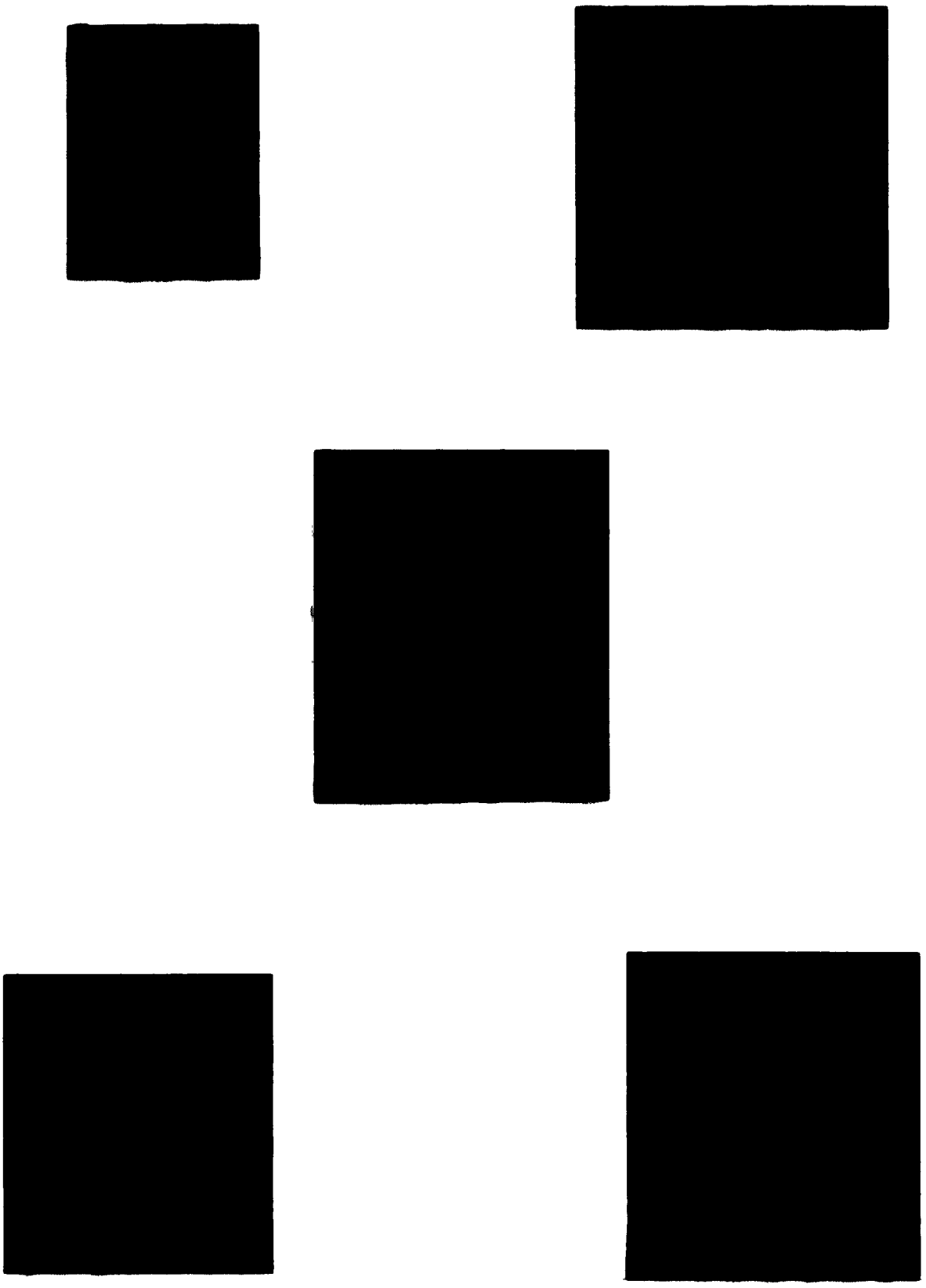

FIG. 21

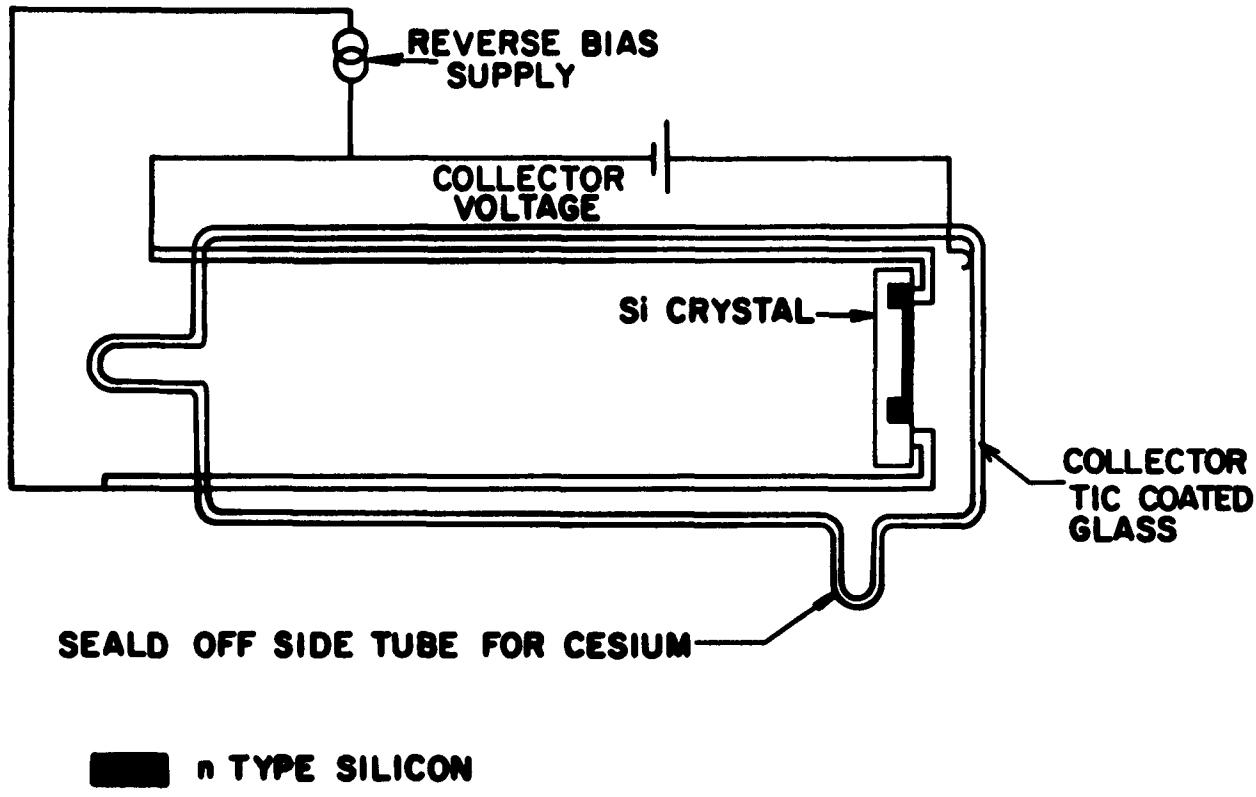
REVERSE BIAS SUPPLY
COLLECTOR VOLTAGE
Si CRYSTAL
COLLECTOR TIC COATED GLASS
SEALD OFF SIDE TUBE FOR CESIUM
n TYPE SILICON

FIG. 22

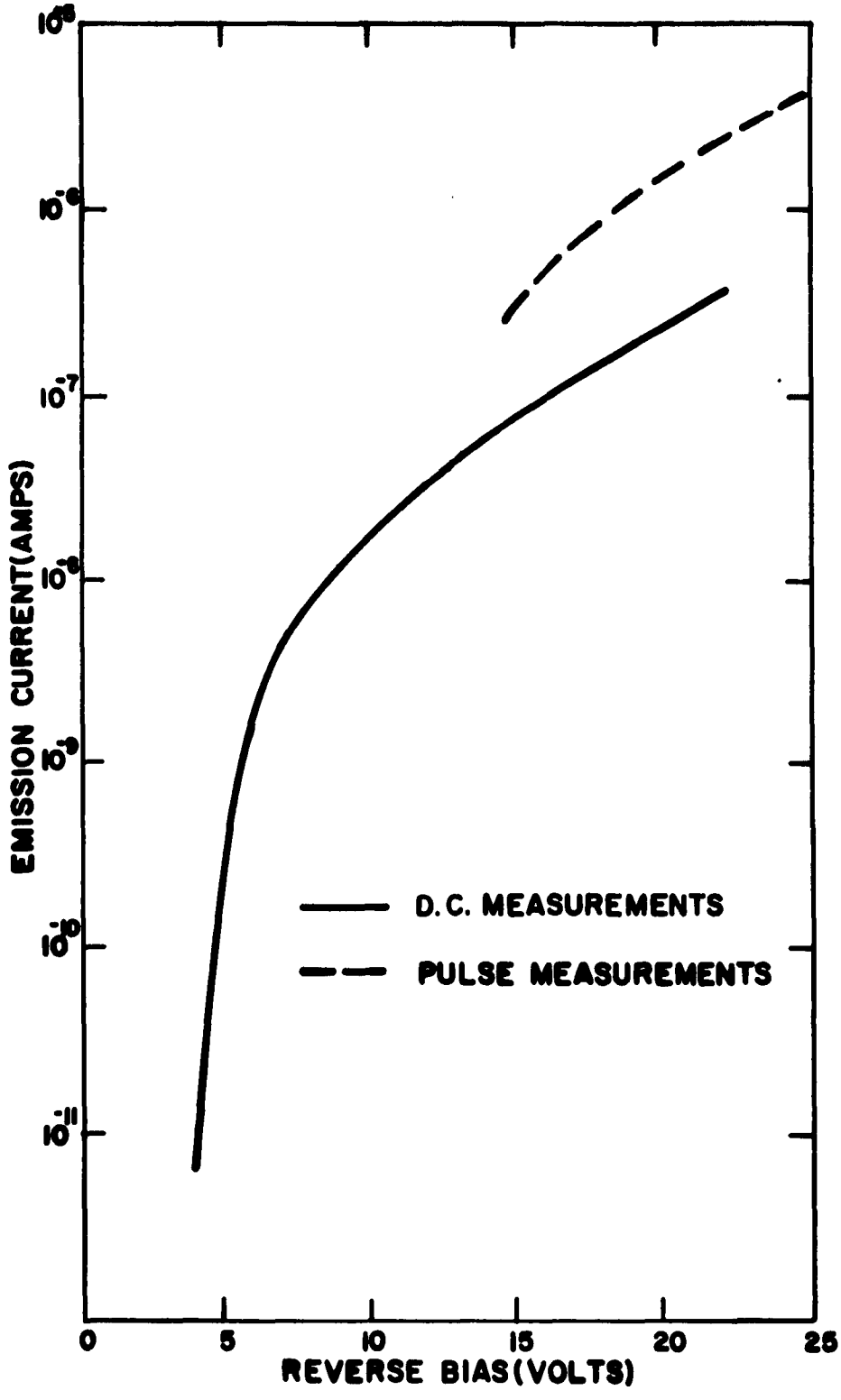
EMISSION CURRENT(AMPS)
D.C. MEASUREMENTS
PULSE MEASUREMENTS
0
5
10
15
20
25
REVERSE BIAS(VOLTS)

FIG. 23

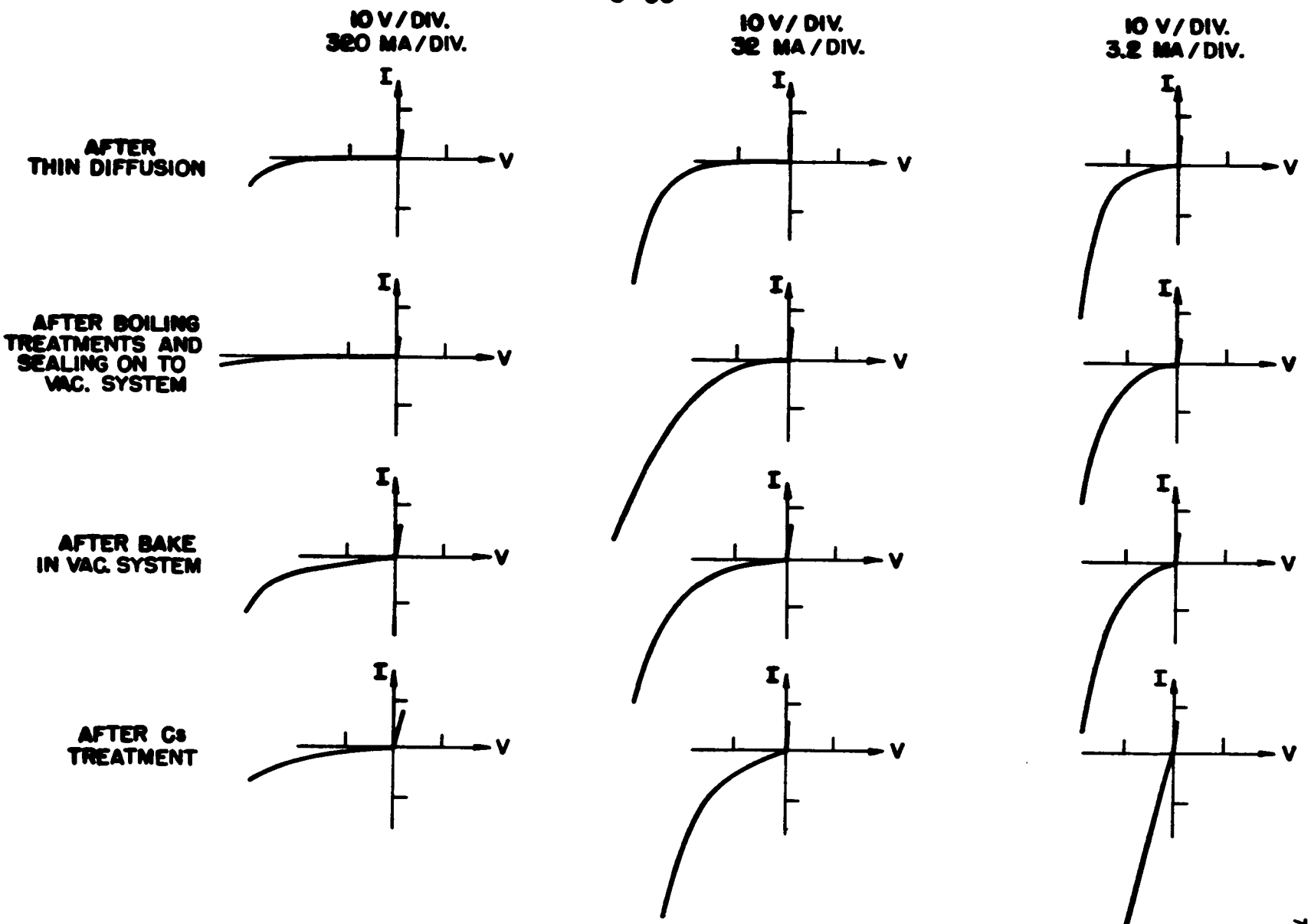
10 V / DIV.
320 MA / DIV.
10 V / DIV.
32 MA / DIV.
10 V / DIV.
3.2 MA / DIV.
AFTER THIN DIFFUSION
AFTER BOILING TREATMENTS AND SEALING ON TO VAC. SYSTEM
AFTER BAKE IN VAC. SYSTEM
AFTER Cs TREATMENT
I
V

FIG. 24

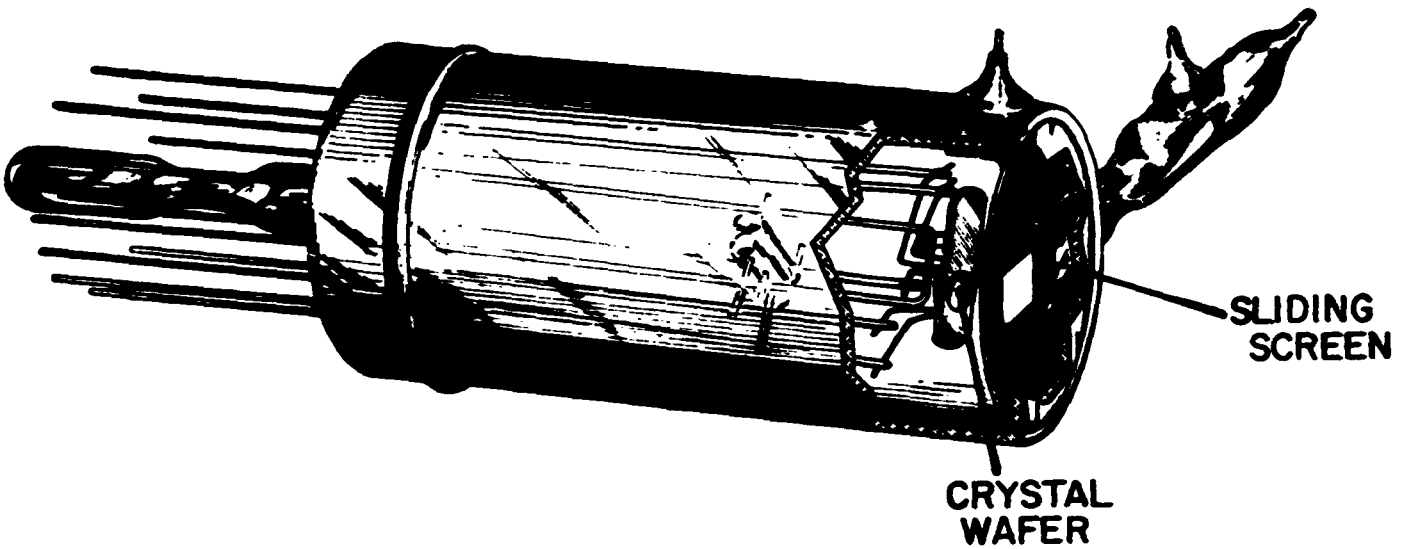

FIG. 25

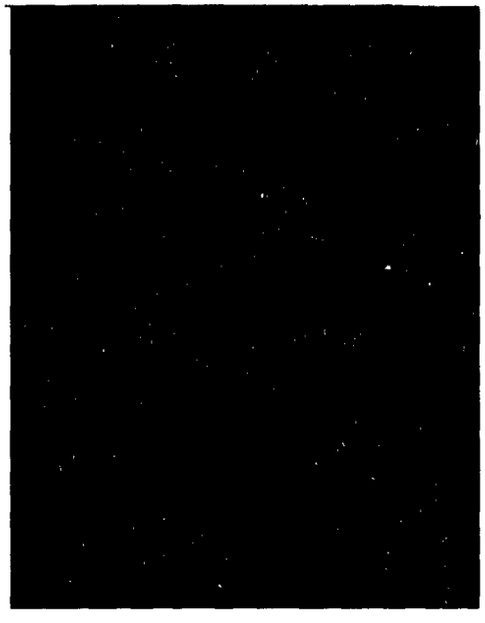

LIGHT EMITTING SPOTS
15 SEC. EXPOSURE

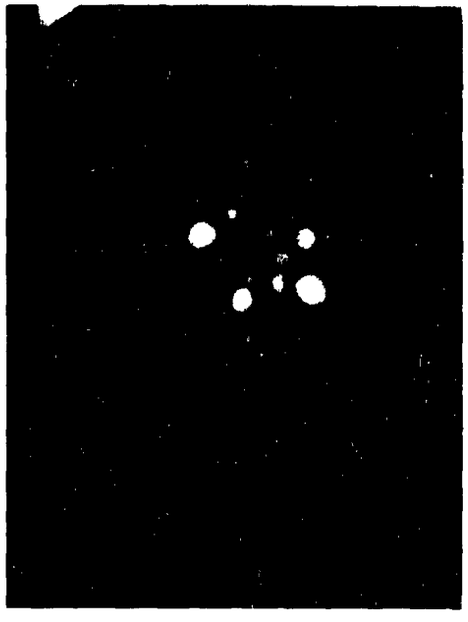

IMAGING WITH 1500 VOLTS
ON PHOSPHOR

LIGHT EMITTING SPOTS
15 MIN. EXPOSURE

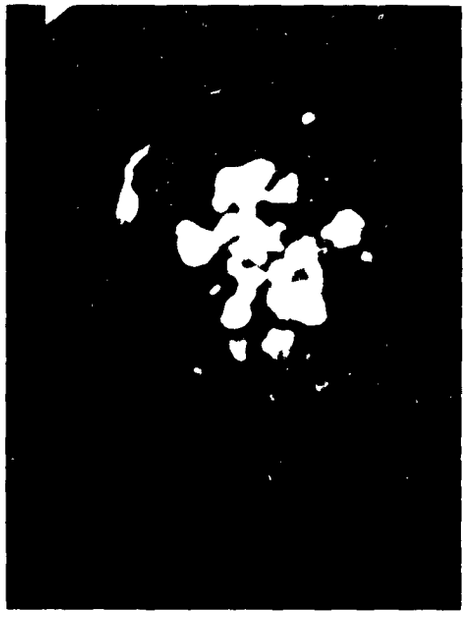

IMAGING WITH 2500 VOLTS
ON PHOSPHOR

FIG. 26

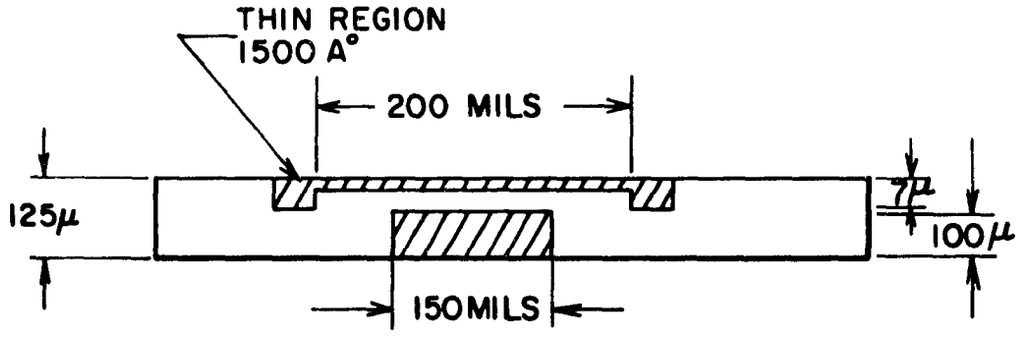

P TYPE Si

N TYPE Si

FIG. 27

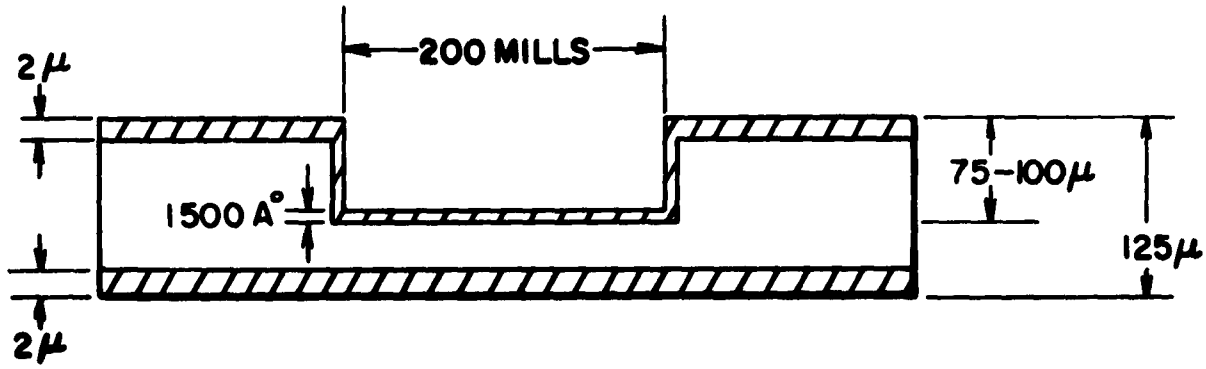

n TYPE Si

P TYPE Si

FIG. 28

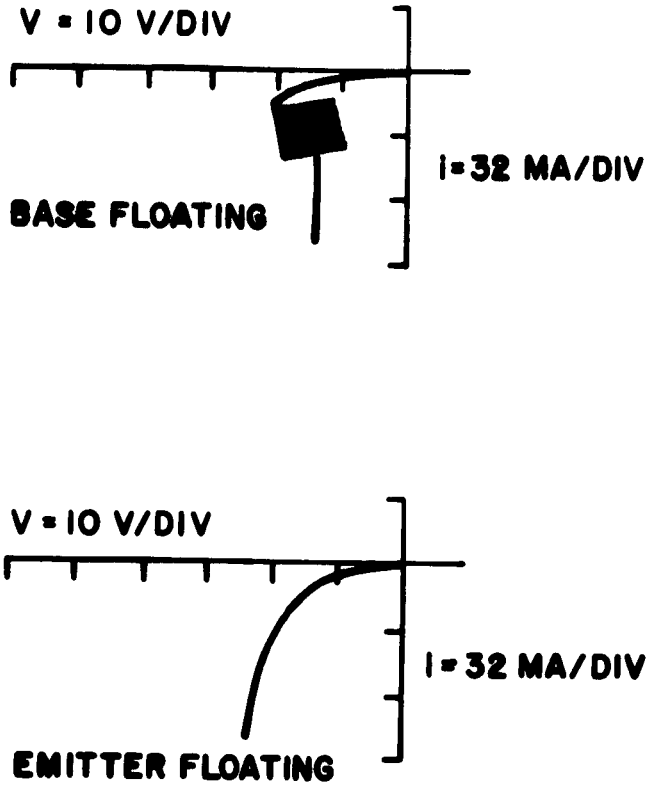
V = 10 V/DIV
I = 32 MA/DIV
BASE FLOATING
V = 10 V/DIV
I = 32 MA/DIV
EMITTER FLOATING

FIG. 29

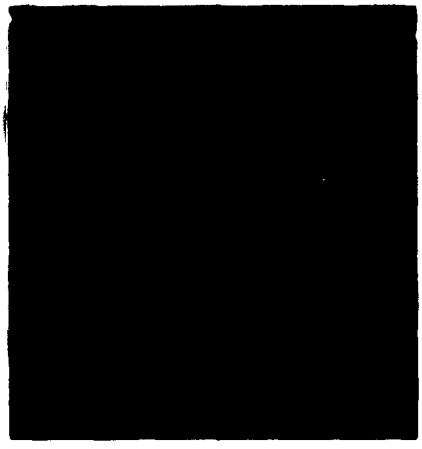

LUMINESCENCE OF DEVICE WITH EMITTER REGION FLOATING

LUMINESCENCE OF DEVICE WITH BASE REGION FLOATING

FIG. 30

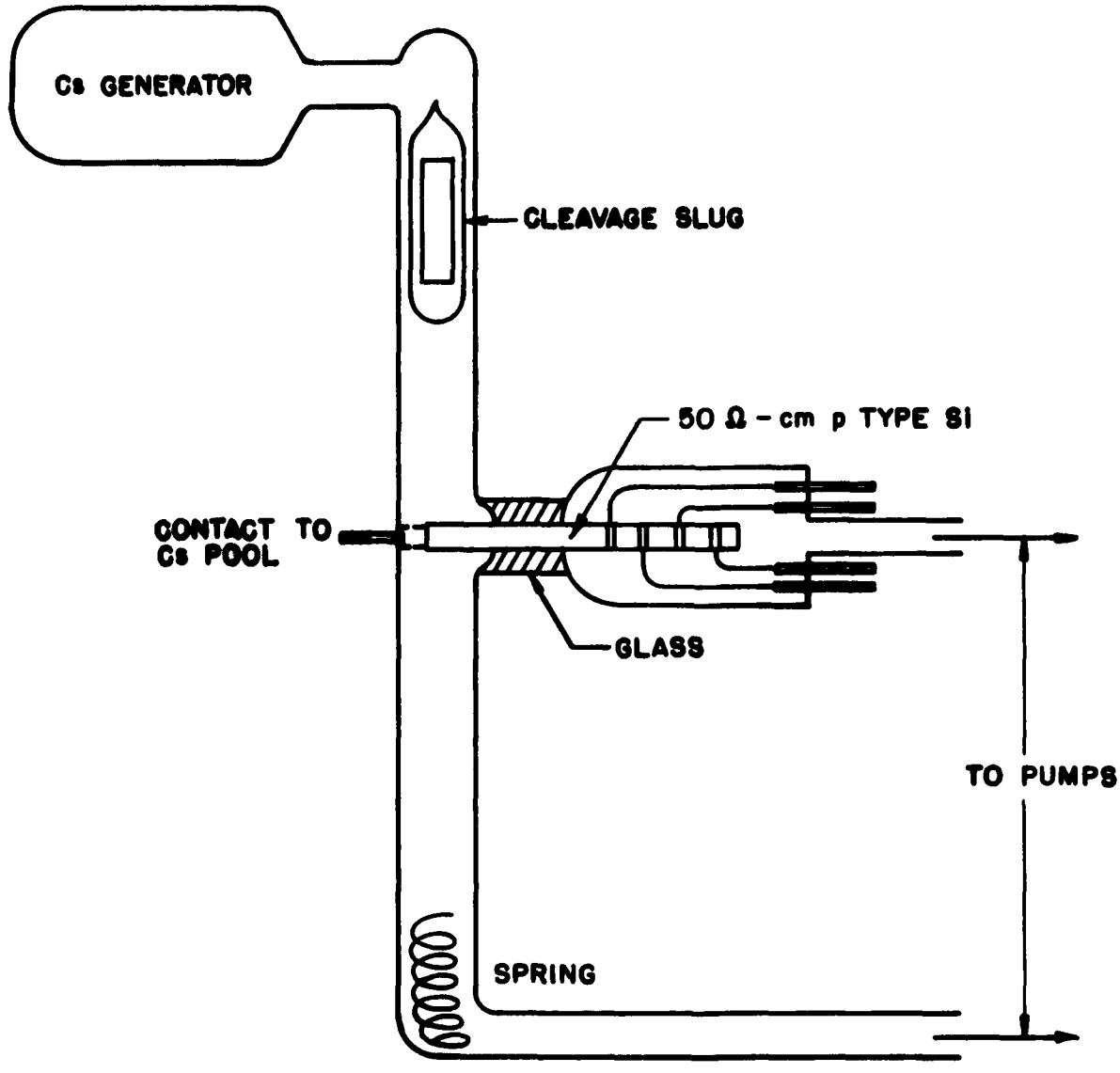
Cs GENERATOR
CLEAVAGE SLUG
50 Ω - cm p TYPE Si
CONTACT TO
Cs POOL
GLASS
TO PUMPS
SPRING

FIG. 31

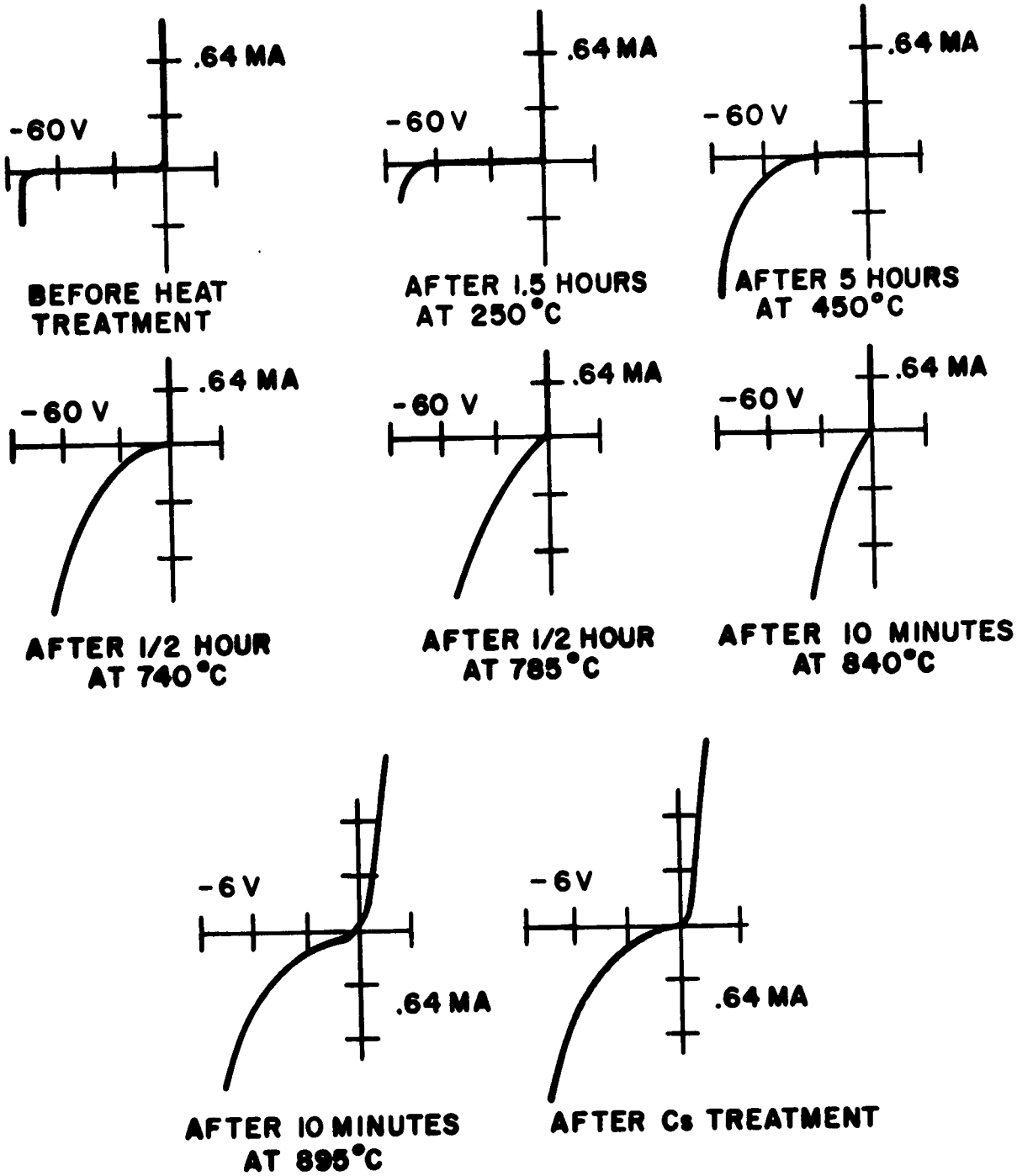
.64 MA
-60 V
BEFORE HEAT TREATMENT
.64 MA
-60 V
AFTER 1.5 HOURS AT 250°C
.64 MA
-60 V
AFTER 5 HOURS AT 450°C
.64 MA
-60 V
AFTER 1/2 HOUR AT 740°C
.64 MA
-60 V
AFTER 1/2 HOUR AT 785°C
.64 MA
-60 V
AFTER 10 MINUTES AT 840°C
-6 V
.64 MA
AFTER 10 MINUTES AT 895°C
-6 V
.64 MA
AFTER Cs TREATMENT

FIG. 32

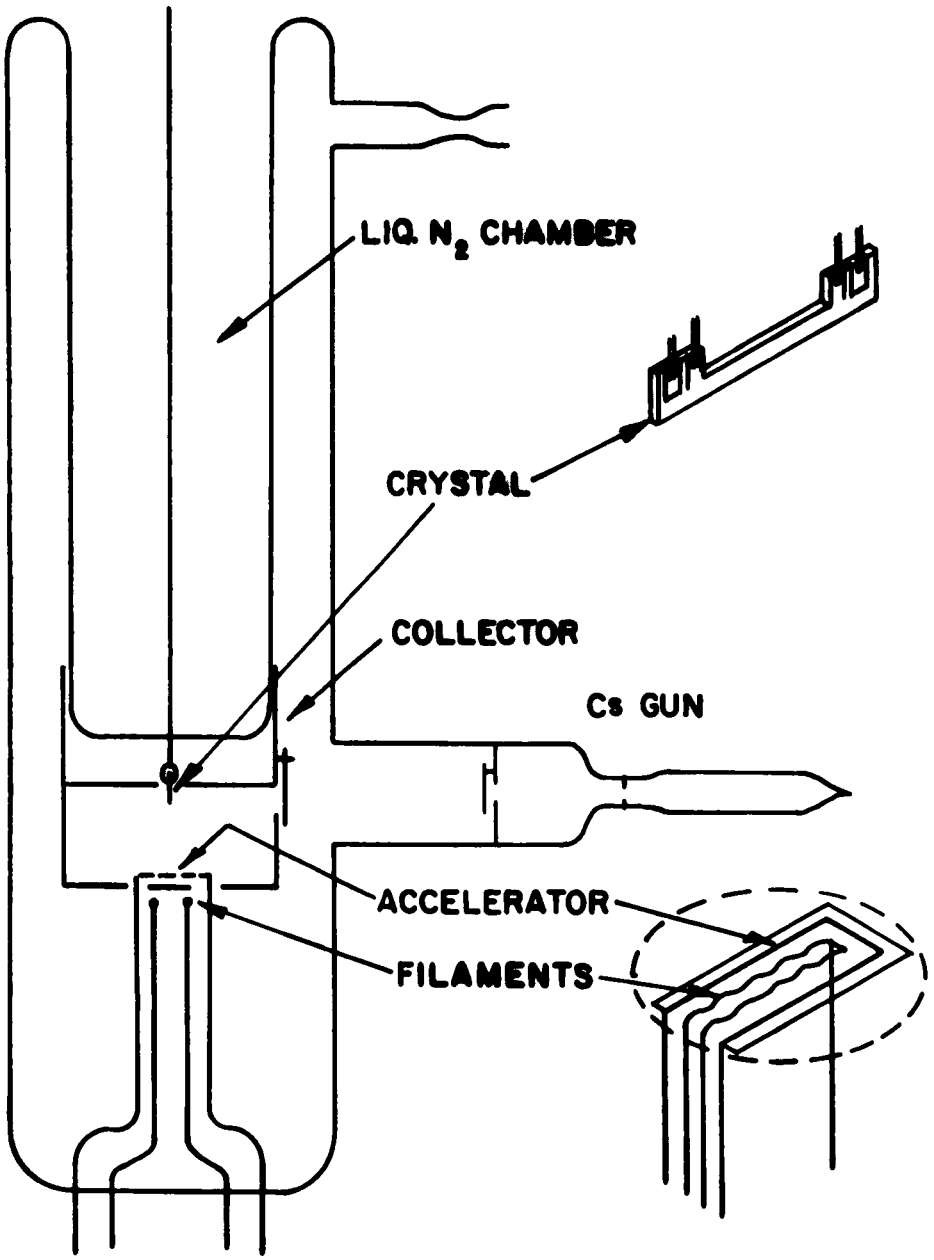
LIQ. N_2 CHAMBER
CRYSTAL
COLLECTOR
Cs GUN
ACCELERATOR
FILAMENTS

FIG. 33

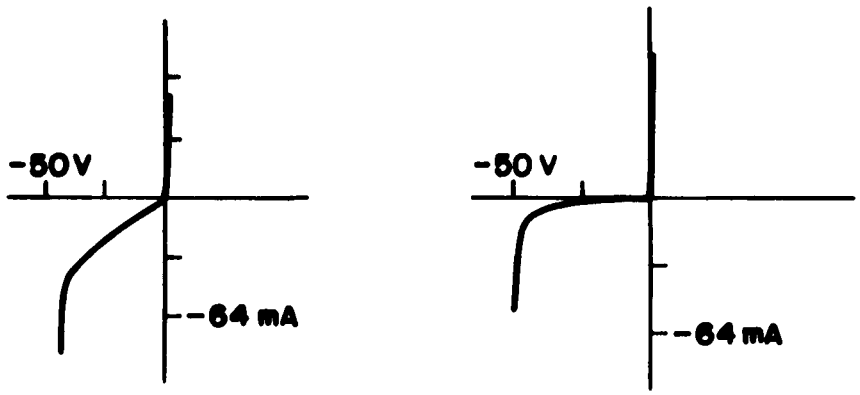

a)- BEFORE BOMBARDMENT b)- AFTER BOMBARDMENT

FIG. 34

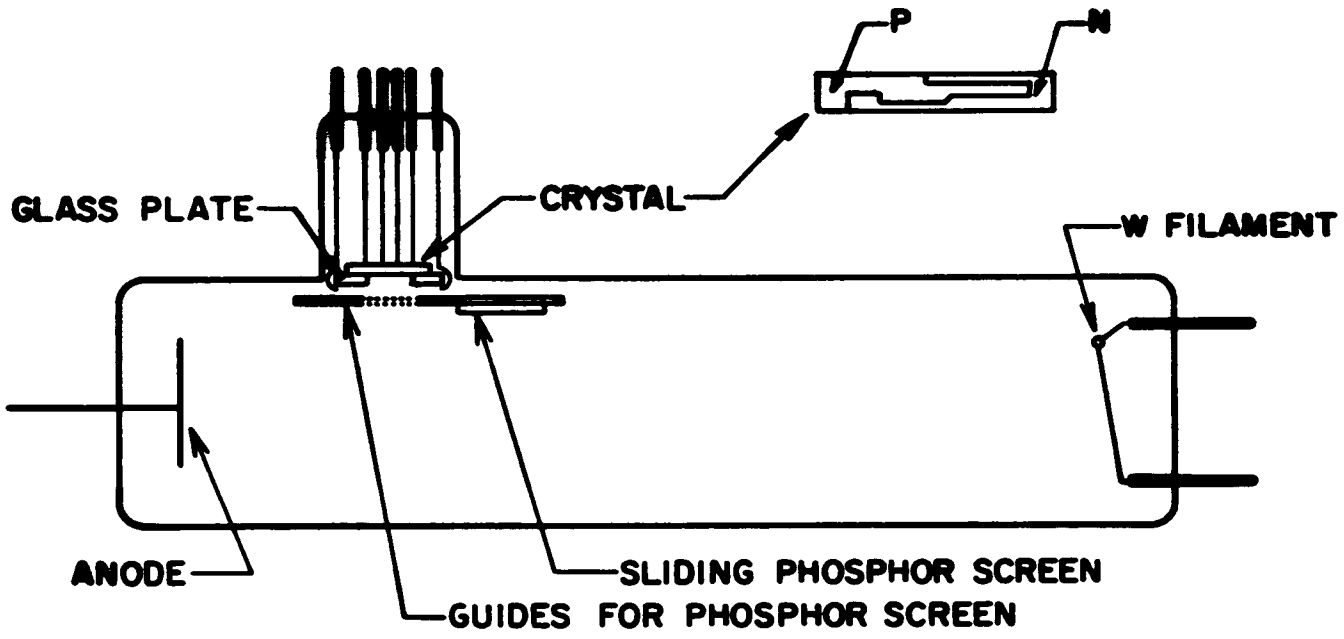

ARGON BOMBARDMENT TUBE

FIG. 35

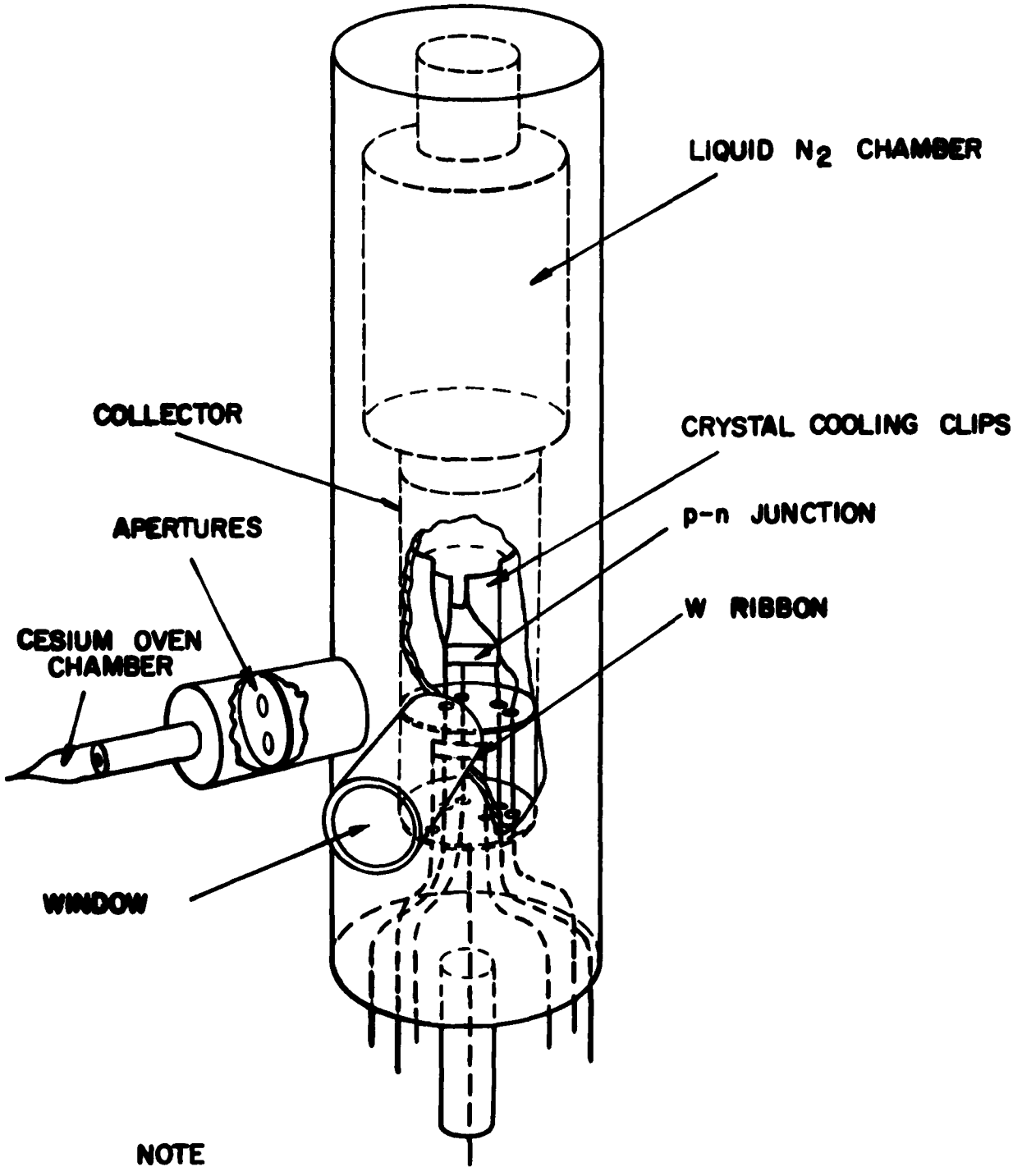

NOTE

APERTURES IN COLLECTOR AND APERTURE SHUTTERS ARE NOT SHOWN.

FIG. 36

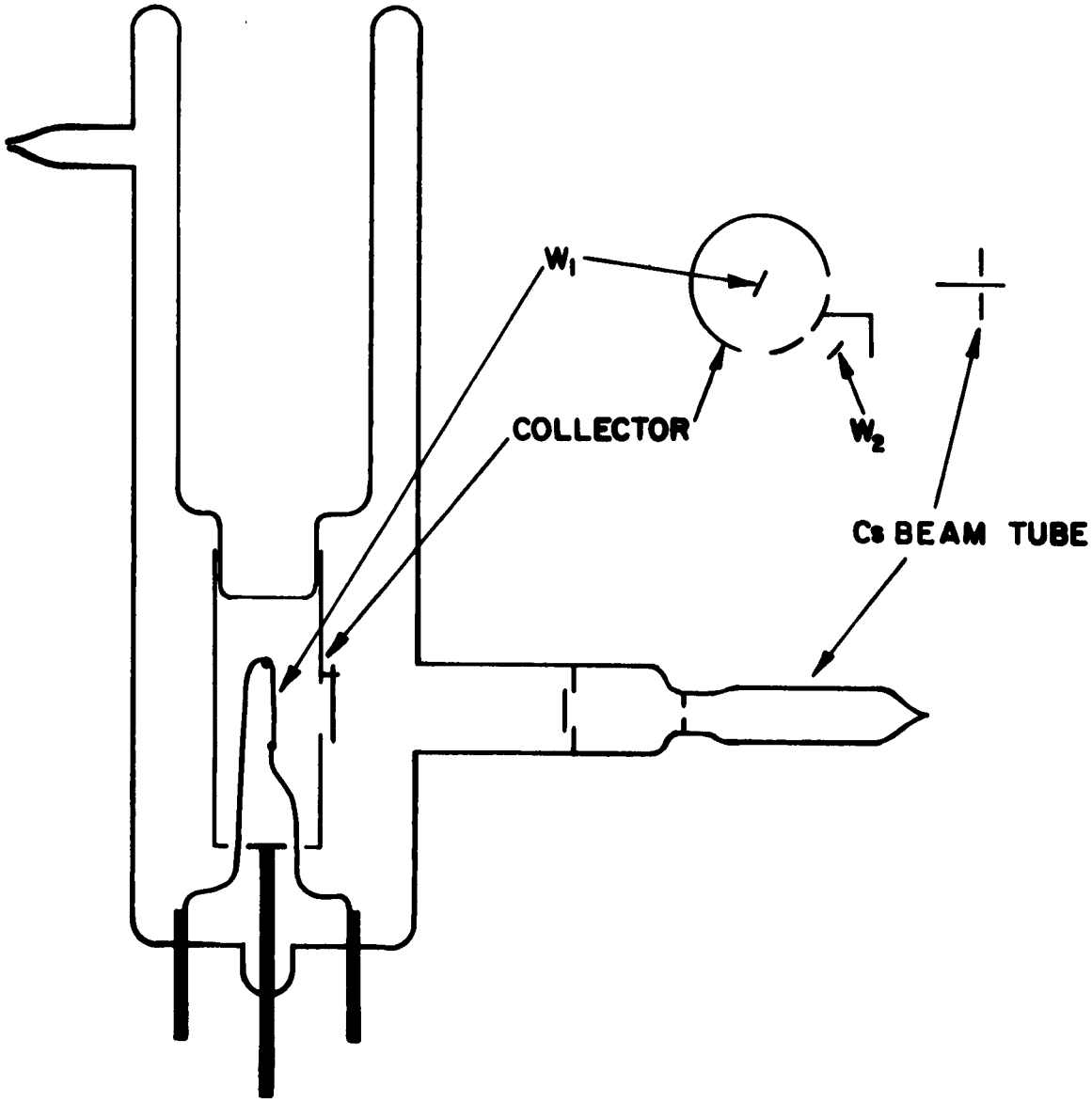

FIG. 37

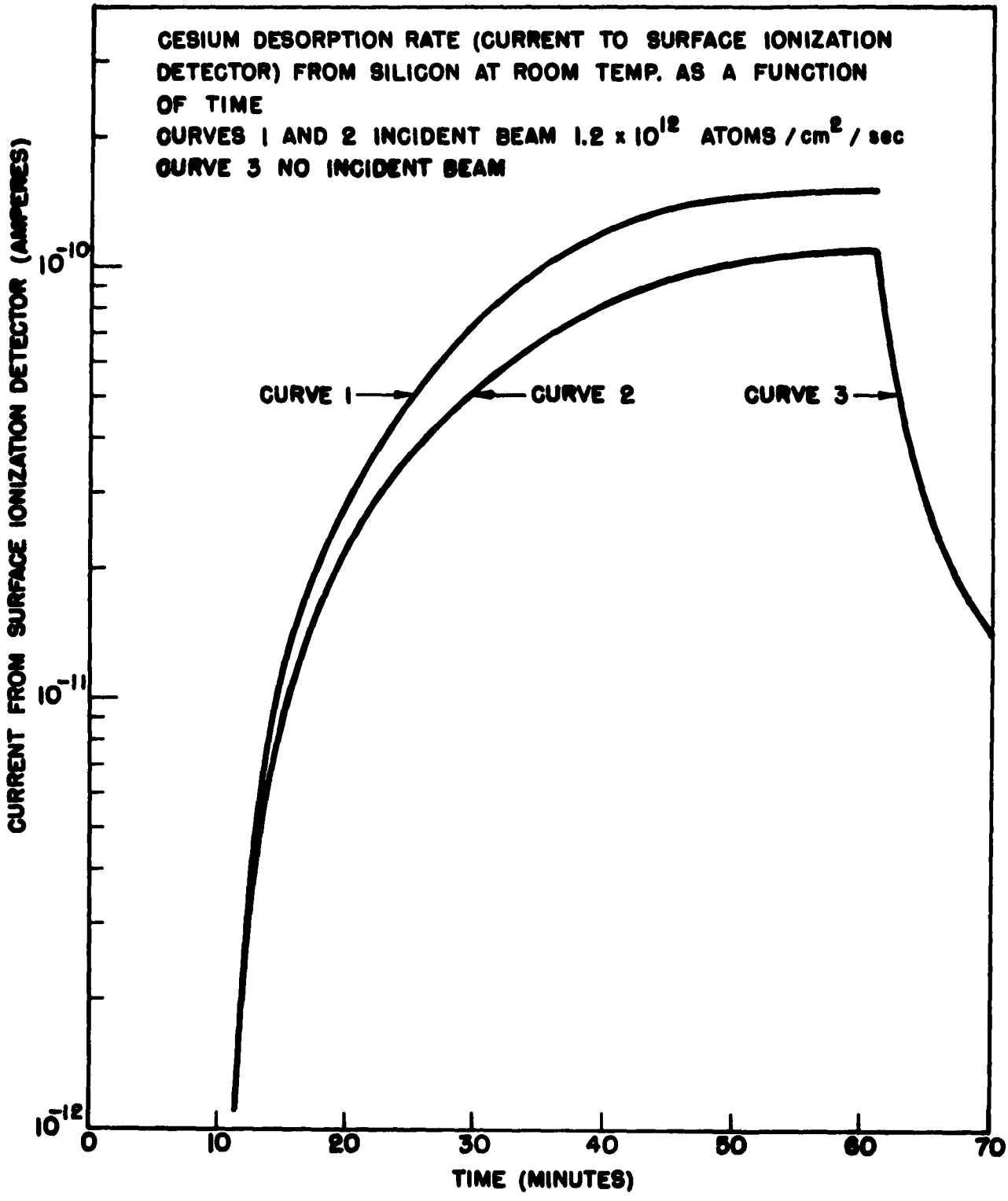
CESIUM DESORPTION RATE (CURRENT TO SURFACE IONIZATION DETECTOR) FROM SILICON AT ROOM TEMP. AS A FUNCTION OF TIME
CURVES 1 AND 2 INCIDENT BEAM 1.2 x 10^12 ATOMS / cm^2 / sec
CURVE 3 NO INCIDENT BEAM
CURRENT FROM SURFACE IONIZATION DETECTOR (AMPERES)
10^-10
10^-11
10^-12
CURVE 1
CURVE 2
CURVE 3
0
10
20
30
40
50
60
70
TIME (MINUTES)

FIG. 38

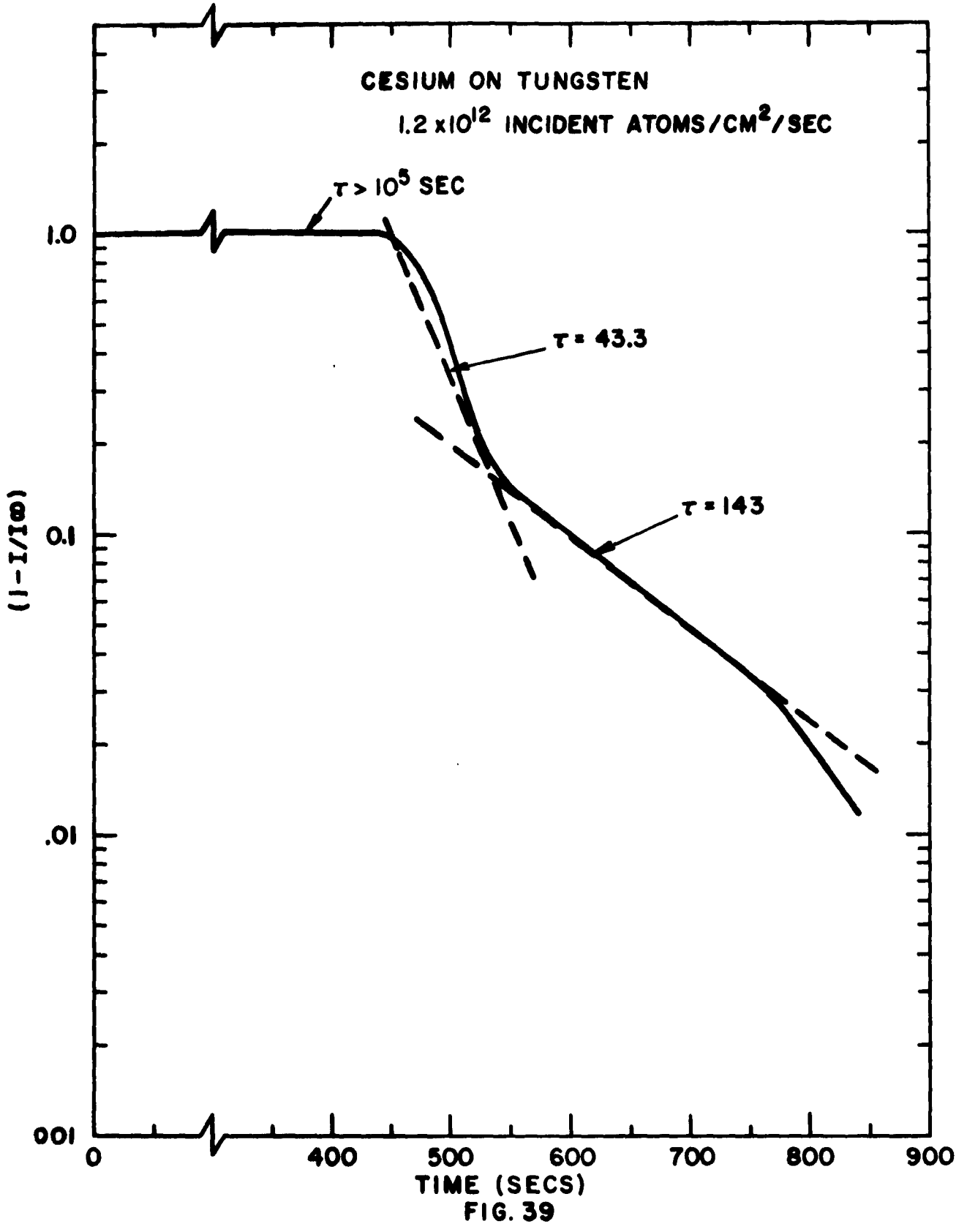
CESIUM ON TUNGSTEN
1.2 x10^12 INCIDENT ATOMS/CM^2/SEC
τ > 10^5 SEC
τ = 43.3
τ = 143
(1-I/I0)
1.0
0.1
.01
001
0
400
500
600
700
800
900
TIME (SECS)

FIG. 39

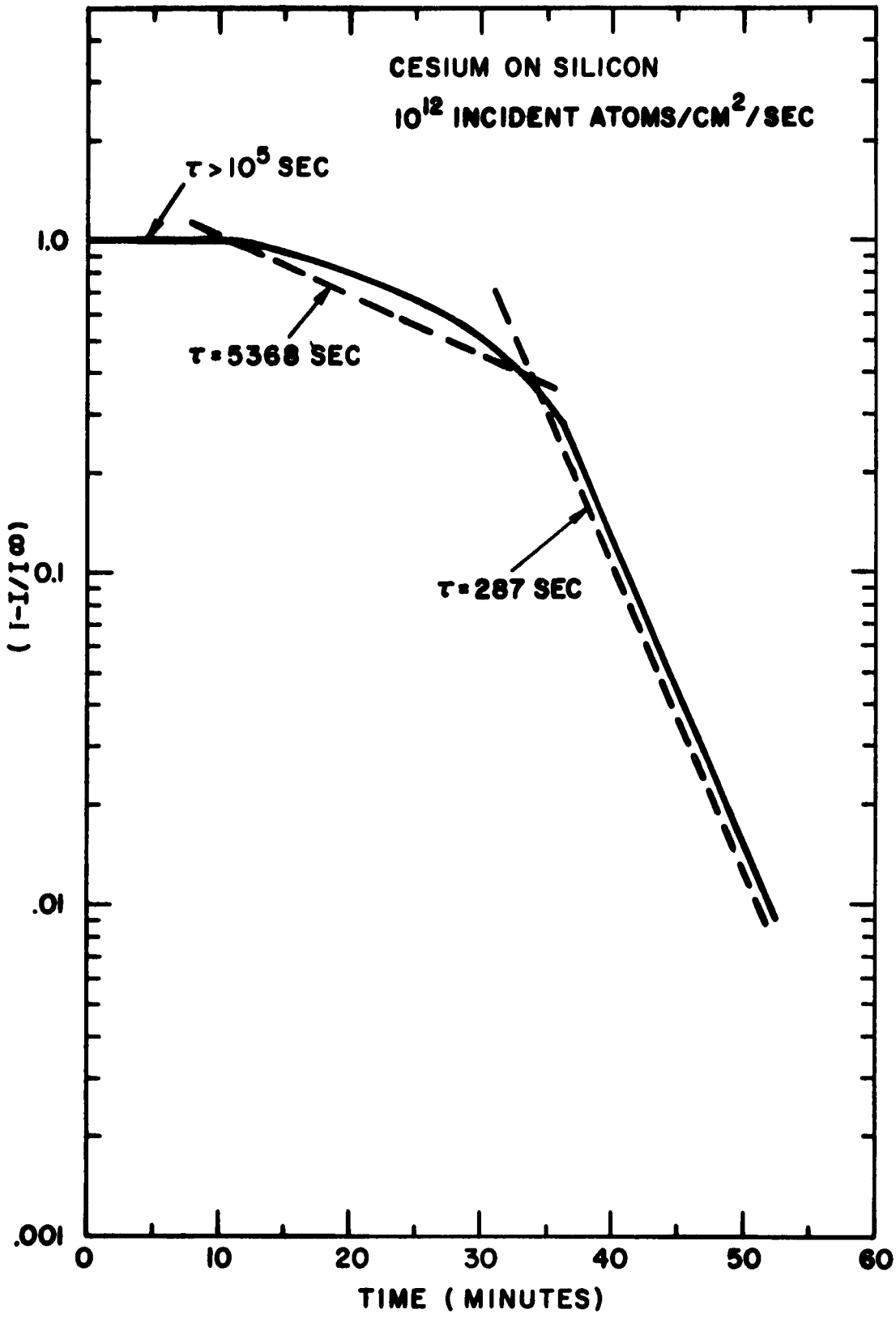
CESIUM ON SILICON
10^12 INCIDENT ATOMS/CM^2/SEC
τ > 10^5 SEC
τ = 5368 SEC
τ = 287 SEC
1.0
0.1
.01
.001
(I-I/I0)
0
10
20
30
40
50
60
TIME (MINUTES)

FIG. 40

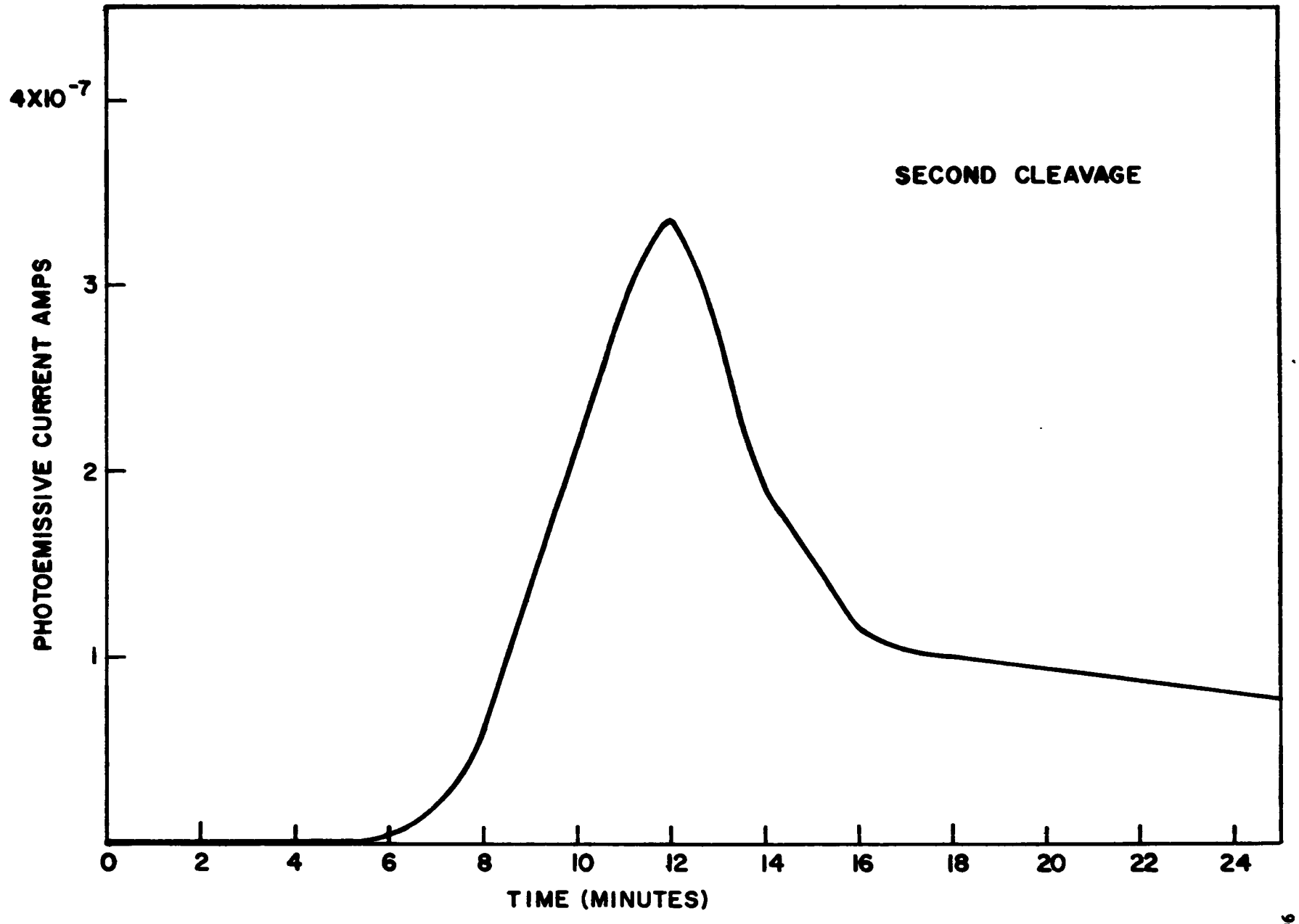
4X10⁻⁷
3
2
1
PHOTOEMISSIVE CURRENT AMPS
SECOND CLEAVAGE
0
2
4
6
8
10
12
14
16
18
20
22
24
TIME (MINUTES)

FIG. 41

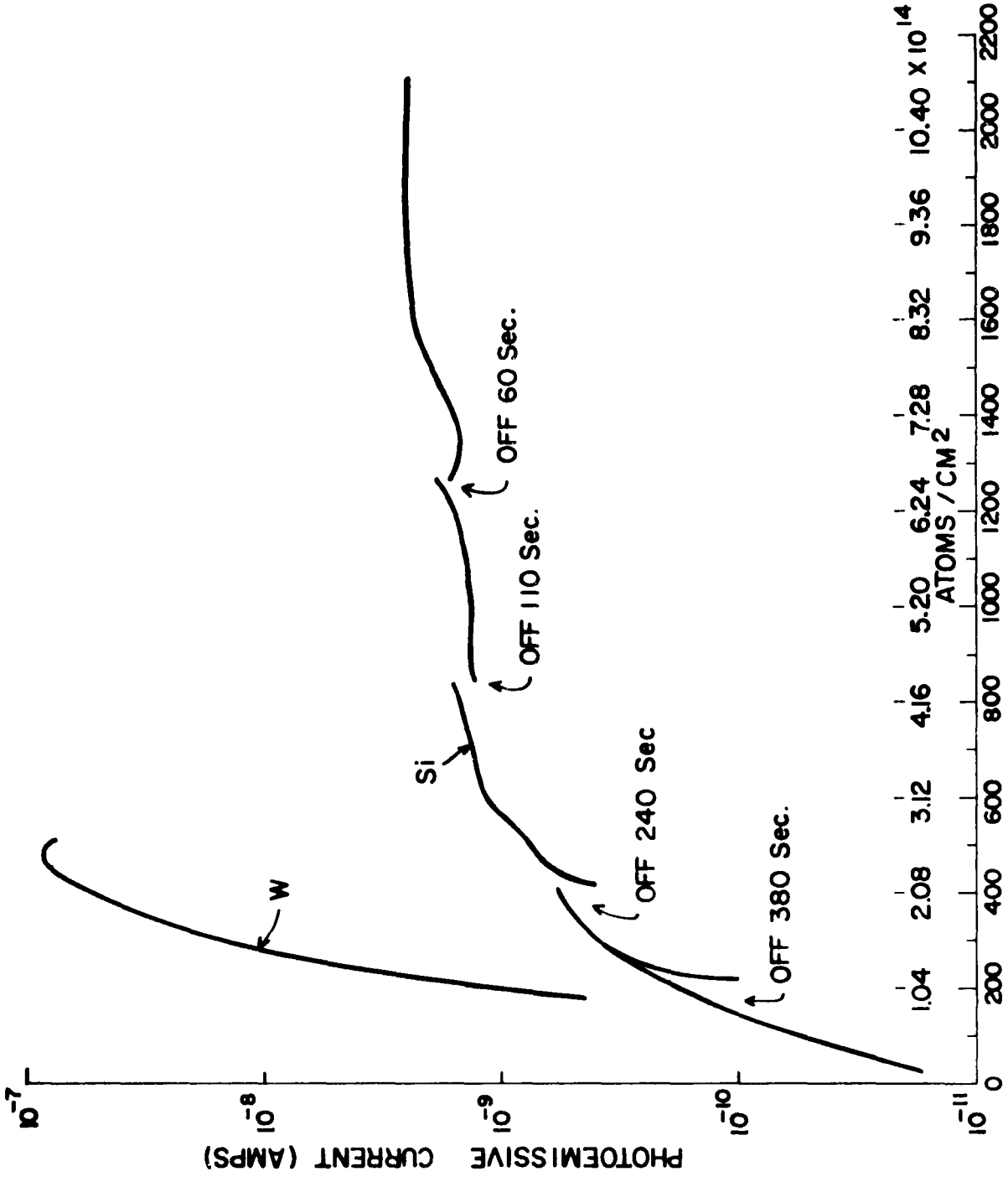
PHOTOEMISSIVE CURRENT (AMPS)
10^{-7}
10^{-8}
10^{-9}
10^{-10}
10^{-11}
W
Si
OFF 60 Sec.
OFF 110 Sec.
OFF 240 Sec
OFF 380 Sec.
0
200
400
600
800
1000
1200
1400
1600
1800
2000
2200
TIME Sec.
1.04
2.08
3.12
4.16
5.20
6.24
7.28
8.32
9.36
10.40 X 10^{14}
ATOMS / CM^2

FIG. 42

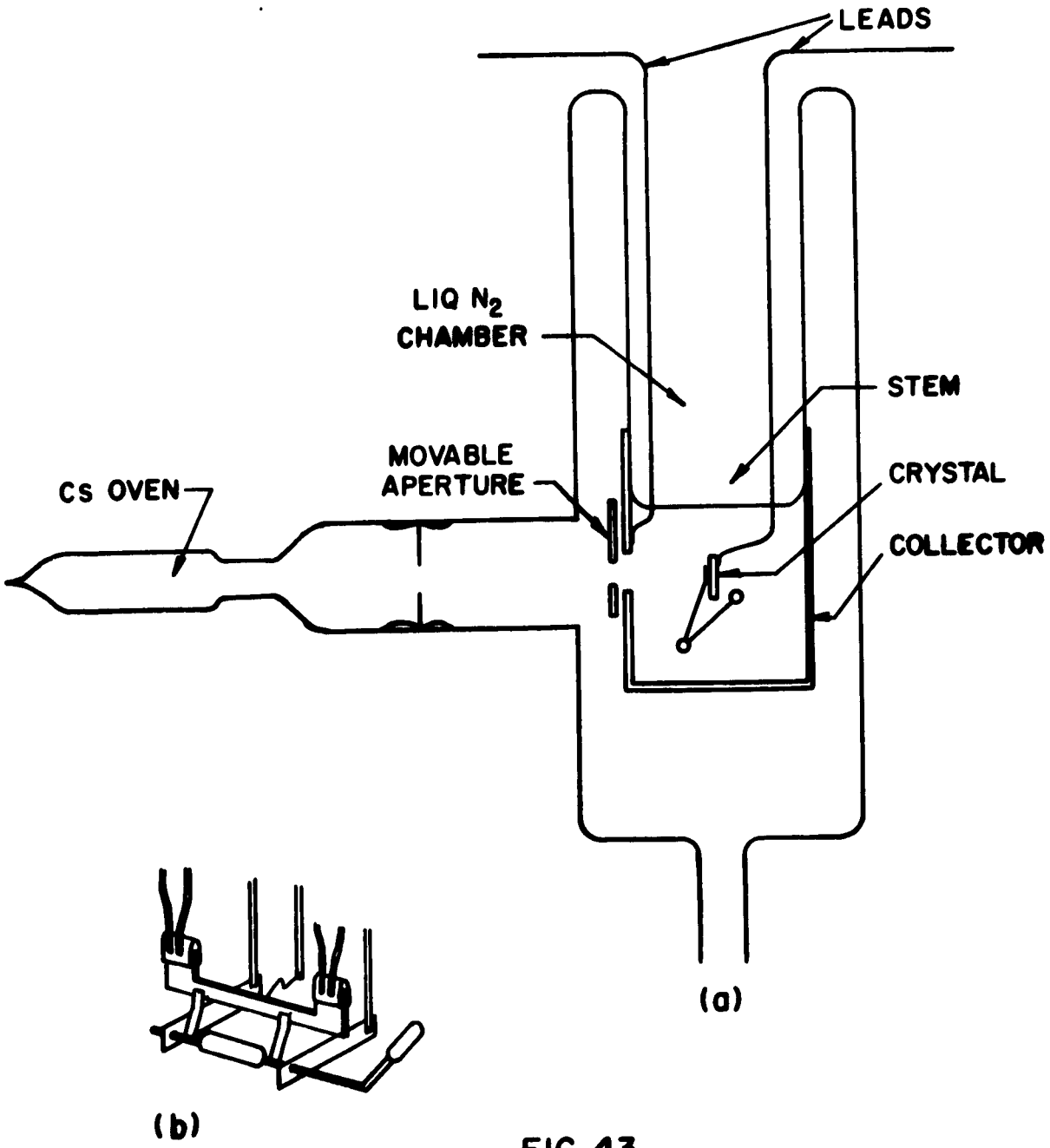
LEADS
LIQ N_2
CHAMBER
STEM
MOVABLE
APERTURE
CRYSTAL
Cs OVEN
COLLECTOR
(a)
(b)

FIG. 43

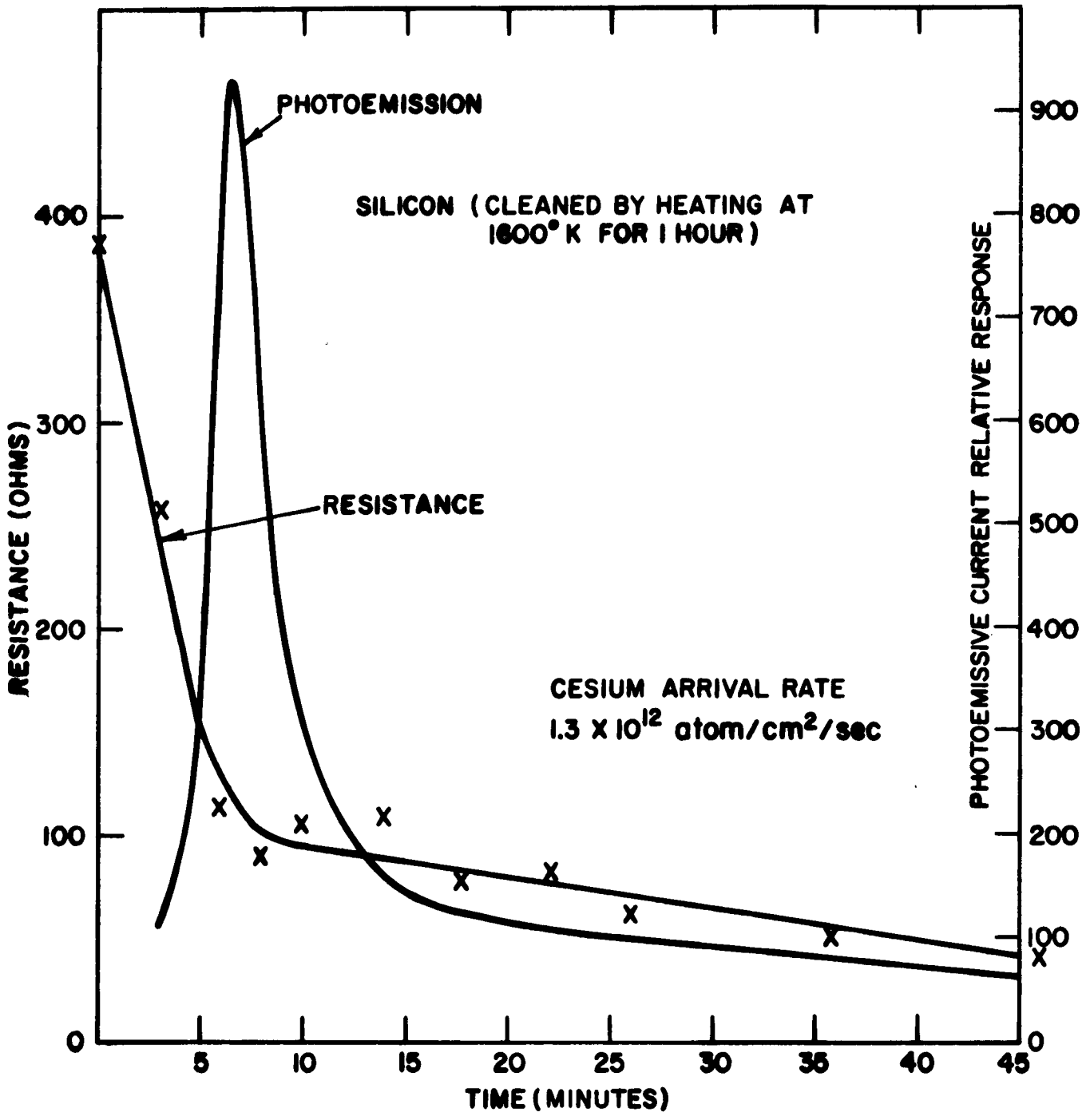
PHOTOEMISSION
SILICON (CLEANED BY HEATING AT 1600° K FOR 1 HOUR)
RESISTANCE
CESIUM ARRIVAL RATE
1.3 X 10^12 atom/cm^2/sec
RESISTANCE (OHMS)
PHOTOEMISSIVE CURRENT RELATIVE RESPONSE
TIME (MINUTES)
0
100
200
300
400
500
600
700
800
900
5
10
15
20
25
30
35
40
45

FIG. 44

AD ______________ Div. 8/4, 25/6

RCA Laboratories, Princeton, N. J.
RESEARCH IN ELECTRON EMISSION FROM SEMICONDUCTORS, R. E. Simon, Project Engineer
Final Report for 1 October 1960 to 30 September 1962
105 pages, incl. illus. – (Contract DA36-039-SC-87388)
Unclassified report.

The work performed under this contract directed toward the study of hot electron emission from semiconductors is reviewed and summarized. These studies include: (1) a review of the literature on hot electron effects in semiconductors, (2) the theoretical study of electron-electron interactions in semiconductors and metals, (3) the requirements for a p-n junction hot electron emitter, (4) a method of preparation of these emitters of Si and their properties, (5) an emitter with an injecting contact, (6) attempts to clean silicon in vacuum by low temperature heating and by argon bombardment without annealing, and (7) measurements on the interaction of cesium with silicon. While it has not yet been possible to produce an emitter with optimum conditions, the groundwork for such an emitter has been laid.

UNCLASSIFIED

1. Hot electron emission
2. Electron-electron interactions
3. Properties of p-n junction emitter
4. Properties of p-n junctions
5. Clean surfaces
6. Cesium-silicon interaction

I. Title: Research in Electron Emission from Semiconductors
II. R. E. Simon
III. U.S. Army, Electronics Research and Development Laboratory, Ft. Monmouth, New Jersey
IV. Contract DA36-039-SC-87388
V. Contract DA36-039-SC-78155

AD ______________ Div. 8/4, 25/6

RCA Laboratories, Princeton, N. J.
RESEARCH IN ELECTRON EMISSION FROM SEMICONDUCTORS, R. E. Simon, Project Engineer
Final Report for 1 October 1960 to 30 September 1962
105 pages, incl. illus. – (Contract DA36-039-SC-87388)
Unclassified report.

The work performed under this contract directed toward the study of hot electron emission from semiconductors is reviewed and summarized. These studies include: (1) a review of the literature on hot electron effects in semiconductors, (2) the theoretical study of electron-electron interactions in semiconductors and metals, (3) the requirements for a p-n junction hot electron emitter, (4) a method of preparation of these emitters of Si and their properties, (5) an emitter with an injecting contact, (6) attempts to clean silicon in vacuum by low temperature heating and by argon bombardment without annealing, and (7) measurements on the interaction of cesium with silicon. While it has not yet been possible to produce an emitter with optimum conditions, the groundwork for such an emitter has been laid.

UNCLASSIFIED

1. Hot electron emission
2. Electron-electron interactions
3. Properties of p-n junction emitter
4. Properties of p-n junctions
5. Clean surfaces
6. Cesium-silicon interaction

I. Title: Research in Electron Emission from Semiconductors
II. R. E. Simon
III. U.S. Army, Electronics Research and Development Laboratory, Ft. Monmouth, New Jersey
IV. Contract DA36-039-SC-87388
V. Contract DA36-039-SC-78155

AD ______________ Div. 8/4, 25/6

RCA Laboratories, Princeton, N. J.
RESEARCH IN ELECTRON EMISSION FROM SEMICONDUCTORS, R. E. Simon, Project Engineer
Final Report for 1 October 1960 to 30 September 1962
105 pages, incl. illus. – (Contract DA36-039-SC-87388)
Unclassified report.

The work performed under this contract directed toward the study of hot electron emission from semiconductors is reviewed and summarized. These studies include: (1) a review of the literature on hot electron effects in semiconductors, (2) the theoretical study of electron-electron interactions in semiconductors and metals, (3) the requirements for a p-n junction hot electron emitter, (4) a method of preparation of these emitters of Si and their properties, (5) an emitter with an injecting contact, (6) attempts to clean silicon in vacuum by low temperature heating and by argon bombardment without annealing, and (7) measurements on the interaction of cesium with silicon. While it has not yet been possible to produce an emitter with optimum conditions, the groundwork for such an emitter has been laid.

UNCLASSIFIED

1. Hot electron emission
2. Electron-electron interactions
3. Properties of p-n junction emitter
4. Properties of p-n junctions
5. Clean surfaces
6. Cesium-silicon interaction

I. Title: Research in Electron Emission from Semiconductors
II. R. E. Simon
III. U.S. Army, Electronics Research and Development Laboratory, Ft. Monmouth, New Jersey
IV. Contract DA36-039-SC-87388
V. Contract DA36-039-SC-78155

AD ______________ Div. 8/4, 25/6

RCA Laboratories, Princeton, N. J.
RESEARCH IN ELECTRON EMISSION FROM SEMICONDUCTORS, R. E. Simon, Project Engineer
Final Report for 1 October 1960 to 30 September 1962
105 pages, incl. illus. – (Contract DA36-039-SC-87388)
Unclassified report.

The work performed under this contract directed toward the study of hot electron emission from semiconductors is reviewed and summarized. These studies include: (1) a review of the literature on hot electron effects in semiconductors, (2) the theoretical study of electron-electron interactions in semiconductors and metals, (3) the requirements for a p-n junction hot electron emitter, (4) a method of preparation of these emitters of Si and their properties, (5) an emitter with an injecting contact, (6) attempts to clean silicon in vacuum by low temperature heating and by argon bombardment without annealing, and (7) measurements on the interaction of cesium with silicon. While it has not yet been possible to produce an emitter with optimum conditions, the groundwork for such an emitter has been laid.

UNCLASSIFIED

1. Hot electron emission
2. Electron-electron interactions
3. Properties of p-n junction emitter
4. Properties of p-n junctions
5. Clean surfaces
6. Cesium-silicon interaction

I. Title: Research in Electron Emission from Semiconductors
II. R. E. Simon
III. U.S. Army, Electronics Research and Development Laboratory, Ft. Monmouth, New Jersey
IV. Contract DA36-039-SC-87388
V. Contract DA36-039-SC-78155

Radio Corporation of America
Contract DA36-039-sc-87388

Final Report

DISTRIBUTION LIST

	No. of Copies
OASD (R&E) Attn: Technical Library Room 3E1065, The Pentagon Washington 25, D. C.	1
Commander Armed Services Technical Information Agency Attn: TISIA Arlington Hall Station Arlington 12, Virginia	10
Advisory Group on Electron Devices 346 Broadway New York 13, New York	2
Director U. S. Naval Research Laboratory Attn: Code 2027 Washington 25, D. C.	1
Commanding Officer and Director U. S. Navy Electronics Laboratory San Diego 52, California	1
Chief, Bureau of Ships Department of the Navy Attn: 681A-1 Washington 25, D. C.	1
Commander Aeronautical Systems Division Attn: ASAPRL Wright-Patterson Air Force Base, Ohio	1
Commander Air Force Cambridge Research Laboratories Attn: CCRR L. G. Hanscom Field Bedford, Massachusetts	1
Commander Air Force Cambridge Research Laboratories Attn: CCSD L. G. Hanscom Field Bedford, Massachusetts	1

	No. of Copies
Commander Air Force Cambridge Research Laboratories Attn: CRZC L. G. Hanscom Field Bedford, Massachusetts	1
Commander Air Force Cambridge Research Laboratory Attn: CRXL-R, Research Library L. G. Hanscom Field Bedford, Massachusetts	1
Commander Rome Air Development Center Attn: RAALD Griffiss Air Force Base, New York	1
AFSC Scientific/Technical Liaison Office U. S. Naval Air Development Center Johnsville, Pennsylvania	1
Chief of Research and Development Department of the Army Washington 25, D. C.	1
Chief, U. S. Army Security Agency Arlington Hall Station Arlington 12, Virginia	2
Deputy President U. S. Army Security Agency Board Arlington Hall Station Arlington 12, Virginia	1
Commanding Officer U. S. Army Electronics Research Unit P. O. Box 205 Mountain View, California	1
Commanding Officer Harry Diamond Laboratories Attn: Library, Room 211, Building 92 Connecticut Avenue and Van Ness Street, N. W. Washington 25, D. C.	1
Commander U. S. Army Missile Command Attn: Technical Library Redstone Arsenal, Alabama	1

	No. of Copies
Commanding Officer U. S. Army Electronics Command Attn: AMSEL-RD Fort Monmouth, New Jersey	3
Commanding Officer U. S. Army Electronics Materiel Support Agency ATTN: SELMA-ADJ Fort Monmouth, New Jersey	1
Corps of Engineers Liaison Office U. S. Army Electronics R & D Laboratory Fort Monmouth, New Jersey	1
Marine Corps Liaison Officer U. S. Army Electronics R & D Laboratory Attn: SELRA/LNR Fort Monmouth, New Jersey	1
Commanding Officer U. S. Army Electronics R & D Laboratory Attn: Director of Research Fort Monmouth, New Jersey	1
Commanding Officer U. S. Army Electronics R & D Laboratory Attn: Technical Documents Center Fort Monmouth, New Jersey	1
Commanding Officer U. S. Army Electronics R & D Laboratory Attn: Technical Information Division (FOR RETRANSMITTAL TO ACCREDITED BRITISH AND CANADIAN GOVERNMENT REPRESENTATIVES) Fort Monmouth, New Jersey	3
Commanding Officer U. S. Army Electronics R & D Laboratory Attn: SELRA/PR - (Mr. Garoff) Fort Monmouth, New Jersey	1
Commanding Officer U. S. Army Electronics R&D Laboratory Attn: SELRA/PR - (Mr. Hanley) Fort Monmouth, New Jersey	1
Commanding Officer U. S. Army Electronics R&D Laboratory Attn: SELRA/PRG - (Mr. Zinn) Fort Monmouth, New Jersey	1

	No. of Copies
Commanding Officer U. S. Army Electronics R & D Laboratory Attn: SELRA/PRM - (Mr. Hersh) Fort Monmouth, New Jersey	1
Commanding Officer U. S. Army Electronics R & D Laboratory Attn: Logistics Division (For: SELRA/PRT, Project Engineer) Fort Monmouth, New Jersey	1
Commanding Officer U. S. Army Electronics R & D Laboratory Attn: SELRA/PRT, Record File Copy Fort Monmouth, New Jersey	1
Commanding General U. S. Army Materiel Command Attn: R & D Directorate Washington 25, D. C.	1
Commanding General U. S. Army Combat Developments Command Attn: CDCMR-E Fort Belvoir, Virginia	1
Commanding Officer U. S. Army Communication & Electronics Combat Development Agency Fort Huachuca, Arizona	1
Headquarters Electronic Systems Division Attn: ESAT L. G. Hanscom Field Bedford, Massachusetts	1
Director, Fort Monmouth Office U. S. Army Communication & Electronics Combat Development Agency Fort Monmouth, New Jersey	1
U. S. Continental Army Command Liaison Office U. S. Army Electronics R & D Laboratory Fort Monmouth, New Jersey	3
Commanding General U. S. Army Electronic Proving Ground Attn: Technical Library Fort Huachuca, Arizona	1

	No. of Copies
Commanding Officer U. S. Army Electronics Materiel Agency Attn: SELMA-R2a 225 South 18th Street Philadelphia, Pennsylvania	1
Commander Aeronautical Systems Division Attn: ASRNET Wright-Patterson Air Force Base, Ohio	1
ITT Industrial Laboratories 3700 East Pontiac Street Fort Wayne, Indiana Attn: Michael F. Toohig Mgr, Storage Tube Develop	1
Massachusetts Institute of Technology Lincoln Laboratory Lexington 73, Massachusetts Attn: M. A. Granese Documents Librarian	1
National Aeronautics and Space Administration Ames Research Center Moffett Field, California Attn: Mrs. Lucille D. Baker, Chief Admin. Services Division	1
Texas Instruments, Inc. 13500 N. Central Expressway P.O. Box 5012 Dallas, Texas Attn: Patricia L. Brown	1
Sandia Corporation Sandia Base Albuquerque, New Mexico Attn: Mrs. Bertha Allen	1
Stanford Research Institute Menlo Park, California Attn: Mr. D. Geppert	1
Commander Air Force Cambridge Research Center L. G. Hanscom Field Bedford, Massachusetts Attn: CRRCPV, J. Bloom	1

	No. of Copies
Chief, West Coast Office U. S. Army Electronics R & D Laboratory 75 South Grand Avenue Pasadena 2, California	1
Tung-Sol Electric, Inc. 200 Bloomfield Avenue Bloomfield, New Jersey Attn: Dr. A. M. Skellett	1
Sperry Gyroscope Company A Division of Sperry Rand Corporation Great Neck, New York Attn: Mr. T. Sege, Mail Station 1B40	1
Battelle Memorial Institute 505 King Avenue Columbus 1, Ohio Attn: Dr. G. Gaines	1
General Electric Company Power Tubes Division Schenectady, New York Attn: V. J. DeSantis	1
General Telephone & Electronics, Inc. Bayside, New York Attn: Dr. T. Polanyi	1
Philco Corporation C & Tioga Streets Philadelphia, Pennsylvania Attn: Dr. M. E. Lasser	1
Linfield Research Institute McMinnville, Oregon Attn: Dr. W. P. Dyke	1
Massachusetts Institute of Technology Cambridge, Massachusetts Attn: Prof. W. B. Nottingham	1
University of Missouri Columbia, Missouri Attn: Dr. E. P. Hensley	1
University of Minnesota Minneapolis 14, Minnesota Attn: Prof. W. G. Shepherd	1

	No. of Copies
University of California Lawrence Radiation Laboratory Technical Information Division P. O. Box 808 Livermore, California Attn: Clovis G. Graig	1
Sylvania Electric Products, Inc. Emporium, Pennsylvania Attn: Dr. R. A. Palmateer	1
U. S. National Bureau of Standards Washington 25, D. C. Attn: Dr. Glenn F. Rouse	1
General Electric Research Laboratory Schenectady, New York Attn: Dr. Ralph Bondley	1
Nuclear Corporation of America Denville, New Jersey Attn: Dr. N. Sclar	1
Commander Rome Air Development Division Griffiss Air Force Base Rome, New York Attn: W. Quinn	1
Stanford Research Institute Applied Physics Group Menlo Park, California Attn: Dr. C. A. Rosen	1
Sylvania Electric Products, Inc. Mountain View Components Laboratory Mountain View, California Attn: Mr. Leon Lerman	1
Dr. John Moll, Solid State Electronics Laboratory Stanford Electronics Laboratories Stanford University Stanford, California	1
Commanding Officer U. S. Army Electronics R & D Laboratory Attn: SELRA/PF (Dr. Jacobs) Fort Monmouth, New Jersey	1

	No. of Copies
Technical Library G. E. Microwave Laboratory 601 California Avenue Palo Alto, California	1
TRG Incorporated 2 Aerial Way Syosset, New York Attn: Mr. J. D. Maiman	1
Eitel-McCullough, Inc. San Carlos, California Attn: Research Library	1
General Electric Company Owensboro, Kentucky Attn: Mr. A. P. Haase	1
Commanding Officer U. S. Army Engineer Research and Development Laboratories Fort Belvoir, Virginia Attn: Mr. Ernest A. Meredith Warfare Vision Branch	1

This contract is supervised by the Techniques Branch, Electron Tubes Division, ECD, USAECTRDLAB, Fort Monmouth, New Jersey. For further technical information contact Dr. D. Dobischek, Project Engineer, Telephone 201-59-61402.